



**B cell recruitment in spontaneous relapsing  
remitting (RR) experimental autoimmune  
encephalomyelitis (EAE)**

**Dissertation**

zur Erlangung des Doktorgrades der Humanbiologie  
an der Medizinischen Fakultät der  
Ludwig-Maximilians-Universität München

Zakeya Nasser Salem Hamad Al-Rasbi

München

July 2014



**B cell recruitment in spontaneous relapsing  
remitting (RR) experimental autoimmune  
encephalomyelitis (EAE)**

**Dissertation**

Zakeya Nasser Salem Hamad Al-Rasbi

# Eidesstattliche Versicherung

---

Name, Vorname

Ich erkläre hiermit an Eides statt,  
dass ich die vorliegende Dissertation mit dem Thema

selbständig verfasst, mich außer der angegebenen keiner weiteren Hilfsmittel bedient und alle Erkenntnisse, die aus dem Schrifttum ganz oder annähernd übernommen sind, als solche kenntlich gemacht und nach ihrer Herkunft unter Bezeichnung der Fundstelle einzeln nachgewiesen habe.

Ich erkläre des Weiteren, dass die hier vorgelegte Dissertation nicht in gleicher oder in ähnlicher Form bei einer anderen Stelle zur Erlangung eines akademischen Grades eingereicht wurde.

---

Ort, Datum

---

Unterschrift Doktorandin/Doktorand

## **Dedication**

I dedicate this work to my beloved family.

I thank my brothers, Salem, Bader, Hamad, Khamis, Matar, Humaid and Salah Al-Rasbi for their emotional support and cracking jokes at my bad days, which kept me going.

To my very special, and loving sisters, Rahma, Salema, Fatma, Haila, Shaika, Saada, Shumysa and Maryam Al-Rasbi who never spared any piece of advice to make a better version of me and of my work.

I thank Dr. Anwar Al-Zaabi for being caring, loving and believing in me and his continuous support and encouragement. He was so patient, listened, empathized and advised in both my studies and potential career.

To my mother, Murra, I am so grateful to Allah to be your daughter and thank you for your understanding and bearing with me missing so many family occasions, without your prayers I would never have reached this far.

## **Acknowledgement**

First and foremost, I offer my sincerest gratitude to my supervisor Prof. Hartmut Wekerle. The research presented in this thesis could not have been completed without his support and I thank him for welcoming me to his laboratory and everything he has done for me. I am thankful for all continuous support and encouragement throughout my studies. He shared his knowledge with me and gave me his time to complete this thesis.

I would like to extend my deepest thanks to my mentor, Dr. Gurumoorthy Krishnamoorthy for his guidance and support throughout my PhD studies. His training and mentorship inspired the abilities and confidence required to complete this journey, thank you. I express my gratitude to Prof. Edgar Meinl for accepting to act as my principal supervisor at the medical faculty of the Ludwig Maximilians University, Munich. I also kindly acknowledge the members of my thesis examination board from the Ludwig Maximilians University. I would also like to thank the members of my thesis committee at the Max Planck Institute which included Dr. med. Dieter Jenne, Prof. Edgar Meinl and Dr. Marc Schmidt-Supprian for their support and constructive feedback.

I thank my laboratory colleagues, Kerstin Berer, Marsilius Mues, Michail Koutrolos and my best friend Marina Boziki for their continuous encouragement and help. Also, I thank Irene Arnold-Ammer, Lydia Penner and Nicole Reisser for all technical help. I have been blessed with a friendly and cheerful group of fellow PhD students and technicians. I thank them all for being there for me when I ever needed them, providing the support and encouragement and making the laboratory such a lively, cheerful place.

I would also thank Dr. Klaus Dornmair, Dr. Birigit Obermeier and Reinhard Mentele for all the biochemistry work in antibody purification and all the time consumed in discussion and I thank Prof. Naoto Kawakami for all the help in induced CNS antigen transfer studies and performing the intrathecal injections. Also, I extend my thanks to all our animal caretakers for help with the mouse colony. I simply could not have wished for a better or friendlier environment.

Finally, I thank the Max Planck Institute of Neurobiology for accommodating me and Emirates Foundation for partly funding this project.

## **Abstract**

Endogenously recruited myelin oligodendrocyte glycoprotein (MOG)-binding B cells have been observed in relapsing remitting (RR) experimental autoimmune encephalomyelitis (EAE) mice where all T cells are transgenic and specific for MOG<sub>92-106</sub> peptide. The aim of this study was to characterize MOG-binding B cells and preclinical events in RR mice.

Recombinant fluorescent MOG tetramers were utilized to find MOG-binding B cells which occurred at low frequency in RR mice. MOG-binding B cells were distributed throughout the immune compartments, with a tendency to accumulate in the cervical lymph nodes, which drain the central nervous system (CNS). MOG-binding B cells were mature; isotype switched and preferentially resided within the germinal center (GC). Analysis of affinity purified serum anti-MOG antibodies suggested a heterogeneous population of endogenous MOG-specific B cells in RR mice. Anti-MOG antibodies were found in the serum of encephalitic, and also of healthy RR mice. There is a strong correlation between the number of CNS infiltrating T and B cells and serum titer of anti-MOG antibodies in RR mice.

## **Zusammenfassung**

In dieser Doktorarbeit wurde ein Tiermodell bearbeitet, in dem spontan eine schubförmig-remittierende experimentelle autoimmune Enzephalomyelitis Enzephalitis auftritt (RR-Maus). In dieser RR-Maus sind alle T-Zellen transgen und spezifisch für MOG. Ziel dieser Studie war es, MOG-bindende B-Zellen und Abläufe vor Beginn der Erkrankung in RR-Mäusen zu charakterisieren.

Um MOG-bindende B-Zellen zu finden, die in niedriger Frequenz bei RR-Mäusen auftreten, wurden rekombinante fluoreszierende MOG Tetramere eingesetzt. MOG-bindende B-Zellen waren innerhalb der immunen Kompartimente verteilt, mit einer Tendenz zur Ansammlung in Halslymphknoten, die das zentrale Nervensystem (ZNS) drainieren. MOG-bindende B-Zellen waren ausgereift, Isotop-gewechselt und vorzugsweise innerhalb der Keimzentren lokalisiert. Die Aufreinigung von Serum anti-MOG-Antikörpern zeigte einen heterogenen Bestand von endogenen MOG-spezifischen B-Zellen. Anti-MOG-Antikörper zirkulierten sowohl im Serum enzephalitischer als auch gesunder RR Mäuse. Es gab eine starke Korrelation zwischen der Anzahl von T- und B-Zellen im CNS und dem Serum Titer von anti-MOG-Antikörpern bei RR-Mäusen.

## Table of contents

Eidesstattliche Versicherung .....	i
Dedication .....	ii
Acknowledgement .....	iii
Abstract .....	iv
Zusammenfassung .....	v
1. Introduction .....	1
1.1 Multiple sclerosis (MS) .....	1
1.2 Experimental animal models of MS .....	2
1.2.1 Experimental autoimmune encephalitis/encephalomyelitis (EAE) .....	3
1.2.2 Spontaneous EAE animal models .....	3
1.2.3 The relapsing remitting (RR) mice animal model .....	6
1.3 Immunopathology in MS and EAE .....	6
1.3.1 Neural antigen drainage .....	7
1.3.2 Cellular components of CNS in health and disease .....	9
1.3.3 Role of lymphocytes in MS and EAE .....	11
1.3.3.1 T lymphocytes in MS and EAE .....	11
1.3.3.2 B lymphocytes in MS and EAE .....	12
2. Objectives .....	15
3. Material and Methods .....	17
3.1 Materials .....	17
3.1.1 Cell culture .....	17
3.1.2 RPMI 1640 and DMEM (complemented) .....	17
3.1.3 Buffers and solutions .....	17
3.1.4 Antibodies and staining reagents .....	19
3.1.5 Primers .....	20
3.1.6 Mouse license .....	20



3.2	Methods .....	21
3.2.1	EAE induction:.....	21
3.2.2	Alum immunization:.....	21
3.2.3	Intracardiac perfusion:.....	21
3.2.4	Intrathecal injection: .....	21
3.2.5	Leukocyte isolation from peripheral blood:.....	22
3.2.6	Lymphocyte preparation from isolated organs: .....	22
3.2.7	Cultivation of cell lines:.....	22
3.2.8	Whole organ culture: .....	22
3.2.9	Isolation of CNS mononuclear cells: .....	23
3.2.10	Fluorescence-activated cell sorting (FACS):.....	23
3.2.11	Serum collection:.....	23
3.2.12	Enzyme linked immunosorbent (ELISA) assay:.....	23
3.2.13	Enzyme linked immunospot (ELISPOT) assay: .....	24
3.2.14	Fluorescence microscopy: .....	24
3.2.15	Hybridoma generation:.....	25
3.2.16	Antibodies purification from blood serum: .....	25
3.2.17	Purification of anti-MOG antibodies: .....	25
3.2.18	Antibodies purification from CNS: .....	25
3.2.19	Deglycosylation of purified anti-MOG antibody:.....	26
3.2.20	Two dimensional (2D) gels:.....	26
3.2.21	Native gel: .....	27
3.2.22	F(ab) <sub>2</sub> fragmentation:.....	27
3.2.23	RNA techniques .....	27
3.2.24	Statistical analysis.....	27
4.	Results .....	29
4.1	MOG-binding B cells in RR mice.....	29

4.1.1	mMOG <sub>tet</sub> : A tool to detect MOG-binding B cells .....	29
4.1.2	MOG-binding B cells in lymphoid organs .....	32
4.1.3	MOG-binding B cells in the CNS .....	35
4.1.4	Anti-MOG antibodies purification in RR mice .....	36
4.2	Summary of part 4.1 .....	41
4.3	Preclinical events of EAE development in RR mice .....	42
4.3.1	Neural antigens drainage/ transport and deposition in CNS draining lymph nodes .....	42
4.3.2	Preclinical infiltration of immune cells in the CNS .....	47
4.4	Summary of part 4.3 .....	52
5.	Discussion .....	54
5.1	MOG-binding B cells in CNS drainage lymph nodes .....	54
5.2	MOG-binding B cells in the CNS of RR mice .....	55
5.3	RR mice hybridoma to study anti-MOG antibody clones .....	56
5.4	Neural antigen transportation .....	57
5.5	Preclinical infiltration of lymphocytes .....	58
6.	Conclusion .....	60
7.	Appendix .....	62
8.	References .....	64
9.	Curriculum vitae .....	72

# CHAPTER 1: INTRODUCTION

## 1. Introduction

### 1.1 Multiple sclerosis (MS)

The central nervous system (CNS) which includes the brain, spinal cord and optic nerves is a structurally and functionally unique, immunologically privileged organ (Lassmann et al., 1998). It has been shown that the effective immune surveillance mechanisms are necessary to protect CNS against injurious agents. However, failure to control unwanted auto reactive immune responses in the CNS can result in chronic immunopathological disorders, such as multiple sclerosis (MS) and neuromyelitis optica (NMO) (Lassmann et al., 1998). MS is a chronic autoimmune demyelinating disease of CNS that affects primarily young people (Weinshenker, 1998). The prevalence of MS is about 2.5 million, worldwide (Weinshenker, 1998). MS leads to disability at the level of physiological and cognitive functions with symptoms being primarily depended on the location and the spread of demyelinated CNS areas. Symptoms can be quite diverse ranging from sensibility disorders, fatigue, dizziness, deterioration of vision, up to paralysis (Compston and Coles). The majority of patients develop MS with a relapsing remitting (RR) clinical course, with alternating periods of acute disease and recovery (Compston and Coles). After an initial phase, patients can recover completely and remain free of symptoms until the disease reinitiates. Relapses can last for days or weeks with varying recoveries. Over time, patients with RR MS may develop secondary-progressive MS, which often leads to severe disability. A minority of patients, though, suffers from primary-progressive MS, a rather aggressive form of the disease developing gradually but steadily from the very beginning. MS is mainly believed to be mediated by immune cells that attack myelin sheath produced by oligodendrocytes which leads to axonal damage and ultimately, to neuronal death (Engelhardt and Coisne, 2011).

The etiology of MS is dictated by both genetic and environmental factors (Compston and Coles). One important genetic risk factor is major histocompatibility complex (MHC), human leukocyte antigen (HLA) class II (Hafler et al., 2007). MHC II is vital for CD4<sup>+</sup> T lymphocytes activation by antigen-presenting cells (APC). In addition, genome wide association studies (GWAS) identified numerous immune-related genes, including the cytokine receptors for interleukin (IL)-2 and IL-7, as risk factors supporting the autoimmune pathogenesis of the MS (Fugger et al., 2009).

Environmental influences on MS pathogenesis were suggested by the geographical differences in the occurrence of MS. Northern European and Northern American countries show a higher incidence of MS than regions closer to the equator (Kurtzke, 1993). This might be partly explained by the reduced sun exposure hence vitamin D, leading to a higher probability of developing MS (Smolders et al., 2008). It was also proposed that bacteria such as  $\beta$ -hemolytic

*streptococcus* or viral infections, like the Epstein-Barr virus (Vartdal et al., 1980), could trigger MS by means of molecular mimicry or through bystander activation of the immune system, but so far none has been proven, unequivocally (Lünemann and Münz, 2009).

## **1.2 Experimental animal models of MS**

There are three main experimental demyelination models available to study the MS pathogenesis; these are toxic, viral, and immune mediated. The toxic models of MS include the use of cuprizone (Blakemore, 1973), ethidium bromide (Blakemore and Franklin, 2008), and lysophosphatidylcholine (Low et al., 1983). In the cuprizone model, mice are fed with the copper chelator, cuprizone (2% in chow) for 4–6 weeks. Cuprizone treatment causes mitochondrial dysfunction in oligodendrocytes leading to apoptosis (Matsushima and Morell, 2001). Interestingly, after cessation of cuprizone treatment remyelination ensues thus, making this model useful to study oligodendrocytes cell death, as well as, for examining mechanisms of remyelination. The second toxic model is the microinjection of lysophosphatidylcholine or ethidium bromide into white matter tracts causing rapid demyelination, followed by remyelination (Blakemore and Franklin, 2008). Similar to the cuprizone model, these two toxic models have been used to examine cellular and molecular determinants of remyelination (Blakemore and Franklin, 2008). The pitfall of all toxic models is the absence of ongoing immune activity.

The second experimental demyelination model is the viral model of MS. This model relies on the experimental infection of rodents with Theiler's murine encephalomyelitis virus (TMEV), mouse hepatitis virus (MHV), and Semliki forest virus (SFV), which eventually induces demyelination in the CNS. The best-studied viral demyelination models are TMEV and MHV (McCarthy et al., 2012). Viral models of MS provided insight into mechanisms by which autoimmunity are established (Miller et al., 1997) and some behavioral signs following demyelination of the murine CNS (Rivera-Quinones et al., 1998). However, the downside of this model is that viral-induced demyelination probably differs from that of MS, where persistent viral infection of the CNS has not been demonstrated.

The third, myelin antigen induced animal model, involves an immune mediated demyelination. This model is widely used in experimental studies and is being discussed in extensive detail in the following section as studies conducted during this research focuses on immunopathogenesis of MS in its experimental model EAE.

### 1.2.1 Experimental autoimmune encephalitis/encephalomyelitis (EAE)

EAE is one of the most frequently studied MS animal models. EAE is induced in susceptible mouse strains by active immunization with complete Freund's adjuvant and pertussis toxin together with antigen of interest (McCarthy et al., 2012). Several antigen preparations have been used to induce EAE including whole CNS tissue (Wekerle et al., 1994b), purified myelin (Wekerle et al., 1994a) myelin proteins or peptides from myelin antigens such as myelin oligodendrocytes glycoprotein (MOG), myelin basic protein (MBP), and proteolipid protein (PLP) (Bradl and Linington, 1996). The incubation period between immunization, and disease onset, and the severity of clinical symptoms depends on the genetics (species and strain) of animals and experimental factors. Experimental factors includes mode of immunization, dose and nature of injected antigen (Krishnamoorthy and Wekerle, 2009). Unfortunately, the necessity of adjuvant and pertussis toxin for the induction of active EAE limits the applicability of this model, especially during the initial stages of autoimmune disease processes. These limitations are bypassed when EAE is induced by transfer of pre-activated lymphocytes isolated from immunized donor mice which are reactivated *in vitro* with myelin antigen (Paterson, 1960). Passive EAE develops faster and more homogeneously than active EAE, it avoids CFA inoculation, allows the manipulation of pathogenic T cells *ex vivo*, and facilitates the analysis of effector functions of transferred T cells (Ben-Nun et al., 1981). Nevertheless, it does not facilitate the study of the initial steps of the induction of the disease therefore; a spontaneous EAE model is essential.

### 1.2.2 Spontaneous EAE animal models

Spontaneous CNS autoimmunity can be initiated by neurodegenerative disease, genetic manipulation of inflammatory mediators or T and B cell receptors. Spontaneous EAE models were extensively reviewed by Krishnamoorthy et al. (2007), and they concluded that certain neurodegenerative diseases exhibit EAE-like demyelinating lesions within CNS. One animal model of neurodegenerative disease is Twitcher mouse (Suzuki and Suzuki, 1995). Twitcher mouse is a naturally occurring model of Krabbe disease resulting in dysfunctional metabolism of sphingolipids, one of the vital components of myelin sheath (Suzuki and Suzuki, 1995). Myelin degeneration in Twitcher mice leads to immune cell infiltrates to the CNS (Ohno et al., 1993). In addition, selective expression of specific cytokines/chemokines in the CNS tissue, such as tumor necrosis factor alpha (TNF)- $\alpha$ , interferon gamma IFN- $\gamma$ , IL-6, IL-12 (both p35 and p40), chemokine CC motif ligand (CCL)-21 and CCL-2, might lead in some cases to increased proinflammatory milieu within the CNS and increased immune cell infiltration (Krishnamoorthy et

al., 2007). And increased immune cells infiltration results in a neurological syndrome that resembles, at least in part T-cell mediated EAE yet they do not fully replicate the major features of MS pathology.

T/B cell clones	TCR/BCR specificity	Genetic background (MHC restriction)	Spontaneous autoimmunity	Lesions character and location
19	MBP Ac <sub>1-9</sub>	PL/J or B10.PL (I-A <sup>u</sup> )	100% in RAG deficient background	Mononuclear cell infiltrates in the brain and spinal cord (Lafaille et al., 1994)
172.10	MBP Ac <sub>1-11</sub>	B10.PL (I-A <sup>u</sup> )	14–44%	Macrophage and lymphocyte infiltration in the spinal cord white matter (Goverman et al., 1993)
5B6	PLP <sub>139-151</sub>	SJL.J (I-A <sup>s</sup> )	60–83%	Inflammatory foci in the CNS (Waldner et al., 2000)
4E3	PLP <sub>139-151</sub>	SJL.J (I-A <sup>s</sup> )	45%	Inflammatory foci in the CNS (Waldner et al., 2000)
2D2	MOG <sub>35-55</sub>	C57BL/6 (I-A <sup>b</sup> )	4% EAE and 30% optic neuritis	Optic neuritis, and mononuclear cell infiltrates in meninges and CNS parenchyma (Bettelli et al., 2003)
TCR <sup>1640</sup>	MOG <sub>92-106</sub>	SJL.J (I-A <sup>s</sup> )	80% spontaneous EAE	T and B-lymphocytes infiltrates in the brain and spinal cord. Prominent deposits of Immunoglobulin and some activated complement (Pollinger et al., 2009)
2D2 X IgH <sup>MOG</sup>	MOG <sub>35-55</sub> Anti-MOG 8.18c5	C57BL/6 (I-A <sup>b</sup> )	50% opticospinal (OSE) EAE	Inflammatory and demyelinating lesions in the optic nerve and in the spinal cord (Krishnamoorthy et al., 2006)
Ob.1A12	hMBP <sub>84-102</sub>	Humanized Tg (HLA-DR2)	4% in normal background and 100% in RAG-deficient background	Inflammatory and demyelinating lesions throughout the CNS and composed of neutrophilic granulocytes, activated macrophages and T lymphocytes (Madsen et al., 1999)

**Table 1.1 Transgenic mice with T-cells-specific for CNS autoantigens** (*modified from (Krishnamoorthy et al., 2007)*)

The introduction of myelin antigen-specific T cell receptors (TCR) and B cell receptors (BCR) in transgenic mice overcame aforementioned limitations. These models developed EAE disease without the need of the antigen/CFA immunization. Like any other autoimmune disease spontaneous EAE is determined by intrinsic factors like the genetic background of the mice, TCR affinity to the specific antigen, as well as, environmental factors such as housing

conditions. Those intrinsic and environmental factors have a great influence on spontaneous diseases.

Examples of CD4<sup>+</sup> T cell receptors transgenic mice recognizing different myelin antigen epitopes in the context of MHC class II determinants the development of spontaneous EAE during its adult life with different frequencies, histological and clinical courses as summarized in (Table 1.1) (Krishnamoorthy et al., 2007). Briefly, as seen in Table (1.1) MBP-transgenic mice develop spontaneous EAE when bred on a recombination-activating gene (RAG)-knockout (KO) background, in non-sterile housing conditions (Governman et al., 1993). This effect was attributed to the absence of MBP-specific T regulatory (T<sub>reg</sub>) cells that control autoreactive T cells and passive transfer of wild type CD4<sup>+</sup> CD25<sup>+</sup> T cells prevented spontaneous EAE (Olivares-Villagómez et al., 1998). MOG<sub>35-55</sub> peptide-reactive TCR transgenic mice, 2D2, develop spontaneous optic neuritis without any clinical or histological sign of EAE (Bettelli et al., 2003). However, they develop EAE when immunized with MOG or by injection of pertussis toxin. The clinical differences between EAE models can be attributed to both non-MHC background genes (Storch et al., 1998) and different target antigens which might induce different types of immunopathology (Sobel, 2000). Further improvements by the introduction of MOG-specific B cell receptor transgenes along with 2D2; TCR double-transgenic 2D2 x IgH<sup>MOG</sup>; termed opticospinal EAE (OSE) mice, led to the development of spontaneous EAE at an incidence of about 50% (Krishnamoorthy et al., 2006, Bettelli et al., 2006). OSE mice spontaneously develop an inflammatory demyelinating disease affecting the spinal cord and optic nerves but spares the brain stem and cerebellum, similar to human opticospinal MS or Devic's disease (Krishnamoorthy et al., 2006, Bettelli et al., 2006). Spontaneous EAE in OSE mice is a result of a pathogenic interaction between MOG-specific T and B cells where MOG-specific B cells concentrate and present recombinant MOG to T cells and, T cells induce the B cells to switch immunoglobulin production from IgM to IgG isotypes (Krishnamoorthy et al., 2007).

While table (1.1) only presents transgenic mice with autoreactive myelin-specific CD4<sup>+</sup> T cells, there are also few of myelin-specific CD8<sup>+</sup> T cell transgenic mice, which, failed to develop spontaneous EAE (Huseby et al., 1999, Perchellet et al., 2004). Failure to develop spontaneous EAE by autoreactive myelin-specific CD8<sup>+</sup> might be explained by their suppressive and regulatory role in EAE seen in several studies. One example is, when CD8<sup>+</sup> T cells isolated from EAE-recovered mice and cultured with MBP-activated CD4<sup>+</sup> T cell clones inhibited their activity *in vitro* and prevented disease in the recipients after transfer of those cultured MBP-activated CD4<sup>+</sup> T cell clones to MBP-immunized mice (Jiang et al., 2003).



Finally, the last example of spontaneous EAE animal models are “humanized” transgenic mice, which harbor TCRs that were cloned from human CD4<sup>+</sup> T cells (clone Ob.1A12), recognize MBP<sub>84-102</sub> peptide in the context of an MS-susceptible human MHC class II protein, DR15 (Madsen et al., 1999). Spontaneous EAE incidence in these humanized mice was less than 5% but increased when crossed with RAG knockout mice. Another strain of mice carry humanized TCR, which recognize MBP<sub>85-99</sub> peptide had a EAE frequency of 60%, with more severe clinical deficiencies (Ellmerich et al., 2005).

### **1.2.3 The relapsing remitting (RR) mice animal model**

Relapsing remitting (RR) mice are transgenic mice expressing a T cell receptor (TCR) specific for the MOG peptide 92–106 (MOG<sub>92-106</sub>) in the context of I-A<sup>s</sup> MHC class II. This TCR, consisting of V $\alpha$ 8.3 and V $\beta$ 4 genes, was derived from a MOG-specific encephalitogenic Th1-CD4<sup>+</sup> T cell clone isolated from a WT SJL/J mouse immunized against recombinant MOG (Pollinger et al., 2009). These mice, are kept under specific pathogen free (SPF) conditions, usually develop spontaneous RR diseases at an age older than 8 weeks, with an EAE incidence of over 80% (Pollinger et al., 2009).

Most importantly, these T cells recruit endogenous MOG-specific B cells around the age of 3 weeks (Pollinger et al., 2009). Transgenic RR mice produce high titers of anti-MOG autoantibodies with IgG<sub>1</sub> and IgG<sub>2</sub> isotypes. These endogenous B cells were present in the inflammatory lesions of the CNS. There were also local deposits of immunoglobulin (Ig) along with some activated complement in the CNS (Pollinger et al., 2009).

B cells have an essential role in the spontaneous development of RR-EAE (Pollinger et al., 2009). B cells can contribute to autoimmune responses via secreting humoral antibodies, acting as antigen presenting cells (APCs), releasing cytokines and interacting with autoimmune T cells. In RR-EAE, the humoral response seems to be vital. B cell depletion, using anti-CD20 monoclonal antibodies (mAb) during the neonatal period of the mice life, suppressed RR-EAE, while depletion of B cells in adult mice results in accelerated clinical courses (Pollinger et al., 2009). In addition, MOG-specific B cell expansion critically requires the presence of the endogenous target autoantigen, as MOG-KO RR SJL/J mice never produced anti-MOG autoantibodies (Pollinger et al., 2009).

## **1.3 Immunopathology in MS and EAE**

MS and EAE are immune-mediated diseases of the CNS characterized by initial inflammation, followed by demyelination, and finally axon loss (Lassmann et al., 1998). This initial

inflammation can lead to direct or indirect damage of myelin creating a pro-inflammatory milieu that stimulates drainage and/or transportation of neural autoantigen to the nearest CNS draining lymph nodes (Weller et al., 2009). Neural antigens are taken up by the APCs in the peripheral lymphoid tissue and presented to immune cells in order to stimulate and activate these cells. After activation, T and B cells with improved specificity for selective antigen expand. After clonal expansion, T and B cells infiltrate back to the CNS, and re-encounter their specific antigen. CD4<sup>+</sup> T cells recognize their antigens presented by microglial cells on MHC class II molecules. B cells mature to plasma cells and release large amounts of antibodies that bind to soluble or membrane-bound antigens on expressing cells. Finally, reactivation of these cells leads to heightened production of inflammatory cytokines (Chabas et al., 2001). These cytokines attract other immune cells, such as macrophages, which contribute to inflammation through the release of injurious immune mediators and direct phagocytic attack on the myelin sheath (Figure.1.1).

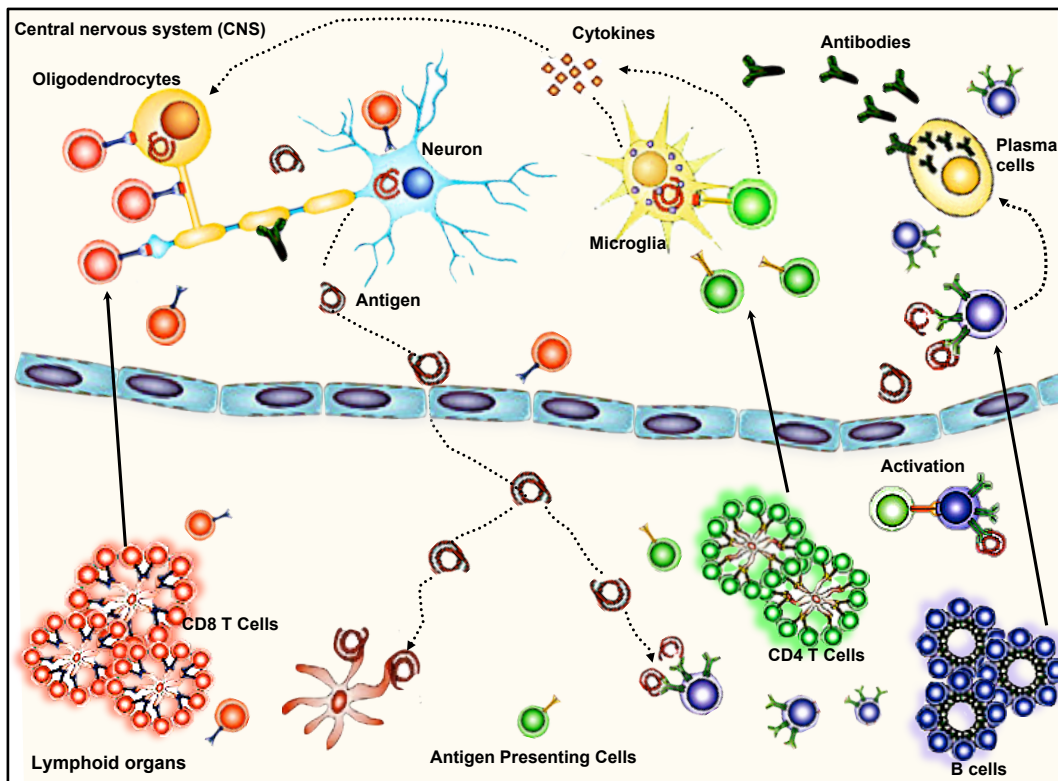


**Figure 1.1. Schematic diagram of immune-pathogenesis in MS and EAE.** (Adopted from *Nature Reviews Neuroscience* (Hemmer et al., 2002))

### 1.3.1 Neural antigen drainage

The CNS has long been recognized as an 'immune privilege' site because of the lack of lymphatic vessel drainage and the tight blood brain barrier (BBB) which reduce immune surveillance in the CNS (Abbott et al., 2010). Yet, adaptive immune responses can be initiated

against CNS antigens, so immune privilege notion of CNS is not absolute (Wekerle, 2006). In fact, CNS is believed to possess a soluble route for antigen drainage to the lymphatic system via the interstitial fluid (ISF) and cerebrospinal fluid (CSF).

ISF is the tissue fluid, which surrounds cells in any given organ. ISF is formed by hydrostatic pressure that pushes water and solutes from small blood vessels to extracellular space and eventually returns to blood via osmotic pressure through blood vascular walls (Weller, 1998). ISF and solutes are believed to travel in reverse manner to blood direction along the basement membrane of arteries between smooth muscle cells in the tunica media (Carare et al., 2008). Injections of different sized fluorescent tracers or labeled antigens in the CNS have revealed that ISF drains within 5 minutes to the basement membrane of blood vessel and diffuses in brain parenchyma (Carare et al., 2008). And after 30 minutes, fluorescent tracers were no longer present in vascular basement or brain parenchyma indicating there is an active ISF drainage in the CNS (Carare et al., 2008). In a similar study by (Szentistvanyi et al., 1984), radioactive tracers injected into the CNS were found in deep cervical lymph nodes and were believed to take a route other than the CSF draining route. The radioactive tracers were found in cranial arteries, which reside at the base of the skull but they were not found in the carotid artery in the neck. Cranial arteries are one of the CSF draining routes but ISF drainage is not merely separated from CSF drainage. After selective injection of trypan blue in the CSF, traces were found in perivascular macrophages that reside along the walls of arteries and capillaries, a route which is taken by ISF (Weller et al., 2009).

CSF is produced by choroid plexus epithelial cells and small percentage of CSF comes from ISF. CSF flows from the ventricles into the subarachnoid space and circulate around the brain and spinal cord (Ransohoff and Engelhardt, 2012). There are two routes for lymphatic drainage of CSF. In the first route, CSF is directly drained via arachnoid villi to the blood and/or adsorbed into blood capillaries in the brain parenchyma (Weller et al., 2009). However, it appears that this route is important only under certain conditions such as elevated CSF pressure (Johnston et al., 2004). Therefore, drainage of CSF from CNS across the cribriform plate along olfactory rootlets to the nasal mucosa and then to the different lymphatics of the deep cervical lymph nodes is regarded as the primary extracranial route (Johnston et al., 2005a). Johnston and his colleagues have injected a silicone rubber compound into subarachnoid spaces in both primates and non-primates and found that the material penetrated the cribriform plate above the nasal cavity. This route also has been proven with other studies like the one where India ink was injected into subarachnoid space and particles of India ink were observed in the perineurial space of the olfactory nerves and they penetrated the cribriform plate (Johnston et al., 2005b).

The lymphatic vessels in the nasopharyngeal mucosa were consequently filled with India ink tracer (Yoffey and Drinker, 1939). Furthermore, infused X-ray contrast medium into the cisterna magna of monkeys revealed that the contrast agent appeared to travel alongside the optic and olfactory nerves to nasal region to reside in the deep cervical lymph nodes reviewed in (Koh et al., 2005).

As stated earlier, the partial immune surveillance of the CNS is believed to be facilitated by the transport of neural antigens via the lymphatic drainage of ISF and CSF to the CNS draining lymph nodes (Carare et al., 2008, Weller et al., 2009). ISF of the CNS drains via perivascular channels that are populated by perivascular macrophages and other APCs able to sample the full range of CNS antigens. Furthermore, the choroid plexus, cerebral ventricles and meninges contain cells that phenotypically resemble DCs and might potentially be capable of traveling to DCLNs (Bulloch et al., 2008). During CNS inflammation, APCs can be found within the brain demyelinating lesions. In fact, active demyelination is defined by the presence of phagocytic macrophages containing myelin protein inclusions. Additionally, some macrophages that expressed CC-chemokine receptor 7 (CCR7), indicating the capability to enter lymph nodes and potentially to present myelin antigens to T cells (Ransohoff and Engelhardt, 2012). However, there is no concrete evidence to support the possibility that APCs migrate from the CNS to the lymphatic system or vice versa.

### **1.3.2 Cellular components of CNS in health and disease**

CNS is a unique organ in terms of function and structure, yet like any organ it requires effective immune mechanisms for protection against infection, despite its perception as a site of immune privilege (Wekerle, 2006). The effective immune surveillance is facilitated by the local innate APCs and infiltrating immune cells. Apart from T and B cells there is no other type of immune cells that have been extensively documented in a healthy CNS.

#### *APC population in the CNS*

The healthy CNS is populated, apart from myelin forming oligodendrocytes, with two main types of glial cells, microglia and astrocytes; they serve as innate sensors of the CNS. Innate APCs or myeloid cells of the CNS can be divided into two main populations (Ransohoff and Cardona, 2010). The first population consists of parenchymal microglial cells, a highly specialized tissue-specific macrophage. Second population consists of epiplaxus cells of the choroid plexus and meningeal, perivascular and ventricular macrophages. Microglia develops early in life and maintained throughout the life by local proliferation. Systemic inflammation, stroke, physical

trauma and neurodegeneration lead to microglia activation (Ransohoff and Brown, 2012). The net results of microglial activation can be either beneficial or deleterious. In fact, neurons constitutively express cell-surface and secreted microglial inhibitors. Consequently, it is likely that neuronal cell death or injury converts the immunosuppressive environment to an inflammatory milieu (Ransohoff and Perry, 2009). Under such inflammatory conditions, CNS myeloid cells can upregulate APC- and DC-associated markers including CD11c, MHC class II and other co-stimulatory molecules (McMahon et al., 2006). CSF also contains a small proportion of monocytes which constitute ~5% of all CSF cells (Trebst et al., 2001).

Astrocytes are best described as neuroglia cells. The main function of astrocytes includes buffering potassium, balancing water, and modulating synaptic activity (Sriram, 2011). Astrocytes also produce neurotrophins, inflammatory mediators and many chemokines (Sriram, 2011). However, constant astrocytic stimulation during chronic inflammation has detrimental consequences as seen by microglial-astrocyte interactions in inflammatory conditions (Vesce et al., 2007, Bezzi et al., 2001). Chemokine C-X-C motif ligand (CXCL)-12 signals to astrocytes to promote physiological release of glutamate during synaptic transmission and to release small amounts of TNF- $\alpha$ . In inflammatory conditions, CXCL12 plus TNF- $\alpha$  from astrocytes and pro-inflammatory conditions signal to microglia to produce large quantities of TNF- $\alpha$  which impairs the capacity of astrocytes to detoxify glutamate, resulting in neuronal loss (Vesce et al., 2007, Bezzi et al., 2001). In addition, astrocytes like microglia in an inflammatory condition can act as APC. Rat astrocytes upregulate MHC class II molecules after treatment with IFN- $\gamma$  as a result gain the capacity to prime autoreactive T cells, and contribute to increased immune reactivity against nervous tissue (Fontana et al., 1984, Wekerle et al., 1987).

#### *T cells in the CNS*

In the late 1980s, it was shown that migration of T cells to CNS occurs even during non-inflammatory conditions (Wekerle et al., 1986, Hickey, 1991). Tracing radioactively labeled encephalitogenic T cell blasts following their intravenous injection into Lewis rats suggested that resting lymphocytes fail to enter the CNS (Wekerle et al., 1986). The activation stage of T cells, rather than the antigen-specificity determines blood brain barrier (BBB) crossing in this model and enter the CNS (Hickey, 1991). After a few hours, however, neuroantigen specificity is needed for lymphoblast persistence in the CNS (Cross et al., 1990).

Under normal physiological conditions, the majority of the immune cells enter the CNS barriers are confined to the perivascular and subarachnoid spaces filled with CSF, leaving the CNS parenchyma largely untouched (Giunti et al., 2003). The CSF of healthy individuals contains 1,000–3,000 cells per ml, with  $\geq 90\%$  of the cells being T cells (Giunti et al., 2003). Those T cells

are mainly CD4<sup>+</sup> memory T cells that have characteristics of both central memory T (TCM) cells and effector memory T (TEM) cells (Sallusto et al., 1999). These cells are furthermore, comparable with the corresponding CD4<sup>+</sup> memory T cell populations in the blood (Kivisakk et al., 2006). It appears that T cells enter the CSF mainly across the choroid plexus in healthy individuals and early in neuroinflammatory disease (Ransohoff et al., 2003). They perform routine immunosurveillance of the CNS, by searching within the CSF-filled subarachnoid spaces for antigens presented by the rich network of subarachnoid-space macrophages (McMenamin, 1999).

### **1.3.3 Role of lymphocytes in MS and EAE**

#### **1.3.3.1 T lymphocytes in MS and EAE**

The most important cellular drivers of MS pathogenesis seem to be T cells, presumably CD8<sup>+</sup> cytotoxic T cells. In contrast, in most models of active EAE, myelin-specific CD4<sup>+</sup> rather than CD8<sup>+</sup> T cells are the central factor of autoimmune pathogenesis. This may be due to the immunization protocol, which favors activation via MHC class II. Similarly, the adoptive transfer of pure encephalitogenic CD4<sup>+</sup> T cell lines, but not CD8<sup>+</sup> T cells, has been successfully used to induce passive EAE (Wekerle et al., 1994b). Nevertheless, in MS patients, the ratio of CD4<sup>+</sup> to CD8<sup>+</sup> T cells in CNS lesions is 1:4, and clonal expansion is detected more frequently among CD8<sup>+</sup> than CD4<sup>+</sup> T cells (Friese and Fugger, 2005). In addition, specific depletion of only CD4<sup>+</sup> T cells in patients did not result in the amelioration of the disease, while treatment with antibodies against CD52, depleted multiple lymphocyte populations, including CD4<sup>+</sup> and CD8<sup>+</sup> T cells resulted in reduced number of circulating lymphocytes (Coles et al., 2012).

Distinct effector T cell subsets have been described to mediate EAE pathogenesis (Friese and Fugger, 2005). Naive CD4<sup>+</sup> T cells can be differentiated into various subclasses of T helper (Th) cells depending on the cytokine milieu. IL-12 and IL-18 induce differentiation into Th1 cells, secreting interferon-gamma (IFN- $\gamma$ ). High concentrations of IL-4, however, yield Th2 cells that produce IL-4, IL-5, and IL-13. A third subpopulation of effector T cells are Th17 cells, secreting IL-17 and IL-22, which can be induced by transforming growth factor beta (TGF- $\beta$ ) and IL-6. In a similar cytokine milieu with high concentrations of TGF- $\beta$  but void of IL-6, naive CD4<sup>+</sup> T cells do not differentiate into Th17 but rather into T<sub>reg</sub> cells, that can reduce inflammatory reactions (Leung et al., 2010). Those different CD4<sup>+</sup> T cell populations get even more complex, since certain plasticity between Th cell subpopulations have been observed. In short, mainly Th1 and Th17 cells drive inflammation and contribute to pathogenesis, while T<sub>reg</sub> cells provide a controlled immunological environment (El-behi et al., 2010).

### 1.3.3.2 B lymphocytes in MS and EAE

The superior importance of T cells as initiator and perpetuator of MS became clear from animal models of EAE. Yet other lines of evidence suggest B cells have a major role in autoimmune diseases either via secreting autoantibodies and cytokines or acting like APCs (Berer et al., 2011b).

Brain and CSF of patients with MS contain high concentrations of antibodies (Kabat et al., 1942). These antibodies forms oligoclonal bands (OCB) of immunoglobulin that mainly involves the IgG<sub>1</sub> and IgG<sub>3</sub> isotypes (Losy et al., 1990). These bands are still an important diagnostic marker for chronic CNS inflammation in MS. Interestingly, the antibody response seems to be stable over long periods and involve a limited number of clonotypes (Walsh et al., 1986). Clonally expanded brain resident B cells are partially accountable for the emergence of these oligoclonal bands, stressing the importance of B cells for the development or course of the disease (Obermeier et al., 2008). Indeed, ectopic lymphoid follicles were described, enriched with B cells and plasma cells in the meninges, potentially providing a suitable microenvironment, where B cells can mature, expand, and locally produce autoantibodies (Serafini et al., 2004).

Autoantibodies also play a major role in EAE, as shown by the transfer of serum from diseased animals which induced subclinical demyelination in recipient animals (Lassmann et al., 1981). Similarly, active EAE was accelerated and showed exacerbated severity in transgenic IgH<sup>MOG</sup> mice, producing high levels of MOG-specific autoantibodies (Litzenburger et al., 1998). In many EAE models, however, the B cell component is missing, since immunization is mostly performed with a short encephalitogenic peptide. Thus, immunization with whole myelin proteins offers a better understanding of the involvement of B cells in disease development, exacerbation or/and protection (Lyons et al., 1999). B cell deficient  $\mu$ MT mice were susceptible to active EAE induced by immunization with MOG<sub>35-55</sub> peptide, but not by recombinant MOG, suggesting differential processing and presentation of the encephalitogenic epitope. On the other hand, (Fillatreau et al., 2002) showed that  $\mu$ MT mice failed to recover from active EAE due to lack of B cell derived IL-10.

B cells can also produce cytokines and chemokines (Lund, 2008). Depending on their cytokine profile, B cells either promote or suppress immune responses in EAE in animal models. B cells produce either Th1 or Th2 associated cytokines when primed with the corresponding Th1 or Th2 cells and antigen *in vitro* (Harris et al., 2000, Harris et al., 2005). However, the existence of such cells *in vivo* remains unclear. The best studied cytokine producing B cells, are murine B<sub>10</sub> or B<sub>reg</sub> cells which produce IL-10 (Fillatreau et al., 2002), which also have been identified in

humans (Duddy et al., 2007). They either inhibit and/or delay the progression of EAE and other autoimmune diseases (Fillatreau et al., 2002).

Antigen presentation by B cells is another important feature that can contribute to the MS pathogenesis. It is of particular importance for the T–B cell interactions observed in the spontaneous EAE models, as mentioned before. IgH<sup>MOG</sup> B cells in the OSE mice model present MOG proteins to MOG-reactive T cells. This results in mutual activation, proliferation, and differentiation and, consequently B cells of those mice produced high titers of MOG-specific IgGs (Bettelli et al., 2006, Krishnamoorthy et al., 2006). In the RR mice model, as well as, the recruitment of MOG-specific B cells from the endogenous repertoire by MOG-reactive transgenic T cells is dependent on the MOG antigen (Pollinger et al., 2009).

In RR-EAE mice, B cells can contribute to the pathogenesis of EAE in two ways: through the production of anti-MOG antibodies seen early in mice lives that contribute to demyelination and deposited in CNS (Pollinger et al., 2009). Alternatively, B cells have also been shown to have both pathogenic and protective functions depending on the age of the mice (Pollinger et al., 2009). Therefore, in experiments conducted as part of this thesis, the phenotype and characterization of endogenous B cells in RR mice were studied either through MOG-specific B cells themselves or anti-MOG antibody titer and their preclinical infiltration in the target tissue (CNS).



## CHAPTER 2: OBJECTIVES

## **2. Objectives**

In RR mice model, MOG-specific T cells are known to recruit MOG-specific B cells from their natural repertoire. These cells can contribute to the susceptibility or resistance to EAE depending on the age of the mice (Pollinger et al., 2009). Therefore, the objectives of the present study are:

1. Phenotype and function of MOG-specific B cells.
2. Clonality of MOG-specific B cells by studying anti-MOG autoantibodies.
3. Release and/or transportation of neural antigens to peripheral lymphoid organs.
4. Immune cells infiltration to the CNS before the onset of spontaneous EAE.

# CHAPTER 3: MATERIAL AND METHODS

### 3. Material and Methods

#### 3.1 Materials

##### 3.1.1 Cell culture

EL4: mouse lymphoma cell line induced in a C57BL/6 mouse by 9, 10-dimethyl-1, 2-benzanthracene treatment (ATCC: TIB-39).

GPE: the retrovirus packaging Ampli-GPE (clone A57) cells were obtained from NIH3T3 fibroblasts

BH-20: the murine monoclonal IgG<sub>2a</sub> clone against mouse neurofilament light generated from SJL/J mouse.

8.18c5: the murine monoclonal hybridoma against native rat MOG

##### 3.1.2 RPMI 1640 and DMEM (complemented)

Media Roswell Park Memorial Institute (RPMI) medium 1640 and Dulbecco's Modified Eagle Medium (DMEM) (Sigma-Aldrich) were complemented with 100 µM non-essential amino acids, 1 mM sodium pyruvate, 50,000 units penicillin, 50 mg streptomycin, 2 mM L-glutamine (Gibco), and 10% fetal calf serum (FCS) (Biochrome). RPMI 1640 medium was further complemented with 200 µM β-Mercaptoethanol. Prior to use FCS was inactivated for 30 minutes at 56°C. Media were sterilized by filtration (pore size 0.2 µm). All quantities refer to 500 ml of medium.

##### 3.1.3 Buffers and solutions

Applied in methods	Buffers and solutions	Composition
3.2	Phosphate buffered saline (PBS)	10 mM Na <sub>2</sub> HPO <sub>4</sub> 1.8 mM KH <sub>2</sub> PO <sub>4</sub> (pH 7.4) 140 mM NaCl 2.7 mM KCl
3.2.3 3.2.14	Paraformaldehyde (PFA) solution	4% PFA in PBS
3.2.5	Heparin solution	5000 units Heparin in PBS
3.2.5	Lysis buffer	150 mM NaCl 20 mM Tris-HCl 1% Triton-X 100
3.2.6	Erythrocytes lysing buffer	0.83% Ammonium chloride in PBS
3.2.9	Isotonic percoll solution	9 parts (v/v) of Percoll 1 part (v/v) of 1.5 M Sodium chloride
3.2.10	Fluorescence-activated cell sorting (FACS) staining buffer	1% BSA 0.1% Sodium azide in PBS
3.2.10	Saponin staining buffer	0.1% (w/v) Saponin in PBS
3.2.12 3.2.13	Blocking buffer	10% FCS in PBS
3.2.12	H <sub>2</sub> O <sub>2</sub> solution	1% H <sub>2</sub> O <sub>2</sub>
3.2.12 3.2.13	Washing buffer	0.05% Tween 20 in PBS

3.2.13	Assay Diluent	0.05% Tween 20 in PBS
3.2.14	Blocking buffer	4% BSA in PBS
3.2.16	Binding buffer	20 mM Sodium phosphate (pH 7.0)
3.2.16	Elution buffer	0.1 M Glycine (pH 2.7)
3.2.16	Neutralization buffer	1 M Tris-HCl (pH 9.0)
3.2.17	Elution buffer	4 M MgCl <sub>2</sub> (pH 6.6-7.2)
3.2.17	Low salt binding buffer	20 mM Sodium phosphate 20 mM NaCl
3.2.17	Ni-NTA column regeneration buffer	1% EDTA 0.05% Tween-20
3.2.18	Binding buffer	1.0% Nonidet P-40 in PBS
3.2.18	Homogenizing buffer	1.0% Nonidet P-40 Mixture of protease inhibitors in PBS
3.2.18	Wash buffer	0.1 M Sodium acetate 0.15 M NaCl
3.2.19	Deglycosylation reaction buffer	1% MEGA-10 in PBS (pH 7.0-7.2)
3.2.19	Dialysis buffer	6 M Urea 20 mM Tris
3.2.20	Agarose solution	0.5 g Agarose 100 ml 1x ELPHO buffer
3.2.20	Ammoniumpersulfate (APS) solution	0.1 g APS in 1 ml H <sub>2</sub> O
3.2.20	Coomassie staining solution	0.1 g Coomassie R-250 50% Methanol 7% Acetic acid
3.2.21		
3.2.20	Destaining solution	50% Methanol 7% Acetic acid
3.2.21		
3.2.20	ELPHO buffer 10x	1% SDS 0.24 M Tris 1.92 M Glycine
3.2.20	Equilibration buffer	6 M Urea 4% SDS 30% Glycerol 50 mM Resolving gel buffer 1.5 M 0.5% Bromophenol
3.2.20	Immobilized pH gradient (IPG) gel rehydration buffer	8 M Urea 2 M Thiourea 2% (v / v) Resolyte 3-10 0.5% Bromophenol
3.2.20	Isoelectric focusing (IEF) loading buffer	6 M Urea 2 M Thiourea 0.5% bromophenol
3.2.20	Non-reducing denaturing sodium dodecyl sulfate (SDS)-loading buffer 5x	0.2 M Tris-HCl (pH 8.0) 1.5% SDS 4.5 ml Glycerol 0.02% Bromophenol
3.2.20	Reducing SDS-loading buffer 3x	0.15 M Tris-HCl (pH 6.8) 15% SDS 45 g Glycerol 6% β-Mercaptoethanol 0.01% Bromophenol
3.2.20	Resolving gel buffer	1.5 M Tris-HCL (pH 8.8) 0.4% SDS
3.2.20	SDS solution	1% SDS

### 3.1.4 Antibodies and staining reagents

FACS markers specificity	Clone	Antibody class	Company
Bcl-6	GI191E	Mouse IgG <sub>1</sub>	eBioscience
CD3 $\epsilon$	145-2C11	Ar Ham IgG <sub>1</sub> , $\kappa$	BD Biosciences
CD4	RM4-5	Rat IgG <sub>2a</sub> , $\kappa$	eBioscience
CD5	53-7.3	Rat IgG <sub>2a</sub> , $\kappa$	BD Biosciences
CD11b	M1/70	Rat IgG <sub>2b</sub> , $\kappa$	BD Biosciences
CD11c	N418	Ar Ham IgG	eBioscience
CD19	1D3	Rat IgG <sub>2a</sub> , $\kappa$	BD Biosciences
CD21	7G6	Rat IgG <sub>2b</sub> , $\kappa$	BD Biosciences
CD23	B3B4	Rat IgG <sub>2a</sub> , $\kappa$	BD Biosciences
CD24	M1/69	Rat IgG <sub>2b</sub> , $\kappa$	BD Biosciences
CD25	PC61	Rat IgG <sub>2b</sub> $\kappa$	eBioscience
CD27	LG.7F9	Ar Ham IgG	eBioscience
CD38	90	Rat IgG <sub>2a</sub> $\kappa$	eBioscience
CD45	30-F11	Rat IgG <sub>2b</sub> , $\kappa$	eBioscience
CD45.1	A20	Ms IgG <sub>2a</sub> $\kappa$	eBioscience
CD45.2	104	Ms IgG <sub>2a</sub> $\kappa$	BD Biosciences
CD45R/B220	RA3-6B2	Rat IgG <sub>2a</sub> $\kappa$	eBioscience
CD95	Jo2	Ar Ham IgG <sub>2</sub> $\lambda$ 2	BD Biosciences
CD138	281-2	Rat IgG <sub>2a</sub> $\kappa$	BD Biosciences
CD154	MR1	Ar Ham IgG <sub>3</sub> $\kappa$	BD Biosciences
F4/80	Cl:A3-1	Rat IgG <sub>2b</sub> $\kappa$	AbD Serotec
GI7	GI7	Rat IgM $\kappa$	BD Biosciences
Ig $\lambda$ 1,2,3 light chain	R26-46	Rat IgG <sub>2a</sub> $\kappa$	BD Biosciences
Ig $\kappa$ light chain	187.1	Rat IgG <sub>1</sub> $\kappa$	BD Biosciences
IgD	11-26c.2a	Rat IgG <sub>2a</sub> $\kappa$	BD Biosciences
IgE	23G3	Rat IgG <sub>1</sub> $\kappa$	eBioscience
IgG <sub>1</sub>	A85-1	Rat IgG <sub>1</sub> $\kappa$	BD Biosciences
IgG <sub>2a/b</sub>	R2-40	Rat IgG <sub>1</sub> $\kappa$	BD Biosciences
IgM	R6-60.2	Rat IgG <sub>2a</sub> $\kappa$	BD Biosciences
IgM	II/41	Rat IgG <sub>2a</sub> , $\kappa$	BD Biosciences
IgM <sup>a</sup>	DS-1	Ms IgG <sub>1</sub> $\kappa$	BD Biosciences
MOG (8.18c5)	8.18-C5	Mouse IgG <sub>1</sub>	Max Planck Institute of Neurobiology
MOG (Z2)	Z2	Mouse IgG <sub>2a</sub>	-
mMOG-biotin-tetramer	-	-	Max Planck Institute of Neurobiology
mOVA-biotin-tetramer	-	-	Max Planck Institute of Neurobiology
Peanut agglutinin	-	-	Sigma
Streptavidin	-	-	eBioscience
Streptavidin-HRP	-	-	eBioscience
TO-PRO-3	-	-	Invitrogen
V $\alpha$ 8.3 TCR	KT50	Rat IgG <sub>2a</sub> $\kappa$	BD Biosciences
V $\beta$ 4 TCR	KT4	Rat IgG <sub>2b</sub> $\kappa$	BD Biosciences
Viability dye	-	-	eBioscience

Enzyme-linked immunosorbent assay (ELISA)	Clone	Antibody class	Company
IgG <sub>1</sub> <sup>a</sup>	10.9	Ms IgG <sub>2a</sub> , κ	BD Biosciences
IgG <sub>1</sub> <sup>b</sup>	B68-2	Ms IgM, κ	BD Biosciences
IgG <sub>2a</sub> <sup>a</sup>	8.3	Ms IgG <sub>2a</sub> , κ	BD Biosciences
IgG <sub>2a</sub> <sup>b</sup>	5.7	Ms IgG <sub>3</sub> , κ	BD Biosciences
IgM <sup>a</sup>	DS-1	Ms IgG <sub>1</sub> , κ	BD Biosciences
IgM <sup>b</sup>	AF6-78	Ms IgG <sub>1</sub> , κ	BD Biosciences
Immunohistochemistry (IHC)	Clone	Antibody class	Company
CD4	RM4-5	Rat IgG <sub>2a</sub> , κ	BD Biosciences
CD45R/B220	RA3-6B2	Rat IgG <sub>2a</sub> , κ	BD Biosciences
DAPI	-	-	Invitrogen
MBP	-	Rat IgG <sub>2a</sub> , κ	Milipore
MOG (Z2)	-	Mouse IgG <sub>2a</sub>	Max Planck Institute of Neurobiology
PLP	Polyclonal	Rabbit IgG	Abcam
Enzyme-linked Immunospot assay (ELISPOT)	Clone	Antibody class	Company
IgG	-	Goat IgG <sub>γ</sub>	Southern Biotech

### 3.1.5 Primers

Primer name	Gene	Oligo sequence (5' -> 3')
mGAPDH sense #1	GAPDH	TCA CCA CCA TGG AGA AGG C
mGAPDH anti-sense #2	GAPDH	GCT AAG CAG TTG GTG GTG CA
mGAPDH probe #3	GAPDH	ATG CCC CCA TGT TTG TGA TGG GTG T
mCD19 sense #1	CD19	GGA AAA GGA AGC GAA TGA CTG A
mCD19 anti-sense #2	CD19	AGA GCA CAT TCC CGT ACT GGT T
mCD19 probe #3	CD19	CGC CAG GAG ATT CTT CAA AGT GAC GC
C3-Vβ4 sense #1	C3 Vβ4 TCR	TGA TGA CTC GGC CAC ATA CTT C
C3-Vβ4 anti-sense #2	C3 Vβ4 TCR	CCT GAG CCA AAA TAC AGC GTT T
C3-Vβ4 probe #3	C3 Vβ4 TCR	TGC CAG CAG CCA AGA ACG GAC AGA T
C3-Vα 8.3 sense #1	C3 Vα8.3 TCR	CCA CGC CAC TCT CCA TAA GAG
C3-Vα8.3 anti-sense #2	C3 Vα8.3 TCR	CAG TAG TAC AGG CCA GAG TCT GAC A
C3-Vα8.3 probe #3	C3 Vα8.3 TCR	AGC AGC TCC TTC CAT CTG CAG AAG TCC

### 3.1.6 Mouse license

Animals used during the studies of this dissertation were bred at the Max Planck Institutes of Biochemistry and Neurobiology animal facilities under specific pathogen free (SPF) conditions. The experimental procedures were approved by the local authorities.

## 3.2 Methods

### 3.2.1 EAE induction:

Mice were injected subcutaneously (s.c) at the back with 200 µl of recombinant MOG (200 µg), which was emulsified in Freund's adjuvant supplemented with 3 mg/ml *Mycobacterium tuberculosis* (strain H37Ra). 200 ng of pertussis toxin was injected intraperitoneal (i.p) on days 0 and 2 after immunization. Clinical scoring of classical paralytic EAE was performed as follows: score 0, healthy; 1, flaccid tail; 1.5, flaccid tail and impaired righting reflex; 2, impaired righting reflex and hind limb weakness; 2.5, one hind leg paralyzed; 3, both hind legs paralyzed with residual mobility in both legs; 3.5, both hind legs completely paralyzed; 4, both hind legs completely paralyzed and beginning front limb paralysis; and 5, moribund or death of the animal after preceding clinical disease.

### 3.2.2 Alum immunization:

Mice were injected with 100 µg of rMOG/OVA i.p 200 µl per mouse. Protein is precipitated (rOVA and rMOG) in 10% alum  $KAl(SO_4)_2$  (Sigma) with 5 N NaOH (Merck). The precipitated protein solution and the alum 1:1 were calibrated to a pH of 6.5-7.5 with NaOH (Merck). Then, the precipitated protein was incubated on ice for 30 minutes, washed 2 times with PBS and resuspended in PBS for i.p injection.

### 3.2.3 Intracardiac perfusion:

In anesthetized mice, the thoracic cavity was opened and a butterfly needle was inserted into the left ventricle of the heart. After incising the right atrium, mice were slowly perfused with 20 ml of PBS then another 20 ml of 4% PFA in PBS for later dissection and histological analysis.

### 3.2.4 Intrathecal injection:

Mice were anesthetized by intraperitoneal injection of ketamine (10 mg/kg of body weight; Imalgene 500; Rhône-Merieux, Lyon, France) and xylazine (1 mg/kg of body weight; Rompun; Bayer). Mouse was fitted into a stereotaxic apparatus, between 10-40 µl of 20 µg of mMOG or mMOG-FITC were slowly injected into the CSF through a 30-gauge needle and a Hamilton syringe inserted in the bregma point of the mouse skull. Full recovery of treated mice and FACS analysis of presence or absence of lymphocytes infiltration to the CNS confirmed appropriate access to the intrathecal space and the success of the procedure.



**3.2.5 Leukocyte isolation from peripheral blood:**

Two to five droplets of blood were collected from anesthetized mice by retro-orbital bleeding into 100 µl of 200 U/ml heparin (Sigma-Aldrich) in PBS. Erythrocytes were lysed by incubation in 1 ml erythrocytes lysing buffer; leukocytes were then centrifuged at 500 relative centrifugal force (rcf) for 5 minutes, washed with 1 ml erythrocytes lysing buffer, and finally resuspended in 200 µl in FACS buffer.

**3.2.6 Lymphocyte preparation from isolated organs:**

Mice were sacrificed and lymphoid organs were collected. Single cell suspensions were obtained by dissociating tissues through 40 µm cell strainers (BD Biosciences). Cells were centrifuged at 500 rcf for 10 minutes at 4°C and resuspended in complemented RPMI for culturing or further downstream analyses. For spleen or bone marrow preparations, an additional erythrocyte lysing step was performed by incubating the cell suspension in 0.83% NH<sub>4</sub>Cl for 3 minutes at room temperature (RT) and washed with RPMI medium.

**3.2.7 Cultivation of cell lines:**

Cell lines or primary cells were cultivated in fully complemented RPMI or DMEM medium in standard cell culture-treated plastic dishes (BD; Nunc, Denmark; Corning) in a humidified incubator (Heraeus) at 37°C and, 5% or 10% CO<sub>2</sub>, respectively. Cells growing in suspension were harvested by resuspending the culture; semi-adherent cells were flushed off the culture dish surface; and adherent cells were first briefly rinsed with PBS and then trypsinized with Trypsin-EDTA (PAA Laboratories) for 3 to 5 minutes at 37°C. Cell densities were regularly determined using a Neubauer hemocytometer (Neubauer). Cultures were kept subconfluent by regular dilution with fresh medium at ratios from 1:2 to 1:10. Cells were pelleted by centrifugation at 250 rcf for 10 minutes at 4°C and resuspended in complemented RPMI for culturing or further downstream analyses.

**3.2.8 Whole organ culture:**

Splenocytes and lymph nodes from mice were dissected and cultivated in fully complemented DMEM medium in standard cell culture-treated plastic dishes (BD; Nunc, Denmark; Corning). These were manually fitted with filters at the bottom of each well (Millipore) in a humidified incubator (Heraeus) at 37°C and 10% CO<sub>2</sub>.

**3.2.9 Isolation of CNS mononuclear cells:**

Mouse brain was dissected out and the entire spinal cord was flushed out with a syringe from the animal and pressed through nylon mesh into RPMI medium (without serum). After centrifugation for 10 minutes at 500 rcf, it was suspended in 5 ml of RPMI and mixed with 2.16 ml of isotonic percoll solution (Amersham Biosciences). The cell suspension was overlaid on 5 ml percoll and centrifuged 1200 rcf for 20 minutes at 20°C. The interface containing the mononuclear cells were collected and washed once with RPMI.

**3.2.10 Fluorescence-activated cell sorting (FACS):**

Cells to be analyzed were transferred into 96-well V-bottom plates and centrifuged at 500 rcf for 10 minutes at 4°C. Cells were washed in 200 µl FACS buffer twice, resuspended in 50 µl FACS buffer containing FC blocker (eBioscience) incubated for 10 minutes and washed with FACS buffer. For surface staining, cells were incubated with directly labeled surface marker-binding antibodies at appropriate dilutions, for 20 minutes at 4°C. After surface staining, cells were suspended in PFA/saponin buffer for 10 minutes in the dark, washed twice with saponin buffer after which fluoro-chrome-labeled antibodies were added and incubated for another 30 minutes. In some samples, viability dyes or TO-PRO-3 were included (eGFP-PLP samples). Biotinylated antibodies were visualized by streptavidin-APC (BD Pharmingen). After washing and resuspension in 100 µl FACS buffer, samples were acquired on a FACS Calibur or FACS Canto or Aria (all FACS machines from BD), and analyzed using FlowJo 7.6 software (TreeStar).

**3.2.11 Serum collection:**

Mice were bled by retro-orbital puncture, and the samples were allowed to clot overnight at 4°C. Serum was collected after centrifugation at 400 rcf for 10 minutes at 4°C and stored at -20°C until further analyses.

**3.2.12 Enzyme linked immunosorbent (ELISA) assay:**

ELISA plates (Nunc) were coated with rMOG (10 µg/ml in PBS), overnight at 4°C. Plates were washed with washing buffer and blocked with assay diluent for 1 hour. They were then washed and incubated with 100 µl of sample at RT for 2 hours. Plates were then washed, and 100 µl of the respective biotinylated secondary antibodies diluted in assay diluent was added and incubated for another 1 hour. After extensive washing, streptavidin-HRP (1:2000) was added and incubated at RT for 30 minutes. After washing, 100 µl of ABTS (2, 2'-Azino-bis-3-ethyl-benzthiazoline-6-sulphonic acid; Sigma) activated with H<sub>2</sub>O<sub>2</sub> was added and absorbance was

measured at 405 nm in an ELISA reader (Victor2™ 1420 Multilabel counter; Perkin Elmer life sciences).

### **3.2.13 Enzyme linked immunospot (ELISPOT) assay:**

Multiscreen HTS filter plates (Millipore) pre-wetted with 15 µl EtOH (35% in PBS) for 1 minute were coated with 50 µl of 20 µg of rMOG in PBS and incubated overnight at 4°C. The next day the plates were blocked with 200 µl of 10% FCS in complete RPMI for 2 hours at 37°C. Total splenocytes or lymph nodes cells were resuspended (10<sup>6</sup>/ml) in complete 10% FCS RPMI medium, seeded in the plates and incubated for 2 hours at 37°C in cell culture incubator (5% CO<sub>2</sub> and 95% H<sub>2</sub>O). After washing the plates, 100 µl of biotinylated antibody diluted in 1% Tween 20 in PBS were added and plates were incubated for 2 hours at 37°C. After which plates were decanted and washed carefully with running water. Plates were treated with 50 µl streptavidin (eBioscience), incubated for 20 minutes and were developed with 25 µl BCIP/NBT (BIOZOL). The reaction was then stopped by running water and spots were counted by an ELISPOT reader (Carl Zeiss).

### **3.2.14 Fluorescence microscopy:**

**Tissue sections:** Organs from PFA perfused mice were fixed in 4% PFA in PBS for 1 hour, and then immersed in 30% sucrose, overnight. Tissues were embedded in tissue-tek O.C.T. compound (Sakura), and 10 µm sections were cut on a CM3050 S Cryocutter (Leica).

**Fluorescence immunohistochemistry:** Tissue sections were fixed in cold acetone for 5 minutes, and blocked with 4% BSA in PBS for 2 hours at RT. Incubation with primary antibody (rat monoclonal, 1:200-400) was done in 4% BSA in PBS for 2 hours or overnight at 4°C. Incubation with fluorescently-labeled secondary antibody (anti-rat IgG goat polyclonal, 1:2000, Invitrogen) was done in 4% BSA in PBS for 2 hours at RT. Cell nuclei were stained with DAPI (Invitrogen) in PBS for 5 minutes at RT, before sections were eventually rinsed with PBS and embedded in anti-fading mounting medium (Sigma-Aldrich). Images were acquired on an inverted SP2 confocal microscope (Leica) or an inverted AxioVert 200 M microscope (Carl Zeiss).

**Image analysis:** Time-lapse images were acquired using Leica LCS software (Leica, Wetzlar), and subsequently processed and analyzed by ImageJ (NIH, Bethesda, MD, USA).

**3.2.15 Hybridoma generation:**

Splenocytes from the RR mice were cultured in unstimulated condition and stimulated condition with 20 µg/ml LPS (*E. coli* serotype O111:B4) *in vitro*. After 3 days, cells were washed extensively to remove the serum. The hybridoma fusion partner cell line, Sp2/0 growing in exponential phase, was also harvested and washed. Splenocytes were mixed with Sp2/0 cells (5:1), and 0.5 ml of 50% polyethylene glycol was added slowly while mixing gently. Cells were kept at 37°C for 1 minutes, diluted with serum-free media, centrifuged and plated in 96-well plates at  $1-2 \times 10^6$  cells/ml in Hybrimax® HAT (Sigma) containing DMEM/20% FCS. Seven days later medium was replaced with Hybrimax® HT (Sigma) containing DMEM/20% FCS and growing clones were expanded in DMEM/10% FCS. Sub-cloning was done manually by serial dilution.

**3.2.16 Antibodies purification from blood serum:**

Diluted serum from mice were filtered and applied to the Hitrap® protein G column (Amersham Biosciences). These were washed extensively with binding buffer to remove non-binding proteins. Antibodies were eluted from the column with the elution buffer and immediately neutralized with the neutralization buffer. The antibodies-containing fractions (measured by OD 280) were pooled and dialyzed against PBS, overnight.

**3.2.17 Purification of anti-MOG antibodies:**

HiTrap chelating HP column was prepared by loading it with 1% NiCl<sub>2</sub> from which excess nickel was removed by washing with H<sub>2</sub>O. Histidine-tagged rOVA protein in low salt binding buffer was loaded to the column and washed extensively. Then, protein G purified antibody from mice serum was passed through the column. The flow-through was collected and passed through another nickel-loaded HiTrap chelating HP column conjugated to mMOG or rMOG. MOG-specific antibodies were eluted with 4 M MgCl<sub>2</sub>. The antibodies-containing fractions (measured by OD 280) were pooled and dialyzed against PBS, overnight.

**3.2.18 Antibodies purification from CNS:**

Frozen brain and spinal cord were thawed and extensively washed with PBS. It was then mashed by pressing it into 100 µm nylon strainers (BD). CNS was homogenized in ice-cold homogenizing buffer using a glass Dounce apparatus (0.1 g of tissue per milliliter of buffer). Insoluble material was removed by centrifugation at 20,000 rcf for 20 minutes (SS-34 rotor: 129,000 rpm at 4°C). The pellet was re-homogenized and centrifuged two additional times. The

supernatants were pooled and clarified by centrifugation at 60,000 rcf (SW-28 rotor: 18257.52 rpm) for 60 minutes (O'Connor et al., 2005). The clarified supernatant was loaded onto a column containing 5 ml of streptavidin agarose conjugated beads (Milipore, Cat 16-126) to remove impurities. The collected flow through, was passed through Protein G (protein G sepharose, CAT 17-0618-01) and the purity of the isolated IgG was assessed by running a SDS-PAGE gel under reducing conditions.

### **3.2.19 Deglycosylation of purified anti-MOG antibody:**

Homogeneity of purified anti-MOG antibodies on IEF gels was increased by heating samples to 95°C for 1 minutes, and incubated for 3 hours at 37°C in the presence of 1 % MEGA-10 (w/v) at pH 7.2 with 100 U/ml N-Glycosidase F recombinant (Roche). The samples were then dialyzed in a D-tube Dialyzer Mini MWCO 12-14 kDa (Novagen) against 6 M urea, for 2 hours using a magnetic stirrer at RT, and then for 15 minutes at 50 V in a flatbed gel electrophoresis chamber to remove residual SDS.

### **3.2.20 Two dimensional (2D) gels:**

**Isoelectric focusing (IEF) first dimension (separation according to charge):** IPG rehydration buffer was added to the eluted samples and loaded onto rehydrated 24 cm Immobiline DryStrip pH 3-10 gel (GE Healthcare). 3100 OFFGEL Fractionator (Agilent) in the in-gel mode was used according to the manufacturer's recommendations, but with two essential exceptions. First, instead of rehydrating the IEF strips together with the eluted samples, the loading cup (8 x 2 mm, conical) was placed onto the rehydrated strip at pH 4.5. Second, the default focusing method was set to a slower voltage-increase and extended duration as follows: for the first 30 minutes the voltage was limited to 500 V and then for 30 minutes to 1000 V. During electrophoresis the maximum values were 8000 V, 50  $\mu$ A and 200 mW until 120 kVh were reached. The IEF strips were then equilibrated for 20 minutes on a slow shaker in equilibration buffer.

**SDS-polyacrylamide gel second dimension (separation by size):** IPG strips, after completion of IEF, were left at RT in equilibration buffer. To fit into the 2D Novex pre-casted gel (Invitrogen), the IPG strips were cut 2 cm shorter from the anode and 1 cm from the cathode and, briefly immersed in 1x ELPHO buffer. An agarose solution was poured and left to be polymerized for 15 minutes. Electrophoresis was then performed in ELPHO running buffer in a mighty small gel chamber (Hoefer) for 4 hours at 10 mA.

**SDS-PAGE:** Separation of proteins was achieved by denaturing, discontinuous, SDS polyacrylamide gel electrophoresis, using precast Novex 4-12% tris-glycine gels (Invitrogen). Protein samples were boiled for 5 minutes at 100°C, before being loaded to each lane. Electrophoresis was performed in running buffer at 100 V for stacking, and at 130 V for resolving of proteins in a mighty small gel chamber (Hoefer). Gels were stained with Coomassie brilliant blue G-250 (Bio-Rad) in order to verify appropriate sample loading.

### **3.2.21 Native gel:**

Protein was separated on a 10% polyacrylamide (19 acrylamide: 1 bis-acrylamide) gel in non-denaturing conditions. Buffers used are similar to those describe for SDS-PAGE except for the removal of SDS and  $\beta$ -mercaptoethanol.

### **3.2.22 F(ab)<sub>2</sub> fragmentation:**

F(ab)<sub>2</sub> fragmentation of Z2 antibody was performed according to manufacturer's protocol (Pierce protein biology products, Thermo scientific) and the products were electrophoresed under non-reducing conditions.

### **3.2.23 RNA techniques**

**RNA extraction:** Total RNA was isolated from purified cells or whole tissue by TRI Reagent (Sigma-Aldrich) following the instructions provided by the manufacturer.

**Reverse transcription:** cDNA was generated from RNA using SuperScript II Reverse Transcriptase (Invitrogen) or the Verso cDNA Kit (Thermo Fisher Scientific), according to the manufacturer's instructions.

**Quantitative PCR:** Real-time qPCR was performed using the Absolute qPCR Mixes (Thermo Fisher Scientific) according to the instructions of the manufacturer. Samples were then amplified using a 7900HT Fast Real-Time PCR System (Applied Biosystems) and analyzed by SDS 2.3 software (Applied Biosystems).

### **3.2.24 Statistical analysis**

Linear regression and unpaired *t* tests analysis were performed using Graphpad software (Graphpad, La Jolla, CA).

## CHAPTER 4: RESULTS

## 4. Results

### 4.1 MOG-binding B cells in RR mice

#### 4.1.1 mMOG<sub>tet</sub>: A tool to detect MOG-binding B cells

Each B cell expresses one B cell receptor (BCR) with a single antigen binding specificity. While, the immune system can react to a vast number of antigens, only few thousands of B cells express receptors that are specific for any given antigen. Therefore, the experimental identification of antigen-specific B cells was a challenging task, due to the low frequency of cells with specific receptors for any particular antigen, which is usually less than 1% (Scheid et al., 2009). Antigen-specific B cells can be detected using fluorescently labeled antigen(s), and to boost the avidity of antigen of interest, antigens tetramerization was routinely used.

To detect MOG-binding B cells in RR mice, the extracellular portion of mouse MOG peptide (MOG<sub>1-125</sub>) was expressed and multimerized (Figure 4.1A). Mouse MOG<sub>1-125</sub> was expressed in human embryonic kidney cells (HEK) transformed with EBNA-1 gene cell line. HEK-EBNA-1 is a mammalian eukaryotic protein expression system that has multiple advantages over prokaryotic systems. The most relevant advantage is those only correctly folded proteins are secreted, namely proteins, which retain their sulfide-sulfide bonds and their correct glycosylation pattern (Figure 4.1C). Purified MOG<sub>1-125</sub> peptides from HEK cells were biotinylated with BirA ligase in order to multimerize them to form tetramers. Tetramerization was achieved based on the ability of streptavidin (SA) to spontaneously assemble stable tetramer-structures composed of four MOG<sub>1-125</sub> peptide monomers (mMOG<sub>tet</sub>) (Figure 4.1D). Additionally, mammalian chicken ovalbumin protein (mOVA) was also prepared in a similar fashion as a control. The construct of both mMOG<sub>tet</sub> and mOVA<sub>tet</sub> contain Igk signal peptides to guide the proteins to the secretory pathway outside of the cell. The synthetic proteins were also biotin tagged for tetramerization purposes and histidine tagged to separate them from other cellular proteins (Figure 4.1A).

Mammalian cell produced mouse MOG tetramers (mMOG<sub>tet</sub>) differ from rat recombinant MOG (rMOG) in many aspects as listed in the table in Figure 4.1C. For example, despite the high homology between rat and mouse, a peptide of mouse- rather than rat- origin such as mMOG might increase binding affinity to MOG-binding B cells in mice. Secondly, and most important, is the preservation of the conformational structure that is only guaranteed by mMOG expressed in a eukaryotic system. Thirdly, the glycosylation pattern of secreted mMOG is preserved as seen by the slightly heavier molecular weight of mMOG monomers in the SDS-PAGE gel (Figure 4.1B). All this might increase the chance of detecting B cells in mice.



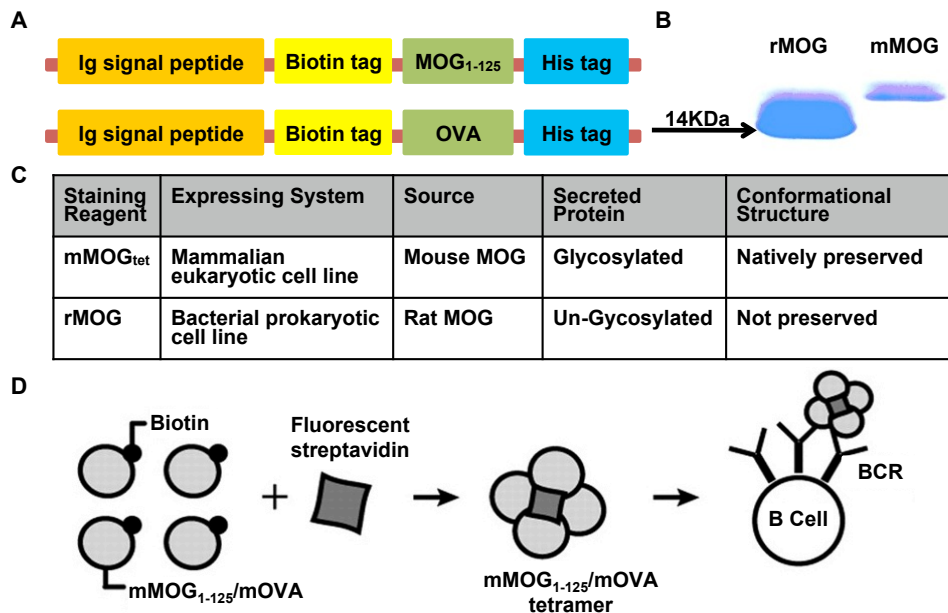


**Figure 4.1. Construction of mMOG tetramer (mMOG<sub>tet</sub>).** A) A schematic diagram of mMOG<sub>1-125</sub> peptide and mOVA protein constructs which consists of Igk signal peptide, biotin tag and histidine-tag. B) SDS-PAGE gel shows molecular weight of rMOG compared to mMOG monomer. C) A table shows major differences between rMOG and mMOG<sub>tet</sub>. D) A schematic diagram shows the principle of tetramerization.

In order to validate the efficiency of mMOG<sub>tet</sub> compared to rMOG in binding to MOG-specific B cells, mMOG<sub>tet</sub> specificity and sensitivity to MOG-binding B cells were evaluated in several experiments. First, the MOG-specific hybridoma cell line 8.18c5 that produces and secretes conformation-dependent anti-MOG monoclonal antibodies (mAb) was used to test the specificity of mMOG<sub>tet</sub> compared to monomeric rMOG. mMOG<sub>tet</sub> had a higher affinity to 8.18c5 hybridoma cell line than rMOG as seen by the shift of signals in the histogram of the mMOG<sub>tet</sub> stained 8.18c5 hybridoma cell line compared to rMOG stained 8.18c5 hybridoma cell line (Figure 4.2A). The staining of irrelevant hybridoma cell line such as the neurofilament light-specific BH-20 hybridoma cell line with either mMOG<sub>tet</sub> or rMOG remained at the background level (Figure 4.2A). Second, B cells in IgH<sup>MOG</sup> transgenic mice, which were engineered to express on its BCR the MOG-specific 8.18c5 immunoglobulin H chain, were used in sensitivity and specificity tests. rMOG bound to about half of MOG-binding B cells in IgH<sup>MOG</sup> mice while mMOG<sub>tet</sub> detected up to 80% of total B cells population in IgH<sup>MOG</sup> mice, presumably labeling even low affinity B cells (Figure 4.2C). A control staining with streptavidin-conjugated fluorochrome (Figure 4.2C) did not produce any staining in IgH<sup>MOG</sup> mice. Also, mMOG monomers captured more serum anti-MOG antibodies from IgH<sup>MOG</sup> compared to rMOG monomers in ELISA assay (Figure 4.2B).

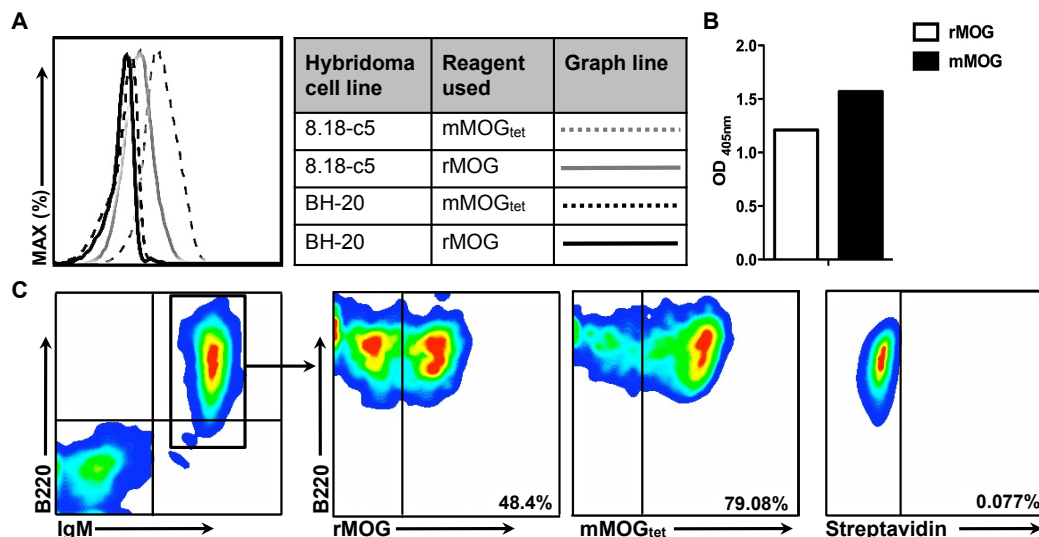


**Figure 4.2. mMOG<sub>tet</sub>: a tool to stain MOG-binding B cells.** A) Histogram shows mMOG<sub>tet</sub> staining compared to rMOG on anti-MOG 8.18c5 hybridoma cell line and a control neurofilament light BH-20 hybridoma cell line. B) ELISA assay shows that IgH<sup>MOG</sup> mice serum antibodies bound better to mMOG compared to rMOG monomers. C) Representative flow cytometric plots of B cells from IgH<sup>MOG</sup> mice stained with rMOG, mMOG<sub>tet</sub> and fluorescent streptavidin as a control. Data are representative of at least two independent experiments.

The specificity of mMOG<sub>tet</sub> was further tested in different experimental settings compared to its staining control tetramer mOVA<sub>tet</sub>. Aluminum hydroxide (alum) was used to precipitate protein of interest (MOG and OVA) and immunize mice to enhance the percentage of antigen-specific B cells. Upon rMOG-alum immunized SJL/J WT mice developed almost 1% of MOG-binding B cells which were detected by mMOG<sub>tet</sub> staining while, rOVA-alum immunized mice showed up to 3% OVA-binding B cells when stained with mOVA<sub>tet</sub> (Figure 4.3A). In addition, there were negligible amount of OVA-binding B cells detected in rMOG-alum immunized mice and vice versa (Figure 4.3A). These results confirmed that mMOG<sub>tet</sub> is a specific reagent that can detect low affinity MOG-binding B cells more efficiently than rMOG. Therefore, mMOG<sub>tet</sub> along with its control reagent mOVA<sub>tet</sub> were used in a sensitivity test. IgH<sup>MOG</sup> C57BL/6 splenocytes were mixed into SJL/J WT splenocytes at different ratios. Serially diluted IgH<sup>MOG</sup> B cells were detected via allotype specific antibody (IgM<sup>a</sup> for C57BL/6 cells) and mMOG<sub>tet</sub>. MOG-binding B cells were found in all dilutions with expected proportions (Figure 4.3B). Percentages of MOG-binding B cells were halved in each diluted sample compared to the previous sample, and it was able to detect MOG-binding B cell of frequency less than 0.2% (Figure 4.3B). These results confirmed that mMOG<sub>tet</sub> is a sensitive reagent that can detect even low affinity MOG-binding B cells compared to rMOG.

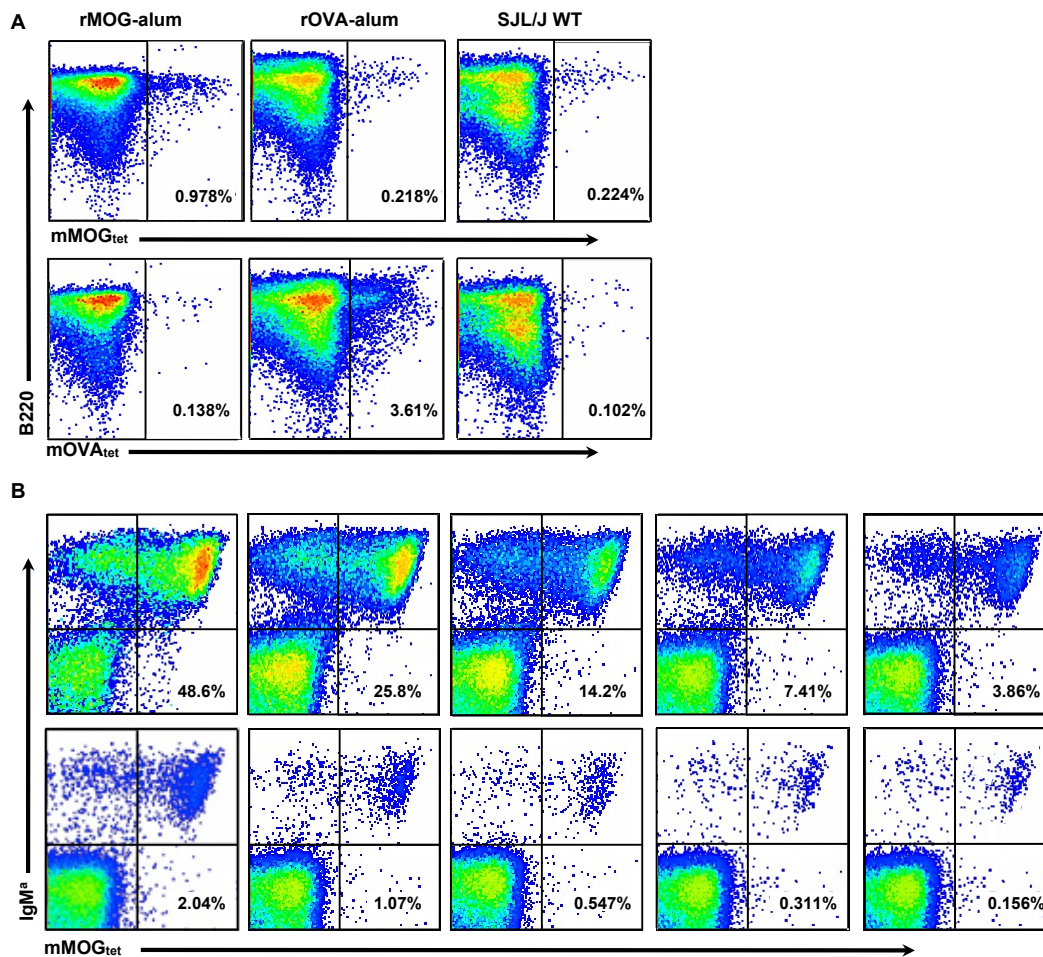


**Figure 4.3. Tetrameric antigens (MOG/OVA) staining were sensitive and specific.** A) Flow cytometric analysis shows MOG- and OVA-binding B cells in splenocytes from rMOG and rOVA alum immunized mice and SJL/J WT mice using mMOG<sub>tet</sub> and mOVA<sub>tet</sub> reagents. B) Flow cytometric analysis of mMOG<sub>tet</sub> binding to IgH<sup>MOG</sup> splenocytes mixed with C57BL6 WT splenocytes at various ratios. Data are representative of at least two independent experiments (n=2/group).

Therefore, mMOG<sub>tet</sub> along with its control reagent mOVA<sub>tet</sub> were used in subsequent experiments.

#### 4.1.2 MOG-binding B cells in lymphoid organs

mMOG<sub>tet</sub> was used to identify naturally recruited MOG-specific B cells in RR mice. MOG-binding B cells were detected within B cell population via mMOG<sub>tet</sub> in RR mice and they are distributed in all lymphoid compartments with different frequencies (Figure 4.4A). Healthy and sick RR mice have significantly more MOG-binding B cells compared to SJL/J WT mice. As anticipated, healthy RR mice have MOG-binding B cells that tend to accumulate in the CNS-draining cervical and lumbar lymph nodes compared to other lymphoid compartments such as axillary and inguinal lymph nodes (Figure 4.4A). Surprisingly, in severely sick RR-EAE mice MOG-

binding B cells are seen in comparable percentages in the CNS draining lymph nodes and the rest of lymphoid compartments, as well as, bone marrow (Figure 4.4A). ELIspot has also revealed that there are antibody-producing cells in RR mice, starting at age of 6 weeks (Figure 4.4B). Splenocytes and bone marrow cells from RR mice and their wild type counterparts at 3 and 6 weeks were cultured overnight without any stimulation, which resulted in the formation of IgG spot forming cells only in RR mice at age of 6 weeks (Figure 4.4B). Collectively, MOG-binding B cells tend to accumulate in CNS draining lymph nodes before the onset of disease and antibody-producing cells are found as early as 6 weeks of age in RR mice.

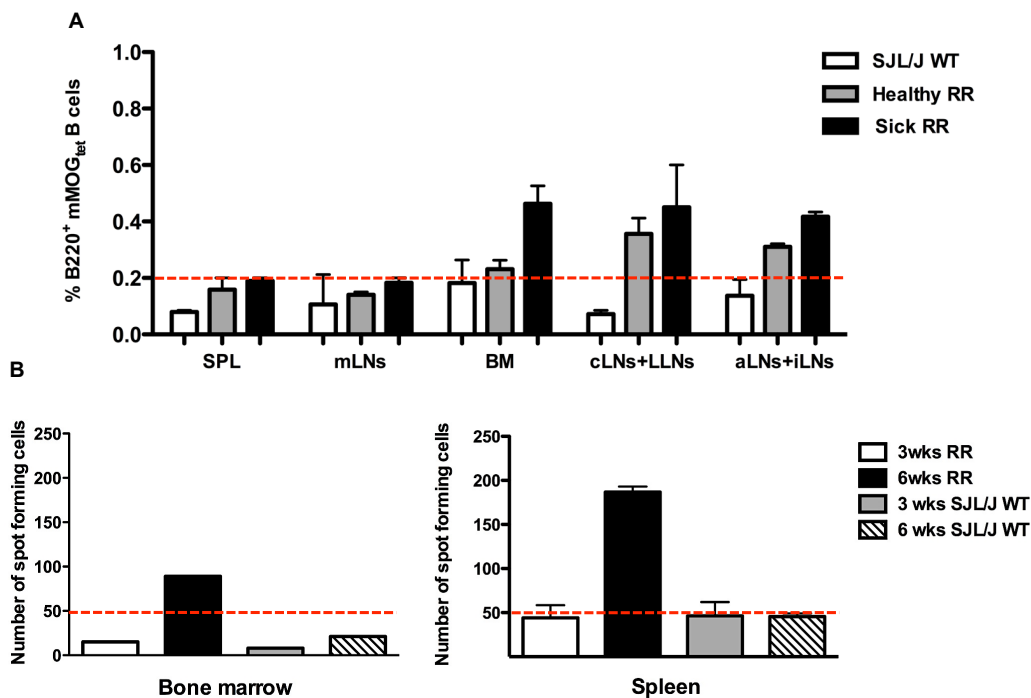


**Figure 4.4. MOG-binding B cells were found in all immune cell compartments in RR mice.** A) Percentage of MOG-binding B cells detected by mMOG<sub>tet</sub> reagent in the indicated immune cell compartments gated on B220<sup>+</sup> B cells (SPL: spleen, mLNs: mesenteric lymph nodes, BM: bone marrow, cLNs: cervical lymph nodes, LLNs: lumbar lymph nodes, aLNs: axillary lymph nodes, iLNs: inguinal lymph nodes). B) ELIspot shows IgG spot-forming cells in 3, 6 weeks old RR and SJL/J WT mice. Graphs are representative of at least two independent experiments (n=2-3/group).

Mature B cells when stimulated with their specific antigen; find their way to enter germinal center (GC) reaction. Germinal centers grant somatic hyper-mutation and isotype switching of B cells to increase their BCR specificity and production. In RR mice, the percentage of MOG-binding B cells in blood lymphocytes increased with disease severity, reaching a maximum of 0.8% of total B cell population (Figure 4.5A). At the same time, during the peak of the disease, the germinal center reaction of the cervical lymph was the highest compared to other lymphoid

organs (Figure 4.5B). Therefore, it was feasible to detect MOG-binding B cells in germinal center reactions of severely diseased RR mice in the CNS draining lymph nodes, that is cervical nodes that contain ~1% to 1.6% of MOG-binding B cells (Figure 4.5C). The specificity and functionality of this population were verified by 10 days *ex vivo* organ cultures assay. Cervical lymph nodes' supernatant contained the highest amount of anti-MOG antibodies compared to other lymphoid organs (Figure 4.5D) in RR mice.

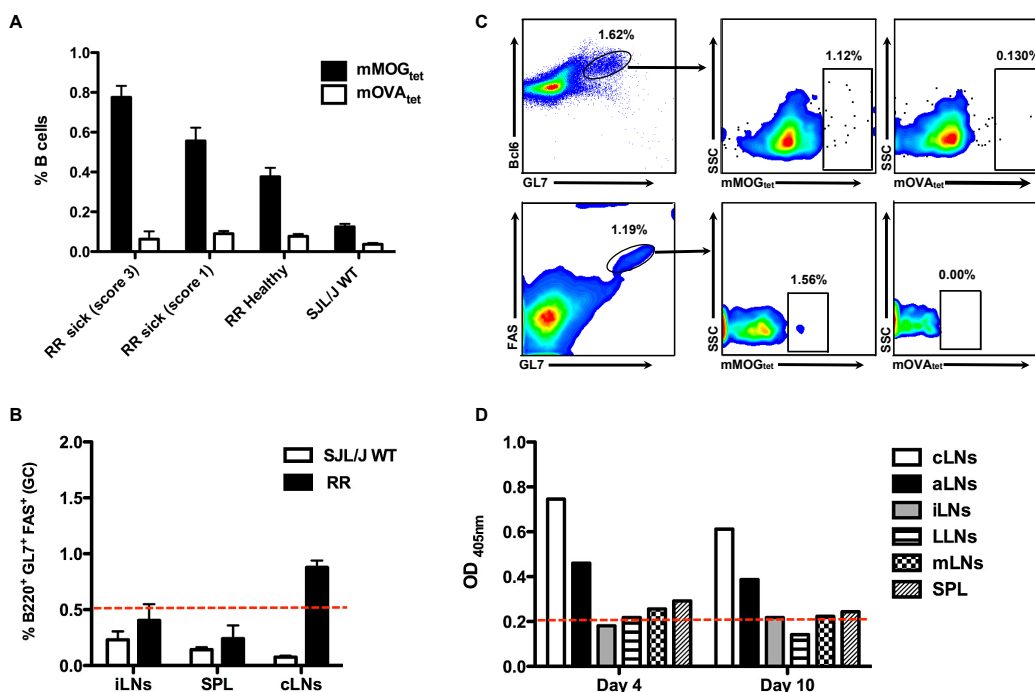


**Figure 4.5. MOG-binding B cells were detected in GC.** A) Frequency of MOG-binding B cells in the blood increased with disease severity. B) GC reaction in different lymphoid compartments of RR mice compared to SJL/J WT mice. C) Flow cytometric plots of cervical lymph nodes from sick RR mice with a score of 3 shows MOG-binding B cells detected in GC reactions seen by GL7, Bcl6 and Fas expression. D) IgG<sub>1</sub> MOG ELISA from supernatant of *ex vivo* organs' culture -at day 4 and day 10-shows MOG-specific GC reaction in spleen and lymph nodes (cLNs: cervical lymph nodes, aLNs: axillary lymph nodes, iLNs: inguinal lymph nodes, LLNs: lumbar lymph nodes, mLNs: mesenteric lymph nodes, SPL: spleen). Data are representative at least of two independent experiments (n=2-4/group).

Usually, germinal center B cells evolve to either plasma blasts or plasma cells. The plasma cell CD138 marker was increased in RR mice lymph nodes compared to SJL/J WT mice (Figure 4.6A). However, unexpectedly, plasma cells did not bind to MOG when stained with mMOG<sub>tet</sub> intracellularly (data not shown). Nevertheless, RR mice contained high percentages of IgG<sub>1</sub> positive cells in immune cell compartments -but not IgG<sub>2a/2b</sub>-compared to SJL/J WT mice (Figure 4.6B), and anti-MOG antibody-producing cells as defined by low expression of B220, and high

expression of isotyped switched Ig (IgG<sub>1</sub>). Thus, MOG-binding B220<sup>low</sup> IgG<sub>1</sub><sup>high</sup> cell population tends to accumulate in CNS draining lymph nodes in RR mice (Figure 4.6C).

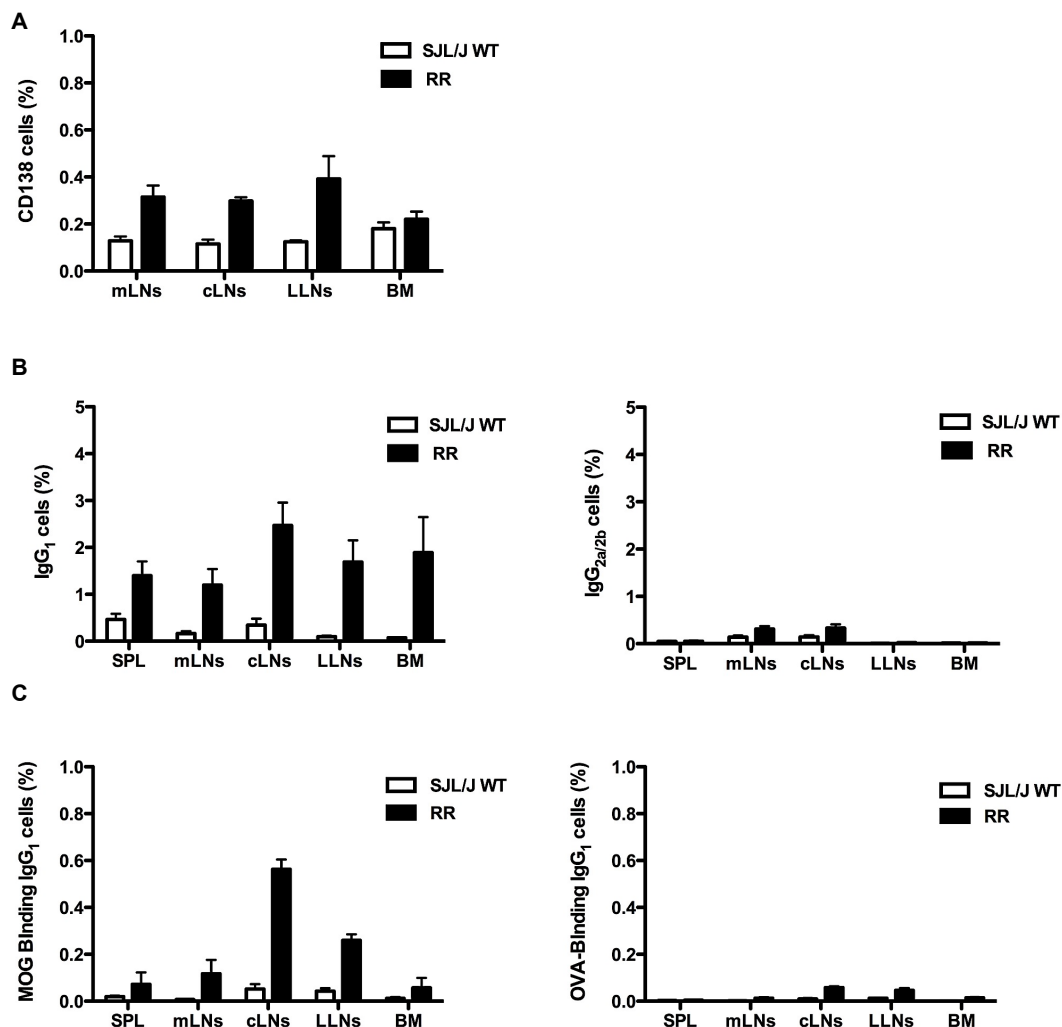


**Figure 4.6. MOG-binding IgG<sub>1</sub> cells.** A) Percentage of total plasma cells stained with anti-CD138 antibodies. B) Percentage of total isotype switched IgG<sub>1</sub> (left hand side) and IgG<sub>2a/2b</sub> (right hand side) B cells. C) Percentage of MOG (left hand side) and OVA (right hand side) IgG<sub>1</sub> binding B cells in RR and SJL/J WT mice. (SPL: spleen, mLNs: mesenteric lymph nodes, cLNs: cervical lymph nodes, LLNs: lumbar lymph nodes, BM: bone marrow). Data are representative of two independent experiments (n=3/group).

#### 4.1.3 MOG-binding B cells in the CNS

RR-EAE mice have higher numbers of CNS infiltrating lymphocytes than healthy or WT SJL/J mice (Figure 4.7A and section 4.3.2). The cell infiltrates contained T cells, B cells and CD11b<sup>+</sup> cells (Figure 4.16); with T cells being more numerous than B cells (Figure 4.7B, 4.17, 4.19). Some reports have documented B cell follicles within the CNS, displayed germinal center-like reactions (Magliozzi et al., 2007, Mitsdoerffer et al., 2010), but there were none found in RR

mice (data not shown). Although, B cell infiltrates were seen in both healthy and sick RR mice, isotype switched B cells were noted mainly in the CNS of sick RR mice and had only anti-MOG IgG<sub>1</sub> isotype but not IgG<sub>2a/2b</sub> isotype (Figure 4.7C). Furthermore, amongst those infiltrating cells, there were negligible amount of plasma cells expressing CD138 detected by flow cytometric analysis (Figure 4.7C). Nevertheless, infiltrating CNS cells of sick mice showed a high production of anti-MOG IgG<sub>1</sub> antibodies in culture, indicating that infiltrating B cells in the CNS are mature MOG-binding and isotyped switched antibody-producing cells (Figure 4.7D).

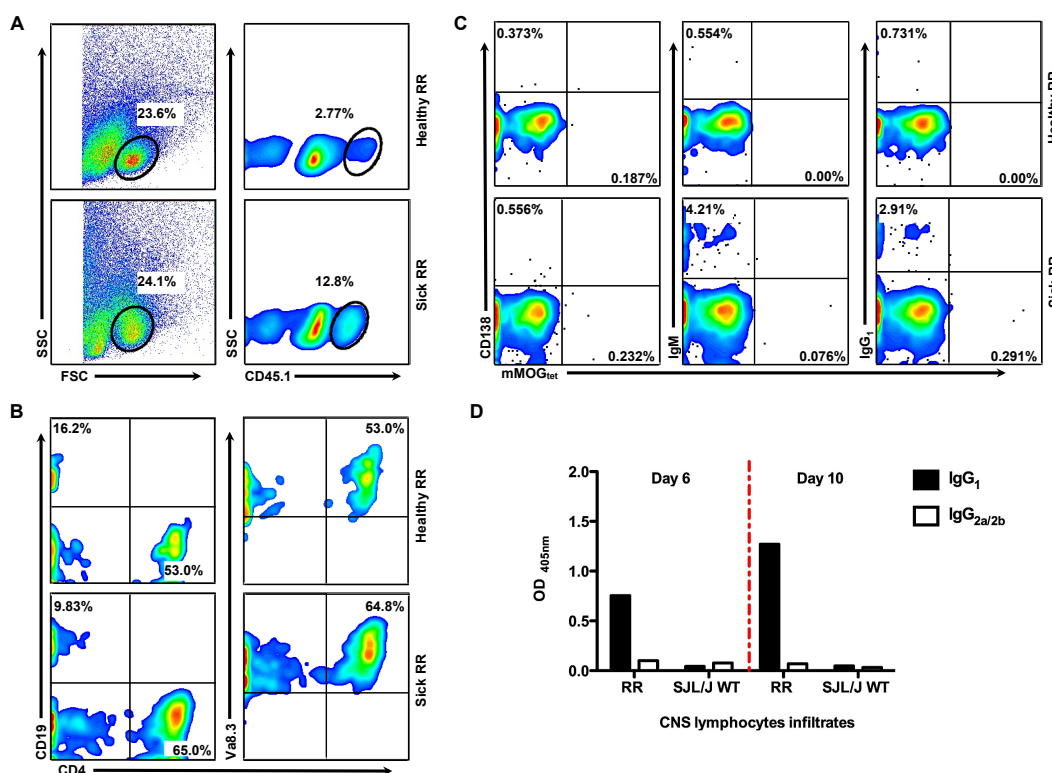


**Figure 4.7. RR mice harbored Ig expressing B cells in the CNS.** A) FACS plots showed gating protocol of infiltrating lymphocytes to the CNS. Lymphocyte population was gated from forward and side scatter plot, and infiltrating lymphocytes were distinguished from resident cells via high expression of CD45. B) Percentage of T and B cells in the CNS of RR mice. C) Percentage of CD138<sup>+</sup>, IgM<sup>+</sup> and IgG<sub>1</sub><sup>+</sup> cells in the CNS of RR mice. D) MOG ELISA assay of CNS derived lymphocytes' supernatant from RR and SJL/J WT mice cultured for 10 days. Flow cytometric plots are representative of three independent experiments (n=2/group). ELISA assay is representative of two independent experiments (n=2/group).

#### 4.1.4 Anti-MOG antibodies purification in RR mice

As stated previously, mMOG monomers bound better to anti-MOG antibodies than to rMOG monomers, which allowed the use of reagent for anti-MOG antibodies clonality studies. Direct purification of anti-MOG antibodies from RR serum by passing antibodies through mMOG columns led to the loss of anti-MOG antibodies, which was largely of IgG<sub>1</sub> isotype (Figure 4.8A).

This loss might be due to poor elution of high affinity anti-MOG antibodies or to loss in the flow through of the column (that contains serum anti-MOG antibodies) due to impurities of serum proteins. The loss of purified antibodies was solved by the introduction of protein G column to isolate all antibodies from other serum proteins (Figure 4.8A), which resulted in purified antibodies uncontaminated by other serum proteins as seen in SDS-PAGE gel (Figure 4.8C). However, despite the fact that protein G had recovered a high proportion of pure anti-MOG antibodies from RR crude serum, there was still some loss of anti-MOG antibodies (both IgG<sub>1</sub> and IgG<sub>2a</sub>) seen by the low OD values from purified anti-MOG antibodies compared to pooled serum before antibody purification in the MOG ELISA assay (Figure 4.8B).

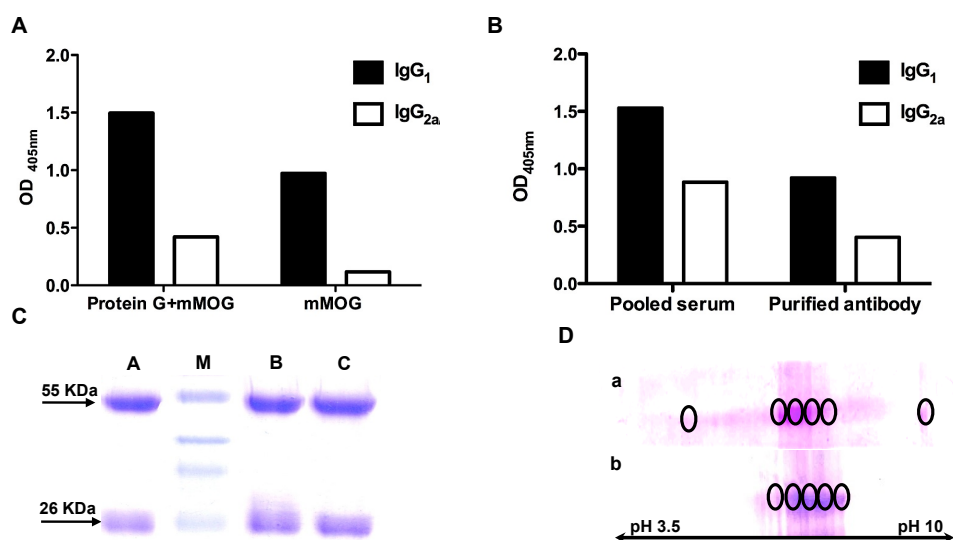


**Figure 4.8. Purification of serum anti-MOG antibodies.** A) MOG ELISA shows that the purification of anti-MOG antibodies (IgG<sub>1</sub>, IgG<sub>2a</sub>) from RR mice directly through mMOG-conjugated column resulted in the loss of antibodies and was improved by enriching antibodies via protein G column. B) MOG ELISA assay of pooled serum anti-MOG antibodies from RR mice before and after purification. C) SDS-PAGE of purified serum antibodies from RR mice and rMOG-alum immunized mice (A: Protein G purified antibodies; B: purified antibodies from rMOG-alum immunized mice; C: purified antibodies from RR mice; M: molecular weight marker). D) 2D-gel shows anti-MOG antibodies from (a) RR mice and (b) rMOG-alum immunized mice, number of circles indicate the number of antibody clones. Data are representative of two independent experiments.

In order to find out how endogenously recruited B cell clonality will differ from induced humoral immunity, SJL/J WT mice were immunized with rMOG-alum and their serum was collected. rMOG-alum anti-MOG antibodies were purified, and these purified antibodies from RR mice and rMOG-alum immunized mice were separated on two-dimensional (2D) gels (Figure 4.8D).

The 2D gels revealed strikingly increased antibody heterogeneity in RR mice than in rMOG-alum immunized mice. Further experiments required to reduce antibody heterogeneity in RR



mice including de-glycosylation of purified antibodies, reduction in the number of mice to only one mouse and introduction of irrelevant intermediate protein (rOVA) to remove a polyclonal population, if there was any. However, firstly, the de-glycosylation step did not reduce much of anti-MOG heterogeneity from pooled RR mice's serum (data not shown). Secondly, 2D gel was impossible to be performed due to the low amount of serum anti-MOG antibodies from a single RR mouse. However, purification of MOG-antibodies from RR-EAE (Figure 4.9A) and healthy mice (Figure 4.9B) had showed that healthy mice might have more free circulating and higher affinity anti-MOG antibodies in their serum compared to sick mice.

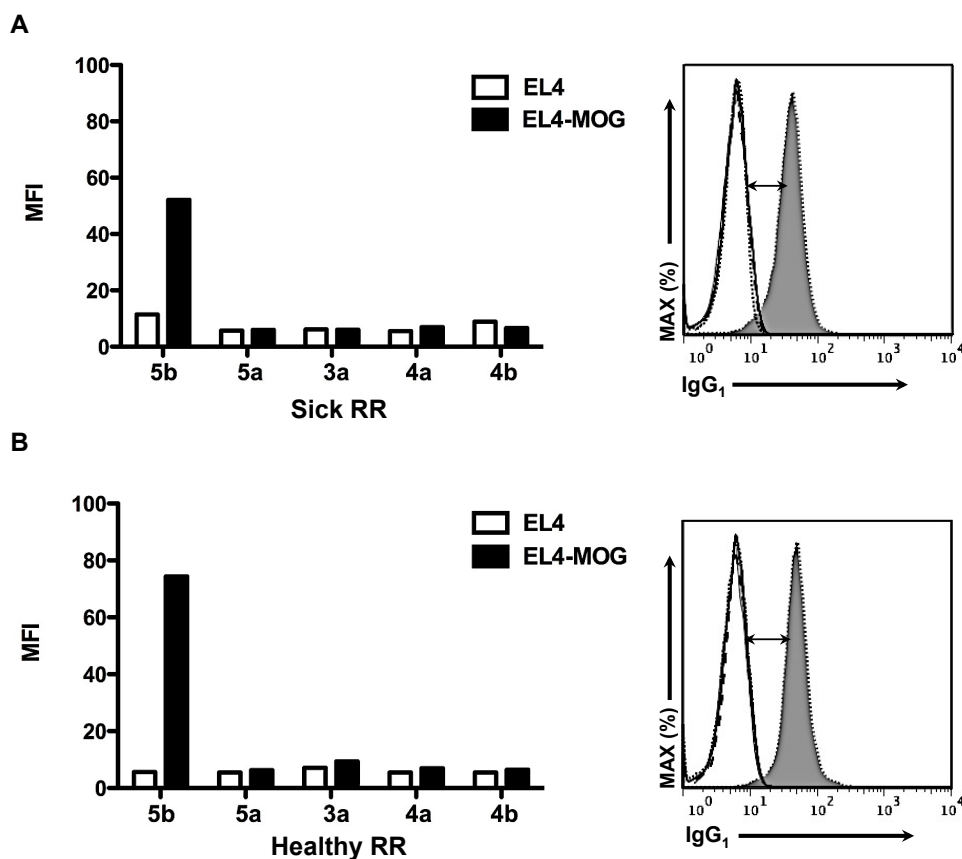


**Figure 4.9. Purification of anti-MOG antibodies from a single mouse.** Mean fluorescence intensity (MFI) and histogram presentation of purified and concentrated anti-mMOG/rMOG antibodies from serum of RR mice (see Appendix 6.1 for detailed protocol 5b: eluted antibodies from mMOG conjugated column, 5a: flow through of mMOG/rMOG conjugated column, 3a: flow through of protein G column, 4a: flow through of irrelevant protein (rOVA), 4b: rOVA eluted antibodies). Graphs showed low levels of free anti-MOG antibodies from (A) sick mouse IgG<sub>1</sub> with lower affinity as seen on the histogram compared to (B) healthy mouse serum. (EL4-MOG cells: dotted gray line and shadowed; EL4 cells: dotted black line; detection antibody only: dashed line; serum without detection antibody: black line). Data are representative of two independent experiments (n=2-3/group).

Therefore, antibodies deposited to CNS were purified. Brain and spinal cord were collected from 22 RR-EAE mice with at least 1.5 of EAE severity scores, which had both anti-MOG IgG<sub>1</sub> and IgG<sub>2a/2b</sub> isotypes in their serum as confirmed by MOG ELISA assay (Figure 4.10A). The purified concentrated antibodies from CNS were visualized by SDS-PAGE gel and detected by silver staining. The gels showed pure and uncontaminated preparations of the RR-EAE CNS purified antibodies (Figure 4.10B). Figure 4.10 C and D prove that recovered antibodies were anti-MOG IgG<sub>1</sub> antibodies when used to detect MOG protein by ELISA assay and antigen cell-bound assay on EL4-MOG cells. Despite those diseased mice had both IgG<sub>1</sub> and IgG<sub>2a/2b</sub> antibodies in serum; only supposedly pathogenic IgG<sub>1</sub> antibodies were recovered from CNS (Figure 4.10D).

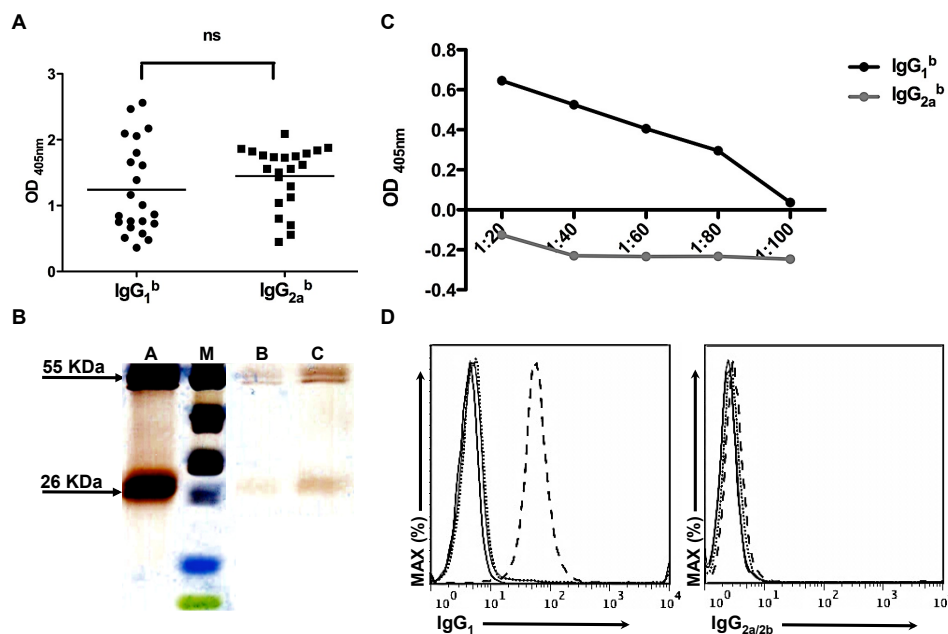


**Figure 4.10. Isolation of MOG-specific antibodies from target tissue in RR mice.** A) MOG ELISA assay of 22 RR mice's serum showed that both anti-MOG Ig isotypes were detected (ns: non- statistically significant i.e. p-value >0.05). B) Silver staining of SDS-PAGE gel shows the heavy chains and light chains of tested antibodies and CNS purified antibodies (A: 8.18c5 positive control antibody; B: 1  $\mu$ g and C: 10  $\mu$ g of CNS purified antibodies; M: molecular weight marker). C) MOG ELISA assay shows that the purified antibodies were functional and detected MOG. D) Isolated IgG<sub>1</sub> antibodies were MOG-specific and bond to conformational MOG expressed on EL4-MOG cells (EL4-MOG cells: dashed line, EL4 cells: black line, detection antibody only: dotted line, serum without detection antibody: gray line). Data are representative of two independent experiments.

The limitation of the antibody quantity isolated from CNS and serum of a single mouse made it difficult to study the clonotypes of B cells in RR mice. Therefore, we decided to generate hybridomas to overcome the quantity problem. Unstimulated splenocytes from RR mice were fused with SP2/0 myeloma cell line. To test the specificity of grown hybridomas, supernatants

were assayed against rMOG and rOVA as irrelevant antigens by ELISA assay. Although the generated hybridomas were still polyclonal, they all were specific to MOG (Figure 4.11B). Moreover, hybridoma produced antibodies were tested for their ability to bind to conformational MOG epitopes expressed by MOG-transfected EL4 cells (Figure 4.11A). Most anti-MOG hybridoma antibodies were of the IgG<sub>1</sub> rather the IgG<sub>2a/2b</sub> isotype as seen in the MOG ELISA assay (Figure 4.11B, and data not shown). However, the mean fluorescence intensity (MFI) of anti-MOG antibodies indicated a binding affinity lower than of the standard anti-MOG monoclonal 8.18c5 (Figure 4.11A), but comparable to antibodies purified from serum and CNS of RR mice (Figure 4.10).

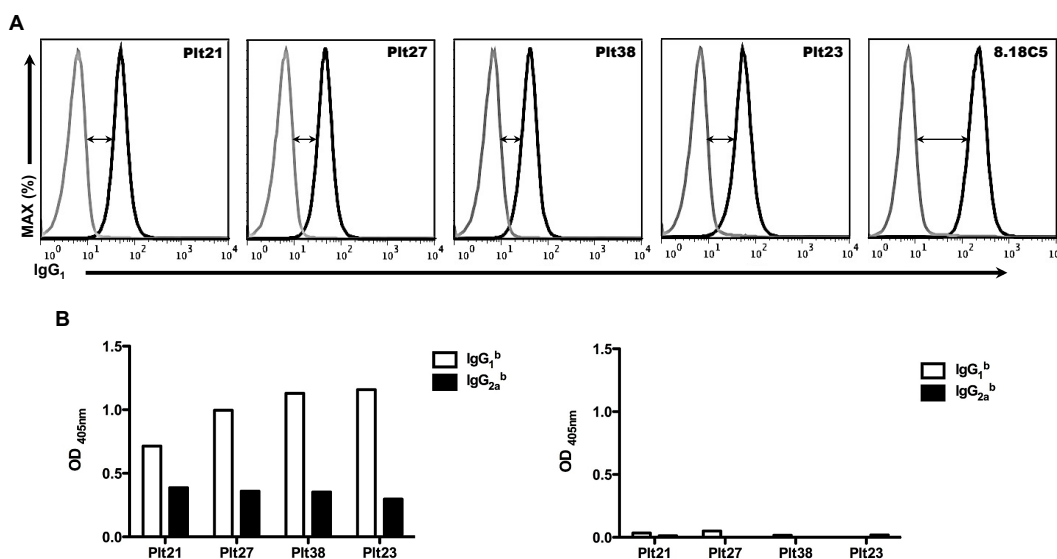


**Figure 4.11. Generation of RR splenocytes hybridomas.** A) Mean fluorescence intensity (MFI) of antibodies purified from hybridomas via protein G columns compared to 8.18c5 (EL4-MOG: black line; EL4: gray line). B) rMOG (left hand side) and rOVA (right hand side) ELISA assay of four selected purified antibodies from RR-hybridomas to verify its specificity to MOG. Data are representative of at least three independent experiments.

These hybridomas provided the opportunity to study endogenous B cell populations via their antibody production without quantity problems as encountered via serum antibody purification and CNS antibody purification.

## 4.2 Summary of part 4.1

Mammalian MOG tetramers (mMOG<sub>tet</sub>) were successfully utilized in RR mice to detect low frequency and low affinity MOG-binding B cells. MOG-binding B cells were broadly distributed through all lymphoid organs with tendency to accumulate in the CNS draining lymph nodes, and they are capable of producing anti-MOG antibodies. Anti-MOG IgG B cells were found in abundance in sick mice CNS. At least part of these antibodies seemed to be produced by CNS-resident B cells because purified lymphocytes from CNS when cultured produced anti-MOG antibodies.

MOG-specific antibodies were found to be heterogeneous in RR mice. RR mice start to produce MOG-specific antibodies from an early age (3 weeks) and continue to populate and develop throughout mice's lifetime, which enabled B cells to evolve and become more heterogeneous and broad yet specific seen by MOG-binding polyclonal monoreactive hybridomas.

### 4.3 Preclinical events of EAE development in RR mice

#### 4.3.1 Neural antigens drainage/ transport and deposition in CNS draining lymph nodes

We hypothesized that capture of antigens from the CNS and their delivery to the nearest lymphoid organs is the first step in eliciting the B cells immune response in EAE. The constant export of these antigens to the CNS draining lymph nodes and epitope spreading might exacerbate the adaptive immune responses of both T and B cells that migrate back to the CNS resulting in an accumulation of damaging immune cells in the CNS. Therefore, studying these early events in spontaneous RR-EAE mice might help in elucidating the pathways by which antigens drainage or transport to the CNS draining lymph nodes occur.

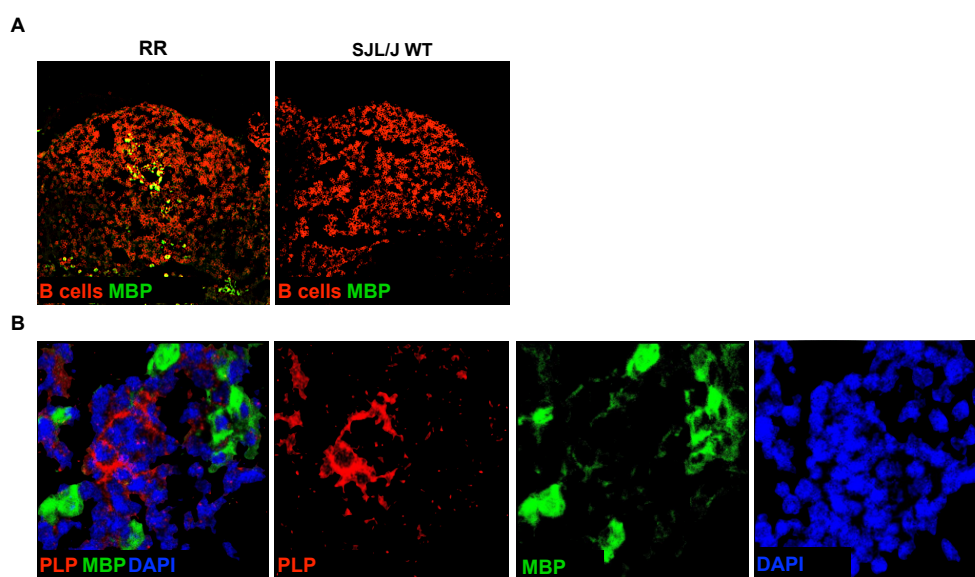
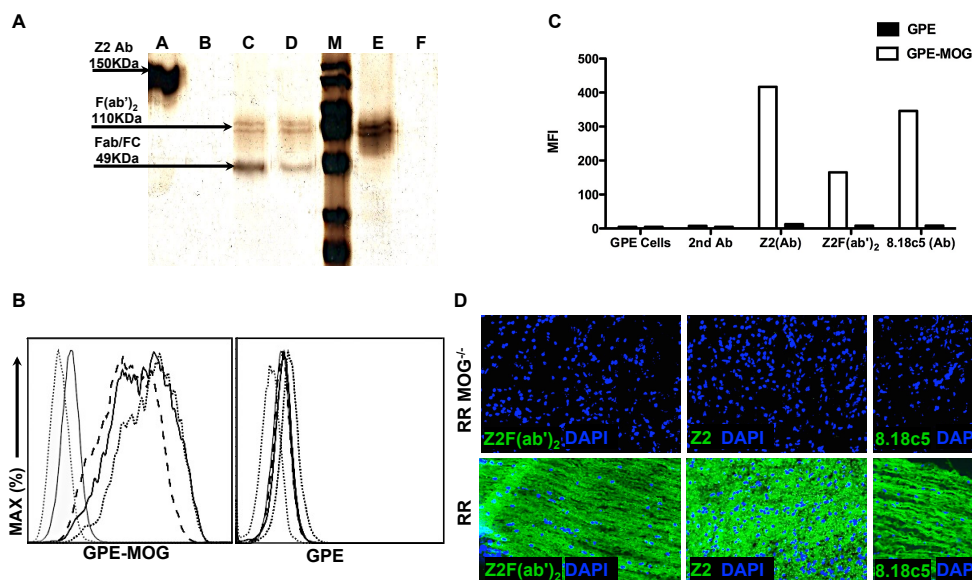


**Figure 4.12. Deposition of neural antigens in RR mice.** A) Fluorescent staining of cervical lymph node sections of RR and SJL/J WT mice for MBP (green) and B220<sup>+</sup> B cells (in red). MBP deposition was seen in RR but not in SJL/J WT mice under 20x magnification. B) Fluorescent staining of RR mice cervical lymph node for PLP (red), MBP (green) and DAPI (blue), at 63x magnification to visualize that PLP was carried on the cell surface, while MBP appeared to be internalized. Data are representative of three independent experiments (n=2-3/group).

Direct immunohistochemistry staining of anti-neural antigens' antibodies in the frozen section of lymphoid organs seemed to be a reasonable way to find myelin debris in CNS draining lymph nodes. In RR mice, myelin basic protein (MBP) was found within B cells compartment (Figure 4.12A), while it was not found in SJL/J WT mice. Moreover, immunohistochemistry staining pattern in RR mice suggested that the proteolipid protein (PLP) was carried on the cell surface while MBP was within the cells (Figure 4.12B). However, one disadvantage of immunohistochemistry is non-specific staining mediated by the FC region of antibody that

interacts with FC cell surface receptors. To circumvent this problem, we decided to produce myelin-specific antibodies lacking the FC region.



We chose the anti-MOG monoclonal antibody Z2 for FC fragmentation for two reasons: firstly, because it largely replicates MBP staining pattern in lymphoid organs seen in RR mice and, secondly for the availability for MOG knockout (KO) RR mice as a negative control. The fragmentation of Z2 antibody into FC and fragment antigen-binding F(ab')<sub>2</sub> was completed (Figure 4.13A). After digesting the FC part of Z2 antibodies, it was important to test Z2 F(ab')<sub>2</sub> capacity to detect MOG peptides on GPE cells (Figure 4.13B,C) and to stain MOG on spinal cord frozen sections (Figure 4.13D). Z2 F(ab')<sub>2</sub> stained GPE-MOG with lower MFI compared to 8.18c5 and complete Z2 antibodies (Figure 4.13B). The Z2 F(ab')<sub>2</sub> staining for MOG in the MOG expressing spinal cord sections was optimal and absent in the spinal cord sections of MOG-KO RR mice (Figure 4.13C). Hence, Z2 F(ab')<sub>2</sub> was eligible to be used in the lymph nodes of RR mice to find out naturally deposited myelin protein and to control MOG staining in MOG knockout mice. Z2, Z2 F(ab')<sub>2</sub> and IgG<sub>2a</sub>k isotype control antibodies were biotinylated, and equal

amounts were used to perform immunohistochemistry staining in different lymphoid organs of RR and MOG-KO RR mice (Figure 4.14). The staining of lymphoid organs with anti-MOG Z2(Fab')<sub>2</sub> in RR and RR-MOG KO was negative; revealing what was thought to be specific staining by anti-myelin antibodies was, FC-mediated staining (Figure 4.14).

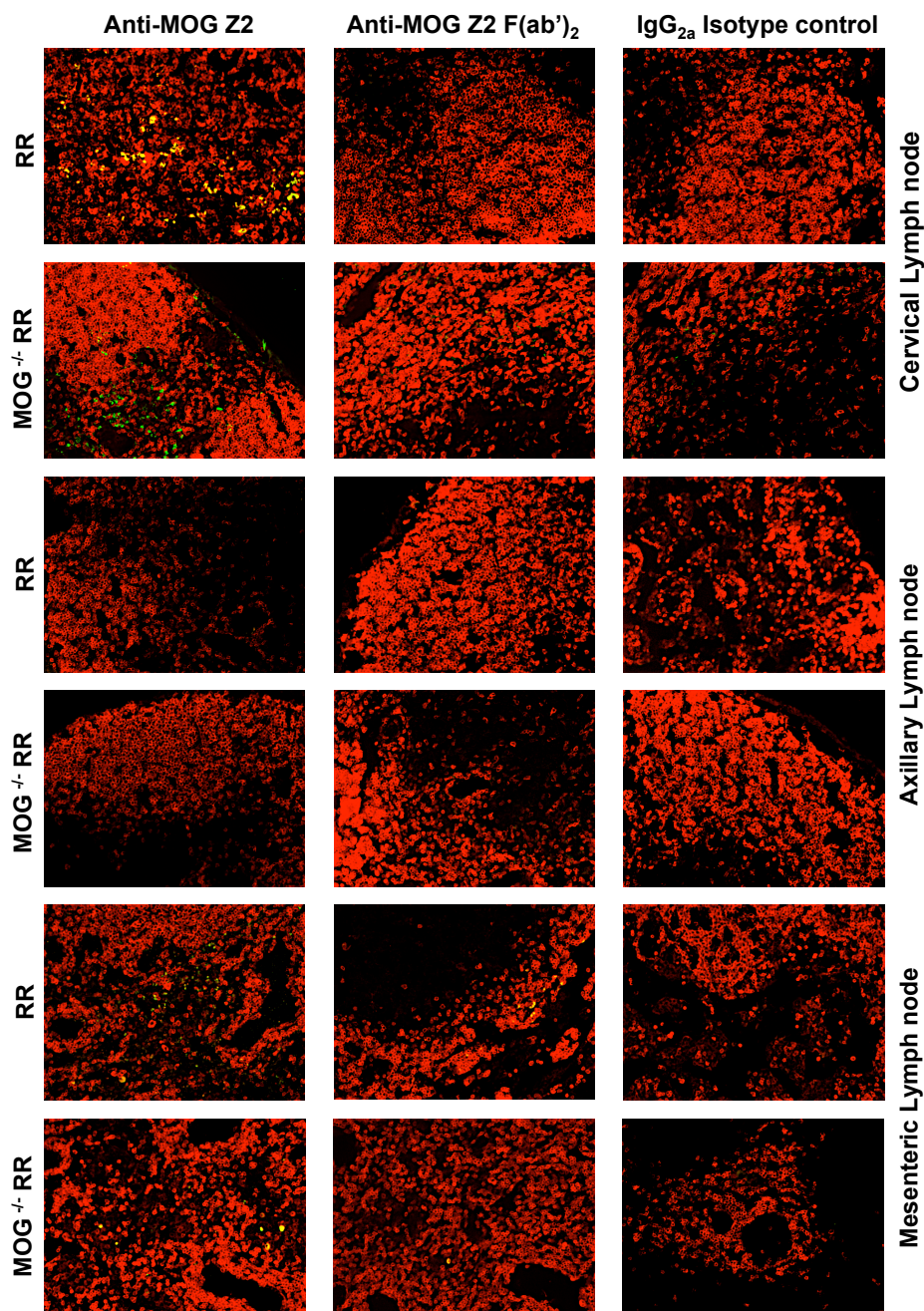


**Figure 4.14. Myelin deposition staining in lymph nodes was FC fragment mediated.** Cryo-sections of selected lymph nodes (10  $\mu$ m) from RR and RR MOG<sup>-/-</sup> mice stained with B220<sup>+</sup> (red) and anti-MOG antibodies Z2, F(ab')<sub>2</sub> fragment of Z2, as well as, IgG<sub>2a</sub> isotype control (green). Pictures were taken at magnification of 20x. Data are representative of two independent experiments (n=2/group).

Thus, these results necessitate a different myelin detection strategy and animal models, like introducing a fluorescent neural protein into the brain and tracing it back to lymph nodes to replicate CNS antigenic drainage or transportation.

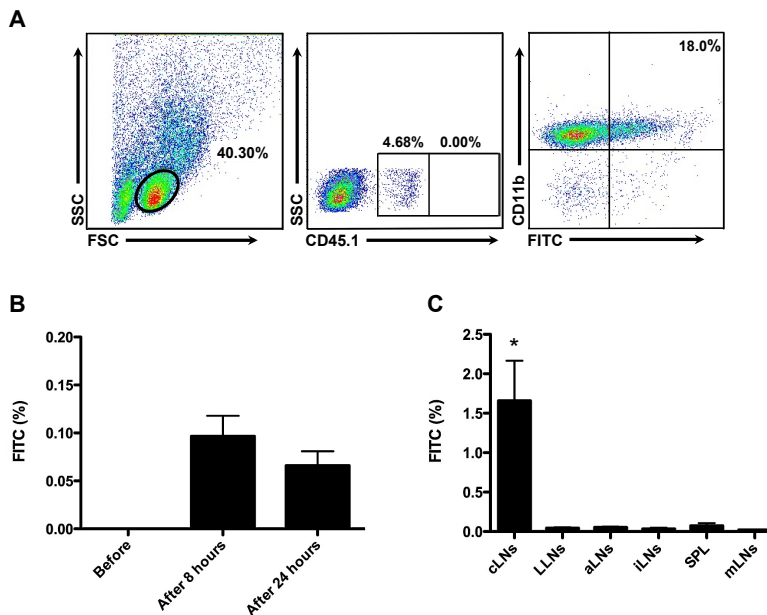


**Figure 4.15. Cervical lymph nodes were the drainage site for intrathecally injected neural antigen.** A) SJL/ J WT mice were intrathecally injected with 20  $\mu$ g of mMOG only or mMOG conjugated with FITC, and organs were harvested after 24 hours for FACS analysis. FACS plots showed CD45<sup>low</sup> population from brain that was mainly CD11b (Microglia) carrying mMOG-FITC. B) Graph showing blood lymphocytes carrying mMOG-FITC after 8 and 24 hours. C) Drainage sites of i.t injected mMOG-FITC in different lymphoid organs (cLN: cervical lymph nodes, LLN: lumbar lymph nodes, aLN: axillary lymph nodes, iLN: inguinal lymph nodes, SPL: spleen, mLN: mesenteric lymph nodes) (\*p-value <0.05). Data are representative of two independent experiments (n=2-3/group).

Experimental simulation of neural antigen drainage was performed by intrathecal injection (i.t) of mammalian MOG peptide conjugated to FITC (mMOG-FITC) followed by a search for the fluorescent proteins. Fluorescence signals were detected in blood lymphocytes after 8 hours and 24 hours. The circulating fluorescence signals gradually decreased from the time of i.t. injection, 8 hours and 24 hours post i.t injection (Figure 4.15B). These FITC molecules in the blood were mainly carried by macrophages that expressed CD11b<sup>+</sup> (data are not shown). In these mice, there were no lymphoid cells that invaded the brain and the spinal cord as indicated by the absence of CD45.1<sup>hi</sup> population (0.00%) in the CNS (Figure 4.18A). Injected mMOG-FITC was mainly retained and engulfed by CNS microglia expressing CD45<sup>low</sup> CD11b<sup>+</sup> (Figure 4.15A), the remainder of FITC molecules was found in blood and cervical lymph nodes. Thus, in



line with previous studies (Weller et al., 2009) and (Carare et al., 2008), our experiments have confirmed that injected mMOG-FITC molecules end up in cervical lymph nodes (Figure 4.15C).

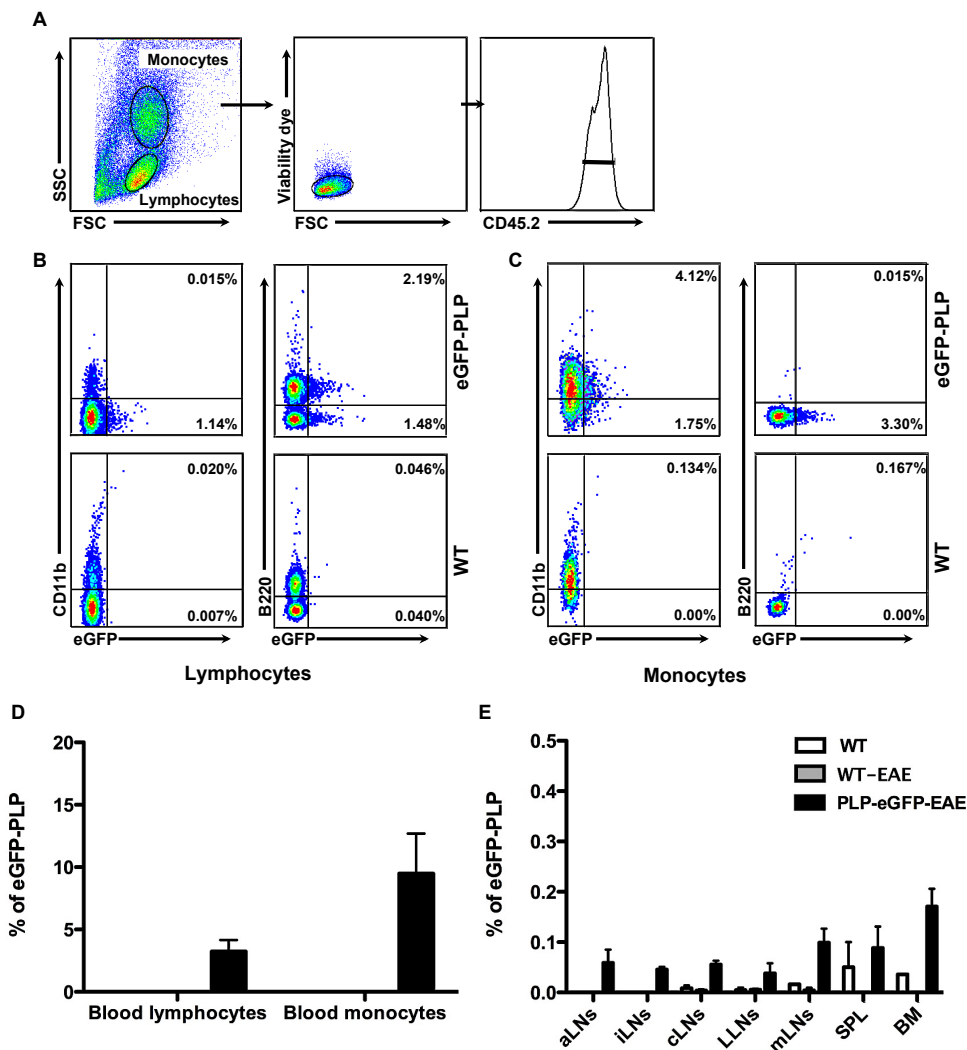


**Figure 4.16. Neural antigens were carried by blood cells in eGFP-PLP mice.** A) Gating protocol to identify GFP positive cells from blood cells. Example of flow cytometric plots showed which cells were carrying eGFP comparing PLP-eGFP C57BL/6 mice to immunized WT C57BL/6 mice in B) blood lymphocytes population and C) monocytes population. D) Quantification of total eGFP-PLP in blood cells and E) in different lymphoid organs (aLNs: axillary lymph nodes, iLNs: inguinal lymph nodes, cLNs: cervical lymph nodes, LLNs: lumbar lymph nodes, mLNs: mesenteric lymph nodes, SPL: spleen, BM: bone marrow). Data are representative of two independent experiments (n=2-3/group).

Furthermore, we used PLP-eGFP mice (C57BL/6 mice with part of the PLP is fused with GFP) to characterize the transport of myelin antigen to the periphery (Figure 4.16). PLP-eGFP mice were immunized and sacrificed at the peak of the disease in order to find any fluorescent signals in lymphoid organs that might indicate PLP drainage from CNS to lymphoid organs. Blood lymphocytes and monocytes were, in fact, the only site where PLP could be detected, however, no eGFP positive cells seen in any of the lymph nodes (Figure 4.16D,E). It is possible

that eGFP might have been digested immediately after uptake by phagocytes before they have reached any lymphoid organs.

### 4.3.2 Preclinical infiltration of immune cells in the CNS

Early activation of B cells can occur in the peripheral lymphoid organs after drainage of neural antigens, or in the CNS after immigration of peripheral immune cells. In either case, anti-MOG antibodies could be used as a marker for pre-clinical immune cell activation because it is easy to non-invasively monitor in blood and anti-MOG antibodies production in RR mice starts very early in mice's lifetime (4 weeks), well before any EAE disease symptoms appear. Lymphocyte infiltration in the CNS was followed by three means: gene expression, immunohistochemistry staining and flow cytometric analysis before and after first sign of anti-MOG antibodies production in RR mice-that is before and after 4 weeks of mice-age-.

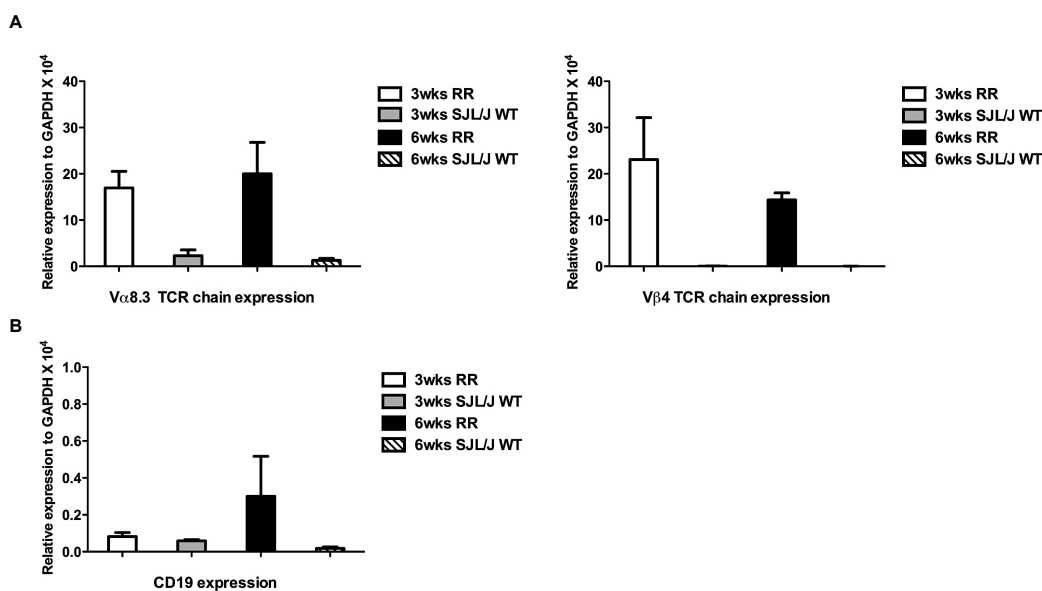


**Figure 4.17. Preclinical infiltration of lymphocytes in RR mice.** Brain tissue (cerebral cortex) from 3 and 6 weeks RR mice showed an early infiltration of A) T cells indicated by their transgenic chains (Vβ4 and Vα8.3), and B) B cells infiltration seen by gene expression of CD19 in relative expression to housekeeping gene GAPDH. Data are representative of two independent experiments (n=2-4/group).

Gene expression analyses of CD19<sup>+</sup> B cells and transgenic T cell receptor genes (Vβ4 and Vα8.3) of 3 and 6 weeks old RR mice indicated an early infiltration of T and B lymphocytes (Figure 4.17). Different CNS regions showed different numbers of infiltrating T and B cells and were most evident at 6 weeks old mice or later (Figure 4.17, 4.18, 4.19 and data not shown). In the brain, cerebellum and brainstem contained more lymphocytes infiltrates than other regions (data not shown); similarly the lumbar spinal cord had more infiltrates than upper regions of

spinal cord. B cells might have been recruited later to the CNS than T cells, as suggested by low expression of CD19 cell marker of B cells in 3 weeks old RR mice compared to 6 weeks old mice (Figure 4.17B), implying that T cells are the pioneer infiltrates to the target tissue opening the door for B cells to follow them to reside and populate in the CNS.

Early lymphocyte infiltration was also demonstrated by immunohistochemistry staining, mainly in RR mice (Figure 4.18). In the CNS of 2 weeks old RR mice, there were few scattered T cells in the cerebellum or brain stem and B cells were completely absent (Figure 4.18). However, in 6 weeks old mice, infiltration of T and B cells were detected easily, with T cells homing alone or in cluster while B cells were only found in aggregates together with T cells (Figure 4.18). Finally, from the previous experiments, it was observed that CNS infiltrates found in different quantities and accumulation preferably, in the cerebellum and brain stem in the brain and lumbar section of the spinal cord with T cells being the pioneer infiltrates.

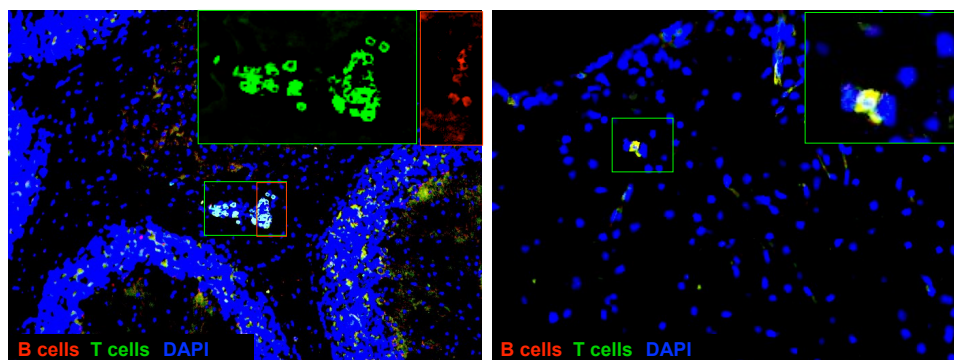


**Figure 4.18. Preclinical infiltration of lymphocytes to the CNS in RR mice.** Cryosections of brain (10  $\mu$ m) from RR mice showed B cells (B220) in red, T cells (CD4) in green and DAPI in blue. Pictures were taken from the brain stem of 2 weeks old mice (right hand side), and the cerebellum of 6 weeks old mouse (left hand side). Pictures were taken at 20x magnification (zoomed in at the top right hand corner). Data are representative of independent three experiments (n=3-4/group).

Finally, anti-MOG antibodies can indicate an immune reaction against MOG in RR mice even before the onset of clinical symptoms and their detection in serum at early age provides an opportunity to study and correlate the initial immune events preceding the development of clinical disease.

Two weeks old RR mice had few lymphocyte infiltrates in the CNS ( $\leq 2000$  infiltrating T cells) (Figure 4.19). At this very young age, the mice did not develop any anti-MOG antibodies both in blood serum and *ex vivo* organ culture's supernatant (Figure 4.21). Collectively, at 2 weeks of mice-age, data suggested that APCs including B cells did not meet their cognate antigens yet to produce antibodies.

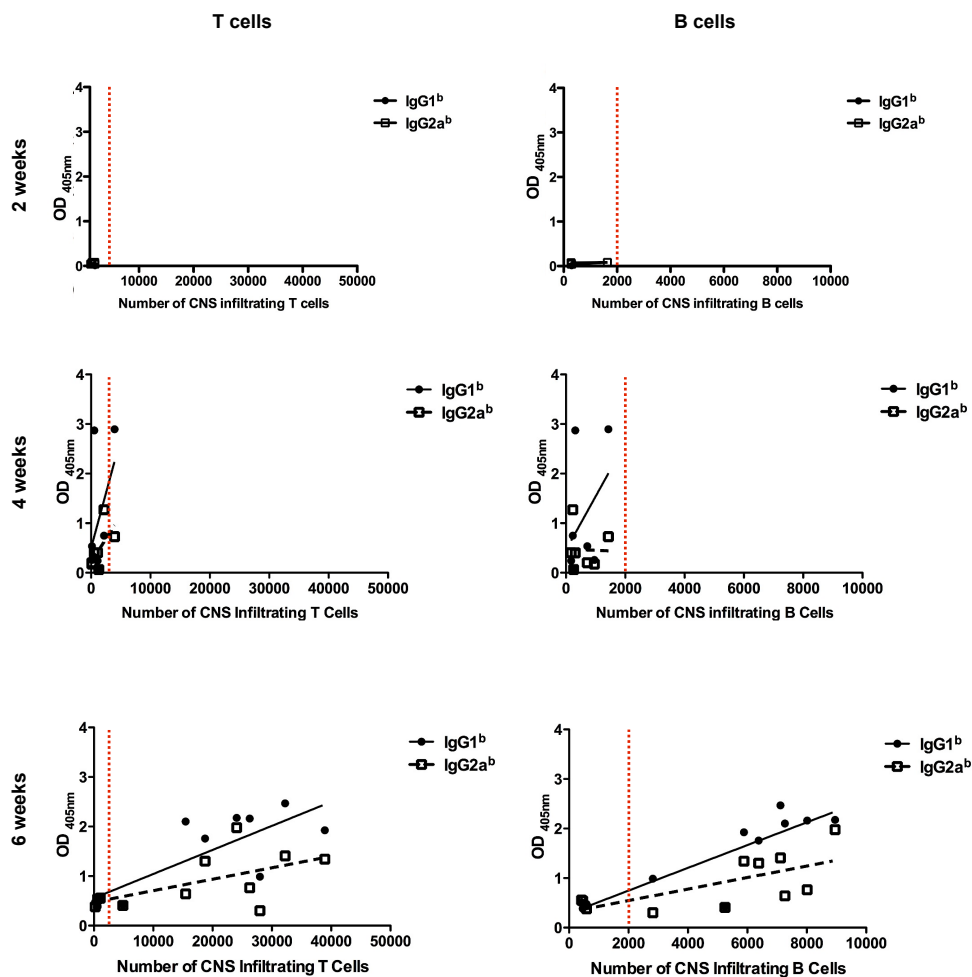


**Figure 4.19. Preclinical infiltration of T and B lymphocytes in relation to anti-MOG serum antibody production.** FACS beads were used to count infiltrating T and B cells in the CNS from RR and SJL/J WT mice at different ages, and blood serum was collected. Serum MOG ELISA readings (X-axis) and the number of infiltrating cells (Y-axis) were plotted into XY graph and on X-axis there is a red dashed line indicates baseline infiltration ( $\approx 2000$  cells). Data are pooled from two independent experiments ( $n=4-6/\text{group}$ ).

Four weeks old RR mice had a higher number of T cells infiltrating the CNS but still few B cells ( $\approx 2000$ ) (Figure 4.19). The B cells at the periphery, however, showed immuno-activation reflected by the production of anti-MOG antibodies IgG<sub>1</sub> in the serum and also by *ex vivo* single organ culture, with the highest anti-MOG antibodies production in the cervical lymph nodes (Figure 4.21). The number of infiltrating lymphocytes did not show any correlation with anti-MOG IgG<sub>1</sub> and IgG<sub>2a/2b</sub> antibodies seen by linear regression analysis (table 4.1). From our i.t injection experiments and the literature (Carare et al., 2008), we learned that antigen release is almost immediate and can be detected in blood already 8 hours after injection. Therefore, we

assumed that antigen release and capture was before the production of anti-MOG antibodies leading to T and B cells infiltration to the CNS, sometimes between week 2 and week 4 (Figure 4. 19, .21).

	4 weeks		6 weeks	
	IgG <sub>1</sub>	IgG <sub>2a/2b</sub>	IgG <sub>1</sub>	IgG <sub>2a/2b</sub>
T cells	0.3162	0.3542	0.6471	0.3453
B cells	0.0997	0.0311	0.7727	0.4670

**Table 4.1. Lymphocytes infiltrated to the RR mice CNS correlates with its serum.** Regression values ( $R^2$ ) of the absolute number of infiltrated lymphocytes (T and B cells) to the CNS compared to anti-MOG IgG<sub>1</sub> and IgG<sub>2a/2b</sub> antibodies from blood serum of RR mice at age of 4 and 6 weeks. Data are pooled from two independent experiments (n=4-6/group) presented in Figure 4.19.

Finally, at 6 weeks of mice-age, autoimmune reactivity was amplified in the brain with an increased number of both T and B cells infiltrating the CNS (Figure 4.19). *Ex vivo* organ cultures of these 6 weeks old mice produced a higher amount of anti-MOG antibodies compared to younger mice with those from cervical lymph nodes being the highest and most persistent (Figure 4.21). At 6 weeks of mice-age, the immune system had reached a balance having tight correlation between infiltrating T and B cells in the CNS to anti-MOG antibodies in mice serum in the periphery (Figure 4. 19 and Table 4.1). Interestingly, the strongest correlation was seen with serum anti-MOG IgG<sub>1</sub> antibodies which are believed to be pathogenic with B cells infiltration of value equal to  $R^2=0.77$ , followed by anti-MOG IgG<sub>1</sub> antibodies with T cells infiltration ( $R^2=0.65$ ) as tested using linear regression analysis (Table 4.1).

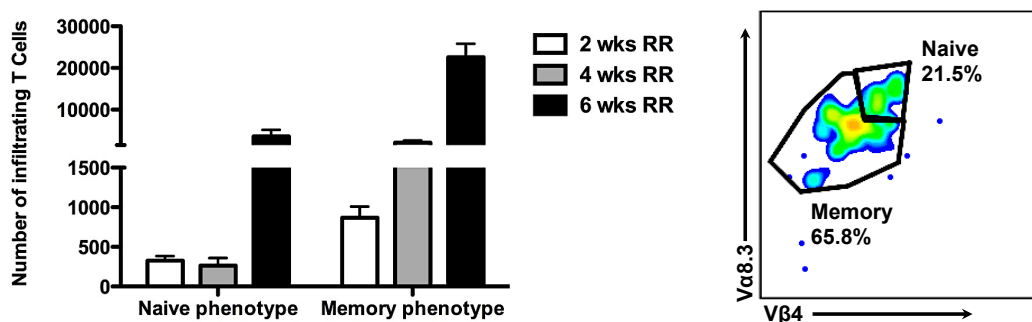


**Figure 4.20. Pre-clinical infiltration of mainly T memory lymphocytes.** FACS beads were used to count the absolute number of infiltrating T cells in the CNS from RR mice at different ages. Absolute number of low and high TCR chains Vβ4 and Vα8.3 expressing T cells (memory, naive phenotype respectively) were depicted. Example of FACS plot is shown on right hand side. Data are pooled from two independent experiments (n=4-6/group).

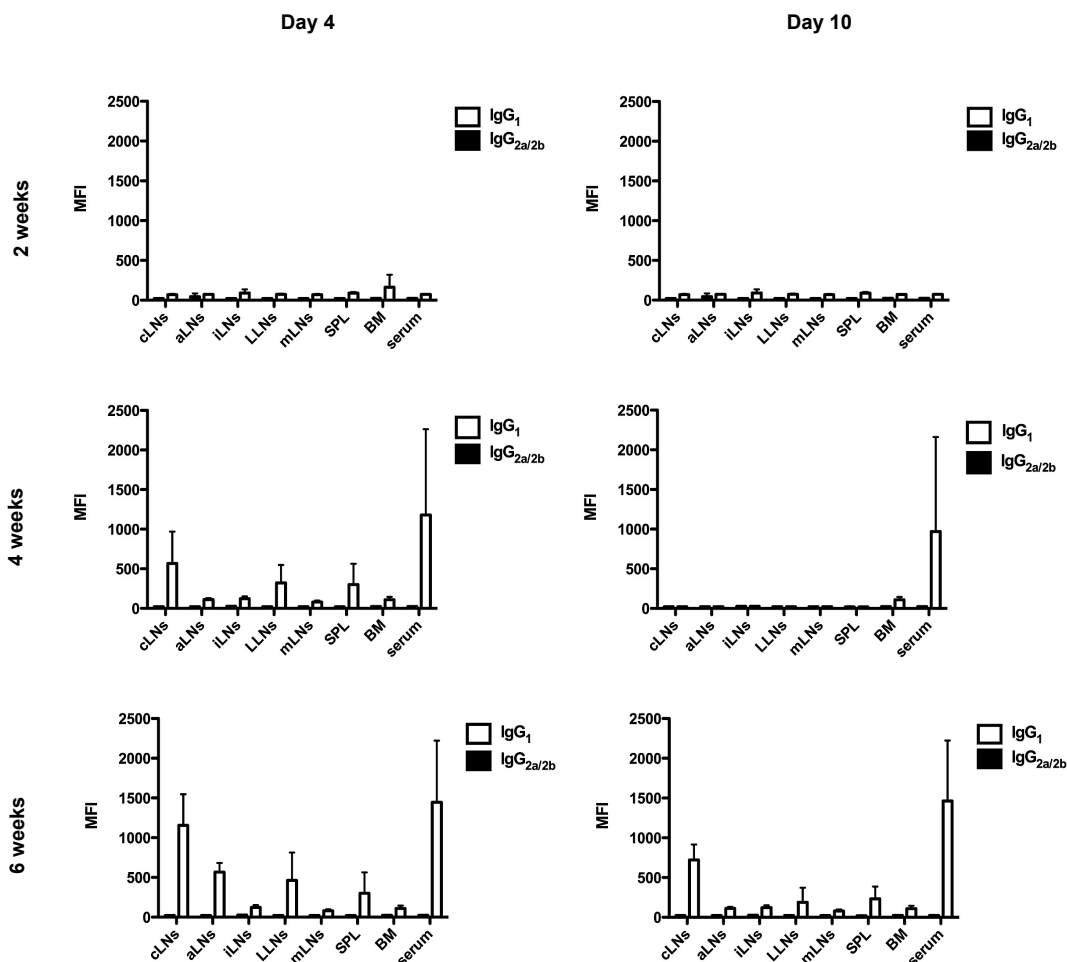


**Figure 4.21. Cervical lymph nodes contributed the most to the serum anti-MOG antibodies in RR mice.** Whole organs were cultured from RR mice at different ages (cLN: cervical lymph nodes, aLN: axillary lymph nodes, iLN: inguinal lymph nodes, LLN: lumbar lymph nodes, mLN: mesenteric lymph nodes, SPL: spleen, BM: bone marrow). Supernatant of organs' culture and serum were used to stain EL4-MOG cells, and mean fluorescence intensity (MFI) was calculated. Data representative of two independent experiments (n=2-3/group).

Moreover, infiltrating T cells to the CNS were mainly expressing a memory phenotype and gradually built up in the CNS with age (Figure 4.20). However, in 6 weeks old mice, we observed a sudden increase in absolute numbers of naïve infiltrating T cells in the CNS, which might suggest that the lymphocytes had found a niche in the site of inflammation to divide and proliferate (Figure 4.21) or simply BBB was “open” for more naïve T cells to arrive at the CNS.

#### **4.4 Summary of part 4.3**

RR mouse model is a unique, spontaneous model, where the preclinical stage of the disease seems to be relatively long allowing for studying preclinical immune events. It was learnt that neural antigens are drained to CNS lymphoid organs. Signs of pre-clinical events of EAE were – here- simplified by increased absolute number of lymphocytes in the CNS and systemic anti-MOG antibodies production. At 4 weeks of mice-age, lymphocytes were peripherally recruited, evident by anti-MOG antibodies production and slightly exceeding baseline infiltration of T cells to the CNS. At 6 weeks of mice-age, peripheral reaction seemed to be tailored to fit the inflammation demands in the CNS as seen by the correlation between anti-MOG antibodies and, the absolute number of both infiltrating T and B lymphocytes to the CNS. This correlation might potentially indicate which of RR mice will remain healthy and which ones are on the verge of disease.

## CHAPTER 5: DISCUSSION



## 5. Discussion

### 5.1 MOG-binding B cells in CNS drainage lymph nodes

B cells express surface immunoglobulin (slg) molecules as antigen binding receptors and each B cell expresses slg with a single antigen binding specificity (Buisman et al., 2009). The identification of antigen-specific B is a challenging task, because in the entire immune repertoire the frequency of cells specific for any particular antigen is usually less than 1% (Scheid et al., 2009, Wu et al., 2010).

Tetramer technology, as introduced by Altman et al. (1996), has become widespread in identifying antigen specific lymphocyte clones. As a method to identify and phenotypically characterize Ag-specific T lymphocytes, it has quickly advanced our understanding of the immune response from a general sense to a more precise sense. This technology is mainly used in flow cytometry to quantify *ex vivo* antigen-specific T cells by binding soluble tetramer MHC-peptide complexes attached to a fluorochrome (Vollers and Stern, 2008). Quantitative analyses of antigen-specific immune cell populations provided valuable information on the natural course of immune responses, such as in viral, bacterial, or parasitic infections, cancer, autoimmune diseases and transplantation. However, this technology has been used less in B cells (Gieseke et al., 2012). We applied tetramer technology to study autoimmune B cells in RR mice, where anti-MOG antibodies are seen from 3-4 weeks of mice-age, and which are produced by a few thousands of antigen-specific B cells. Detection of MOG-binding B cells was hampered by their low affinity and low frequency. Therefore, we expressed MOG peptide 1-125 in HEK EBNA eukaryotic cells, allowing for glycosylation, to keep correct conformational structure, and oligomerized the protein in analogy to MHC tetramers. Therefore, MOG tetramerization technique allowed detecting mMOG-binding B cells in RR mice especially in CNS draining lymph nodes.

It is well established that the high-affinity binding of autoantibodies to self-antigens is critical for their pathogenic activity in autoimmune disease *in vivo* (Shlomchik et al., 1987). This concept has been supported by the demonstration that autoimmune Ig genes, which were clonally expanded, were modified by somatic mutations in GC (Shlomchik et al., 1987). Further support of affinity maturation came from the observation that IgM to IgG class switching coincided with progression of the clinical development of autoimmune diseases, such as in SLE (Tillman et al., 1992, Hirose et al., 1993). However, in RR mice most of the purified antibodies were of low affinity as compared to a classical MOG binding mAb (8.18c5) used as a positive control. Therefore, two points needed to be clarified: Firstly, affinity maturation of autoantibodies in parallel to Ig class switching and somatic hypermutations were not consistently observed. These

results were similar to a study of clonally related anti-IgG<sub>2a</sub> rheumatoid factors from a lupus-prone MRL-lpr/lpr mouse, which had demonstrated limited affinity maturation, despite Ig isotype switching with extensive somatic mutations (Jacobson et al., 1994). During our experiments, we also noted that in the RR mice EAE incidence did not dictate isotype switching or affinity maturation that is IgG<sub>1</sub> and IgG<sub>2a/2b</sub> switching was not shaped by the disease course. Secondly, studies of rheumatoid factor monoclonal autoantibodies disclosed that low-affinity autoantibodies are able to induce immune complex-mediated vasculitis (Berney et al., 1992, Fulpius et al., 1993). Also low affinity IgG anti-mouse RBC monoclonal autoantibodies had a significant role of FcγR-mediated erythrophagocytosis in the development of anemia (Clynes and Ravetch, 1995). Thus, it was speculated that low-affinity B cells could become highly pathogenic (Fossati-Jimack et al., 1999), and are also driven to germinal center formation (Dal Porto et al., 1998). The same was observed in this study where, mMOG<sub>tet</sub> allowed visualizing low affinity MOG-binding B cells within the germinal center, which was not possible to be detected by rMOG. Moreover, about 40% of normal adult B cell population are polyreactive and are the predominant cell type in the newborn up to 90% (Chen et al., 1998). The B1 subset is believed to be the main population producing polyreactive antibodies (Kantor et al., 1995, Hardy et al., 1994). Unlike what we found in RR mice, hybridomas were polyclonal monoreactive to MOG.

## 5.2 MOG-binding B cells in the CNS of RR mice

B cells are known to enter CNS during normal immune surveillance and in disease (Alter et al., 2003). In RR mice, there are more T cells than B cells infiltrated into the CNS. Most of the CNS infiltrating B cells in RR mice were capable of producing anti-MOG antibodies of the IgG<sub>1</sub> isotype. The switch to IgG<sub>1</sub> takes place in germinal centers and requires the presence of T cells and autoantigen. How and where would T cell, B cells and autoantigen meet? One possibility is indicated by Cserr and Berman (1978), who have developed a system in which a fine cannula placed in the brain parenchyma is left in place while the BBB becomes reestablished. Their system allowed infusing minute amounts of an antigen directly into the CNS without traumatically disrupting the reconstituted BBB. When antigens were introduced behind the reconstituted BBB, antigen-specific B lymphocytes and plasma cells accumulate near the tip of the cannula. This observation suggested that activated B lymphoblasts can circulate and pass through CNS tissues in search of their antigens as was observed in early infiltration of B cells in RR mice, and they have populated there.

Antibodies of limited clonality (oligoclonal bands) are found in the CNS and cerebrospinal fluid (CSF) of patients with MS (Kabat et al., 1942). Clonally expanded CNS resident B cells are partially accountable for the emergence of these oligoclonal bands, stressing the importance of B cells for development or course of MS (Obermeier et al., 2008). In RR mice, Ig deposition is evident in the CNS (Pollinger et al., 2009). Deposited Ig in RR mice was MOG-specific and IgG<sub>1</sub> isotype. Despite the fact that these mice were capable of producing both anti-MOG IgG<sub>1</sub> and IgG<sub>2a/2b</sub> isotypes, CNS dissociated anti-MOG antibodies of sick RR mice did not show much IgG<sub>2a</sub> isotype. The aforesaid result might be attributed either to low numbers of isotype switched B cells to IgG<sub>2a/2b</sub> in the CNS or due to high adhesive capacity of IgG<sub>2a</sub> antibodies, as mentioned in several studies (Hazenbos et al., 1996). *In vitro*, it had been shown that murine IgG<sub>1</sub> and IgG<sub>2b</sub> interacted preferentially with the low affinity receptors, FcγRIIB and FcγRIII, and IgG<sub>2a</sub> with the high affinity receptor, FcγRI (Hazenbos et al., 1996). More recently, Nimmerjahn et al. (2005) had shown that FcγRIV bound to IgG<sub>2a</sub> and IgG<sub>2b</sub> with at least 10-fold higher affinity than FcγRIII, but it did not bind to IgG<sub>1</sub> with measurable affinity.

### 5.3 RR mice hybridoma to study anti-MOG antibody clones

We agreed with Zhou et al, 2007 that in analyses of antibody and B cell repertoires, the best way to overcome the low quantity of antibodies *ex vivo* is to create hybridomas from RR mice. MOG-specific antibodies from blood serum recovered less than a few nanograms per ml (data not shown) after extended processing for a single RR mouse (Appendix 6.1) and the heterogeneity of these preparations were also vast.

Hybridomas from normal mice commonly produce polyreactive antibodies that reacted with normal tissues (Coutinho et al., 1995, Dighiero et al., 1983). However, in RR mice it was not the case, RR mice's hybridomas were polyclonal yet monoreactive to MOG. Antigen specificity was determined by ELISA with two antigens rMOG and rOVA, which was amongst the panel of antigens tested by others (Coutinho et al., 1995, Dighiero et al., 1983). Furthermore, our studies using ELISA and FACS proved that RR-hybridomas generated from RR spleen are monoreactive to both linear and conformational MOG epitopes.

Additionally, the affinity of created hybridomas was lower than the anti-MOG antibody 8.18c5. It was, however, comparable to anti-MOG antibodies from RR mice's serum and the extracted from the CNS tissue. It should be noted that the anti-MOG 8.18c5 was created from an immunized mouse while RR hybridomas were derived from naturally and endogenously recruited autoimmune B cells. As stated earlier, low affinity binding antibodies are not necessarily less pathogenic (Fossati-Jimack et al., 1999). In general, we are aware that these

results are very preliminary and just a baseline towards the approach of analyzing clonality of RR B cells in both lymph nodes and CNS. Unfortunately, limited genetic database resources of SJL/J mouse background have also, hindered the study.

#### **5.4 Neural antigen transportation**

Besides immune cell infiltrates in the CNS, CNS draining lymph nodes such as cervical lymph nodes are a possible meeting place for anti-MOG T and B cells. Indeed, transferred IgH<sup>MOG</sup> B cells preferentially homed to the cervical lymph nodes of RR mice (Berer et al., 2011a). But this would require the presence of MOG in these lymph nodes. There are two separate pathways for neural antigen drainage to cervical lymph nodes, via interstitial fluid (ISF) and cerebral spinal fluid (CSF). ISF and solutes drain from the brain along the 100-150 nm wide basement membranes of the walls of the capillaries and arteries (Carare et al., 2008). The failure of APCs to migrate to lymph nodes along perivascular lymphatic draining pathways may be a significant factor in immunological privilege of the brain (Weller et al., 2009). Lymphatic drainage of CSF is predominantly through the cribriform plate into nasal lymphatics (Weller et al., 2009). Several studies have shown that there is antigen drainage in MS and EAE to CNS draining lymphoid organs. Antigen drainage has been shown via PLP detection and different anti-myelin antibodies in cervical lymph nodes. Also, surgically removal of cervical lymph nodes where antigen drains reduced the severity of EAE (Zwam et al., 2009). Using similar methods such as staining for myelin antigen in the CNS draining lymph nodes we also saw MBP and PLP-like material in cervical lymph nodes of RR mice. Unfortunately, further examining this technique by introducing an antigen-deficient animal control has shown anti-MOG antibodies staining in cryosections can be seen in both RR and RR MOG KO mice cervical lymph nodes, implying that the positive staining is most likely to be mediated by unspecific antibody binding to Fc-receptors (Leong, 2004, Holmseth et al., 2006, Fritschy, 2008, Daneshtalab et al., 2010). Still, intrathecal injection of different markers has revealed that antigens drain to cervical lymph nodes (Carare et al., 2008), as was seen by soluble tracers (dextran) draining along the basement membranes of capillaries and arteries in naive mouse brains only 5 minutes after intrathecal injection (Carare et al., 2008). Our study showed that within 8 hours after intrathecal injection of mMOG-FITC, FITC was detected in blood lymphocytes and monocytes. Mathematical modeling suggested that contrary waves drive drainage of interstitial fluid, solutes, and neural antigens away from the brain in reverse perivascular transport, but not perivascular macrophages (Schley et al., 2006). Important to note, intrathecal injection did stimulate infiltration of any CD45<sup>hi</sup> lymphocytes populations or release of CD45<sup>low</sup> from CNS as seen in EAE in eGFP-PLP

mice, which indicated that infiltration of CD45<sup>hi</sup> population was a consequence of antigen drainage, not a cause.

### **5.5 Preclinical infiltration of lymphocytes**

Both transgenic T cells and endogenously recruited B cells infiltrated the CNS from a young age in RR mice. Infiltrated cells were seen mainly in the cerebellum and brain stem of RR mice and in the lumbar section of spinal cord. The first wave of infiltrating lymphocytes was seen by 4 weeks, paralleled by increased anti-MOG antibodies production in the cervical lymph nodes. A similar experiment was performed by Furtado et al, 2008 where in myelin basic protein (MBP)-specific TCR transgenic mice spontaneous disease onset and CNS infiltration of T cells coincided with, priming of T cells in the cervical lymph node and their activation via expression of CD69 and CD44 by the age of 6 weeks. In RR mice, by 6 weeks of age, priming of the immune system was checked by anti-MOG antibodies serum titer detection and it was correlated with the amount of infiltrated T and B cells to the CNS. The number of lymphocytes infiltrating the CNS along with MOG-specific serum antibodies might determine which mice were going to remain healthy or become sick. It may take longer to develop EAE by reduced anti-MOG antibodies titer in serum as compared to mice with increased anti-MOG serum titer. This correlation between disease severity and serum titer was also observed in rheumatoid arthritis (Cambridge et al., 2003). Finally, it has shown that infiltrating T cells to the CNS express memory phenotypes at the peak of EAE (Giunti et al., 2003). In RR mice, however, T cells infiltrating into the CNS have memory phenotype indicated by reduced TCR chain expression from a very young mice and increases gradually with age, which might suggest that T cells have found a niche to populate or memory phenotype is required to enter to CNS.

## CHAPTER 6: CONCLUSION

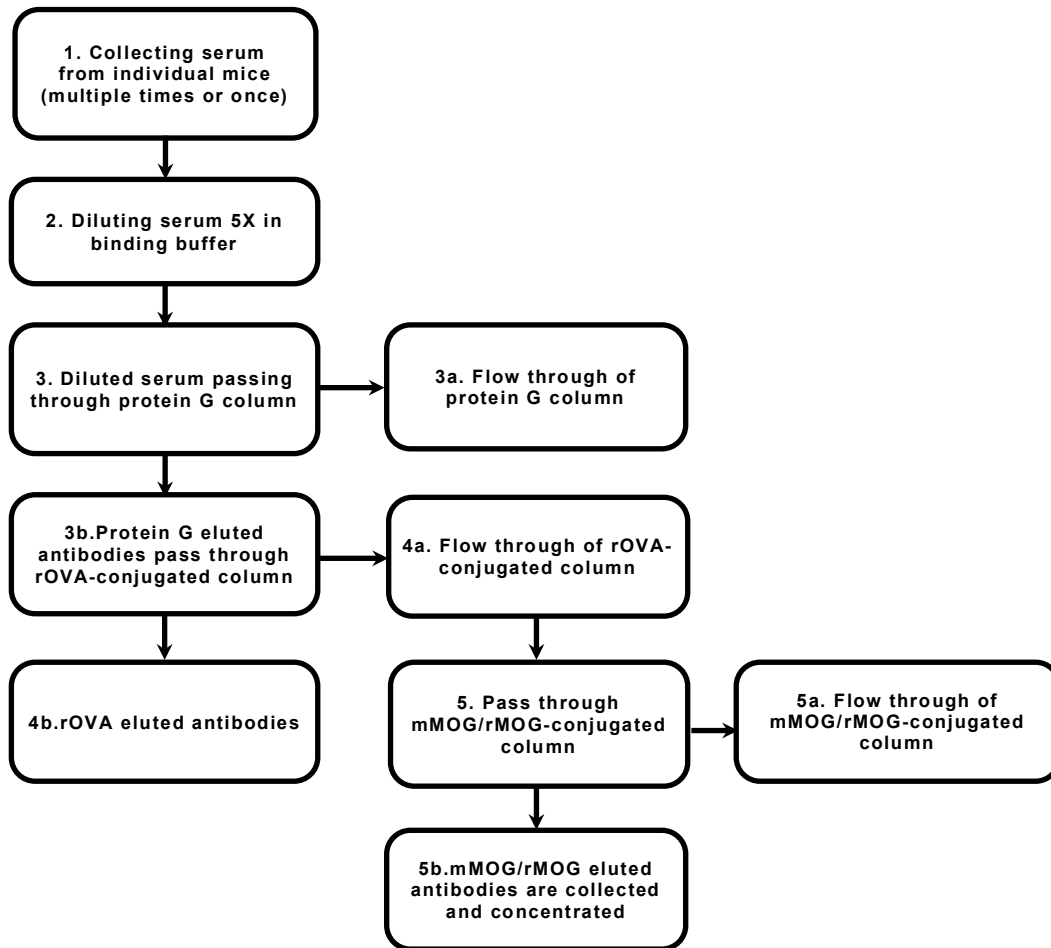
## 6. Conclusion

Mammalian MOG tetramer was successfully utilized in RR mice to detect low frequency and low affinity MOG-binding B cells. MOG-binding B cells were vastly distributed in all lymphoid organs in RR mice with the tendency to accumulate in the CNS draining lymph nodes. MOG-specific antibodies were found to be heterogeneous in RR mice as it evolves from a very young age. Furthermore, neural antigen drainage to lymphoid organs is immediate and neither requires cells of myeloid origin to leave the CNS nor infiltrating cells from the periphery to carry them out of CNS. Signs of pre-clinical events of EAE were –here- simplified by increased absolute number of lymphocytes in the CNS and systemic anti-MOG antibodies production. At 6 weeks old mice, anti-MOG antibody serum titer correlated with the absolute number of both B cells and T lymphocytes infiltrating to the CNS, which might potentially suggest which of RR mice will remain healthy and which ones are on the verge of disease.

# CHAPTER 7: APPENDIX



## 7. Appendix



**Appendix 6.1. Individualization of purifying anti-MOG antibodies.** Adjusted protocol of anti-MOG antibodies purification to reduce its heterogeneity. Single healthy and sick RR mice were bled and serum was collected and processed as described in the chart to finally elute the antibodies of interest (anti-rMOG/mMOG antibodies).

## CHAPTER 8: REFERENCES

## 8. References

- ABBOTT, N. J., PATABENDIGE, A. A. K., DOLMAN, D. E. M., YUSOF, S. R. & BEGLEY, D. J. 2010. Structure and function of the blood–brain barrier. *Neurobiology of Disease*, 37, 13-25.
- ALTER, A., DUDDY, M., HEBERT, S., BIERNACKI, K., PRAT, A., ANTEL, J. P., YONG, V. W., NUTTALL, R. K., PENNINGTON, C. J., EDWARDS, D. R. & BAR-OR, A. 2003. Determinants of Human B Cell Migration Across Brain Endothelial Cells. *The Journal of Immunology*, 170, 4497-4505.
- ALTMAN, J. D., MOSS, P. A. H., GOULDER, P. J. R., BAROUCH, D. H., MCHEYZER-WILLIAMS, M. G., BELL, J. I., MCMICHAEL, A. J. & DAVIS, M. M. 1996. Phenotypic Analysis of Antigen-Specific T Lymphocytes. *Science*, 274, 94-96.
- BEN-NUN, A., WEKERLE, H. & COHEN, I. R. 1981. The rapid isolation of clonable antigen-specific T lymphocyte lines capable of mediating autoimmune encephalomyelitis. *Eur J Immunol*, 11, 195-9.
- BERER, K., MUES, M., KOUTROLOS, M., RASBI, Z. A., BOZIKI, M., JOHNER, C., WEKERLE, H. & KRISHNAMOORTHY, G. 2011a. Commensal microbiota and myelin autoantigen cooperate to trigger autoimmune demyelination. *Nature*, 479, 538-41.
- BERER, K., WEKERLE, H. & KRISHNAMOORTHY, G. 2011b. B cells in spontaneous autoimmune diseases of the central nervous system. *Mol Immunol*, 48, 1332-7.
- BERNEY, T., FULPIUS, T., SHIBATA, T., REININGER, L., VAN SNICK, J., SHAN, H., WEIGERT, M., MARSHAK-ROTHSTEIN, A. & IZUI, S. 1992. Selective pathogenicity of murine rheumatoid factors of the cryoprecipitable IgG3 subclass. *International Immunology*, 4, 93-99.
- BETTELLI, E., BAETEN, D., XE, GER, A., SOBEL, R. A. & KUCHROO, V. K. 2006. Myelin oligodendrocyte glycoprotein–specific T and B cells cooperate to induce a Devic-like disease in mice. *The Journal of Clinical Investigation*, 116, 2393-2402.
- BETTELLI, E., PAGANY, M., WEINER, H. L., LININGTON, C., SOBEL, R. A. & KUCHROO, V. K. 2003. Myelin Oligodendrocyte Glycoprotein–specific T Cell Receptor Transgenic Mice Develop Spontaneous Autoimmune Optic Neuritis. *The Journal of Experimental Medicine*, 197, 1073-1081.
- BEZZI, P., DOMERCQ, M., BRAMBILLA, L., GALLI, R., SCHOLS, D., DE CLERCQ, E., VESCOVI, A., BAGETTA, G., KOLLIAS, G., MELDOLESI, J. & VOLTERRA, A. 2001. CXCR4-activated astrocyte glutamate release via TNF[alpha]: amplification by microglia triggers neurotoxicity. *Nat Neurosci*, 4, 702-710.
- BLAKEMORE, W. F. 1973. Remyelination of the superior cerebellar peduncle in the mouse following demyelination induced by feeding cuprizone. *Journal of the Neurological Sciences*, 20, 73-83.
- BLAKEMORE, W. F. & FRANKLIN, R. J. M. 2008. Remyelination in Experimental Models of Toxin-Induced Demyelination. In: RODRIGUEZ, M. (ed.) *Advances in multiple Sclerosis and Experimental Demyelinating Diseases*. Springer Berlin Heidelberg.
- BRADL, M. & LININGTON, C. 1996. Animal Models of Demyelination. *Brain Pathology*, 6, 303-311.
- BUISMAN, A. M., DE ROND, C. G. H., ÖZTÜRK, K., TEN HULSCHER, H. I. & VAN BINNENDIJK, R. S. 2009. Long-term presence of memory B-cells specific for different vaccine components. *Vaccine*, 28, 179-186.
- BULLOCH, K., MILLER, M. M., GAL-TOTH, J., MILNER, T. A., GOTTFRIED-BLACKMORE, A., WATERS, E. M., KAUNZNER, U. W., LIU, K., LINDQUIST, R., NUSSENZWEIG, M. C., STEINMAN, R. M. & MCEWEN, B. S. 2008. CD11c/EYFP transgene illuminates a discrete network of dendritic cells within the embryonic, neonatal, adult, and injured mouse brain. *The Journal of Comparative Neurology*, 508, 687-710.
- CAMBRIDGE, G., LEANDRO, M. J., EDWARDS, J. C. W., EHRENSTEIN, M. R., SALDEN, M., BODMAN-SMITH, M. & WEBSTER, A. D. B. 2003. Serologic changes following B lymphocyte depletion therapy for rheumatoid arthritis. *Arthritis & Rheumatism*, 48, 2146-2154.
- CARARE, R. O., BERNARDES-SILVA, M., NEWMAN, T. A., PAGE, A. M., NICOLL, J. A. R., PERRY, V. H. & WELLER, R. O. 2008. Solutes, but not cells, drain from the brain parenchyma along basement membranes of capillaries and arteries: significance for cerebral amyloid angiopathy and neuroimmunology. *Neuropathology and Applied Neurobiology*, 34, 131-144.
- CHABAS, D., BARANZINI, S. E., MITCHELL, D., BERNARD, C. C. A., RITTLING, S. R., DENHARDT, D. T., SOBEL, R. A., LOCK, C., KARPUJ, M., PEDOTTI, R., HELLER, R., OKSENBERG, J. R. & STEINMAN, L. 2001. The Influence of the Proinflammatory Cytokine, Osteopontin, on Autoimmune Demyelinating Disease. *Science*, 294, 1731-1735.

- CHEN, Z. J., WHEELER, C. J., SHI, W., WU, A. J., YARBORO, C. H., GALLAGHER, M. & NOTKINS, A. L. 1998. Polyreactive antigen-binding B cells are the predominant cell type in the newborn B cell repertoire. *European Journal of Immunology*, 28, 989-994.
- CLYNES, R. & RAVETCH, J. V. 1995. Cytotoxic antibodies trigger inflammation through Fc receptors. *Immunity*, 3, 21-26.
- COLES, A. J., TWYMAN, C. L., ARNOLD, D. L., COHEN, J. A., CONFAVREUX, C., FOX, E. J., HARTUNG, H.-P., HAVRDOVA, E., SELMAJ, K. W., WEINER, H. L., MILLER, T., FISHER, E., SANDBRINK, R., LAKE, S. L., MARGOLIN, D. H., OYUELA, P., PANZARA, M. A. & COMPSTON, D. A. S. 2012. Alemtuzumab for patients with relapsing multiple sclerosis after disease-modifying therapy: a randomised controlled phase 3 trial. *The Lancet*, 380, 1829-1839.
- COMPSTON, A. & COLES, A. Multiple sclerosis. *The Lancet*, 372, 1502-1517.
- COUTINHO, A., KAZATCHKINE, M. D. & AVRAMEAS, S. 1995. Natural autoantibodies. *Current Opinion in Immunology*, 7, 812-818.
- CROSS, A. H., CANNELLA, B., BROSNAN, C. F. & RAINE, C. S. 1990. Homing to central nervous system vasculature by antigen-specific lymphocytes. I. Localization of <sup>14</sup>C-labeled cells during acute, chronic, and relapsing experimental allergic encephalomyelitis. *Laboratory investigation; a journal of technical methods and pathology*, 63, 162-170.
- CSERR, H. F. & BERMAN, B. J. 1978. Iodide and thiocyanate efflux from brain following injection into rat caudate nucleus. *American Journal of Physiology - Renal Physiology*, 235, F331-F337.
- DAL PORTO, J. M., HABERMAN, A. M., SHLOMCHIK, M. J. & KELSOE, G. 1998. Antigen Drives Very Low Affinity B Cells to Become Plasmacytes and Enter Germinal Centers. *The Journal of Immunology*, 161, 5373-5381.
- DANESHTALAB, N., DORÉ, J. J. E. & SMEDA, J. S. 2010. Troubleshooting tissue specificity and antibody selection: Procedures in immunohistochemical studies. *Journal of Pharmacological and Toxicological Methods*, 61, 127-135.
- DIGHIERO, G., LYMBERI, P., MAZIÉ, J. C., ROUYRE, S., BUTLER-BROWNE, G. S., WHALEN, R. G. & AVRAMEAS, S. 1983. Murine hybridomas secreting natural monoclonal antibodies reacting with self antigens. *The Journal of Immunology*, 131, 2267-72.
- DUDDY, M., NIINO, M., ADATIA, F., HEBERT, S., FREEDMAN, M., ATKINS, H., KIM, H. J. & BAR-OR, A. 2007. Distinct Effector Cytokine Profiles of Memory and Naive Human B Cell Subsets and Implication in Multiple Sclerosis. *The Journal of Immunology*, 178, 6092-6099.
- EL-BEHI, M., ROSTAMI, A. & CIRIC, B. 2010. Current Views on the Roles of Th1 and Th17 Cells in Experimental Autoimmune Encephalomyelitis. *Journal of Neuroimmune Pharmacology*, 5, 189-197.
- ELLMERICH, S., MYCKO, M., TAKACS, K., WALDNER, H., WAHID, F. N., BOYTON, R. J., KING, R. H. M., SMITH, P. A., AMOR, S., HERLIHY, A. H., HEWITT, R. E., JUTTON, M., PRICE, D. A., HAFLE, D. A., KUCHAROO, V. K. & ALTMANN, D. M. 2005. High Incidence of Spontaneous Disease in an HLA-DR15 and TCR Transgenic Multiple Sclerosis Model. *The Journal of Immunology*, 174, 1938-1946.
- ENGELHARDT, B. & COISNE, C. 2011. Fluids and barriers of the CNS establish immune privilege by confining immune surveillance to a two-walled castle moat surrounding the CNS castle. *Fluids and Barriers of the CNS*, 8, 4.
- FILLATREAU, S., SWEENIE, C. H., MCGEACHY, M. J., GRAY, D. & ANDERTON, S. M. 2002. B cells regulate autoimmunity by provision of IL-10. *Nat Immunol*, 3, 944-950.
- FONTANA, A., FIERZ, W. & WEKERLE, H. 1984. Astrocytes present myelin basic protein to encephalitogenic T-cell lines. *Nature*, 307, 273-6.
- FOSSATI-JIMACK, L., REININGER, L., CHICHEPORTICHE, Y., CLYNES, R., RAVETCH, J. V., HONJO, T. & IZUI, S. 1999. High Pathogenic Potential of Low-Affinity Autoantibodies in Experimental Autoimmune Hemolytic Anemia. *The Journal of Experimental Medicine*, 190, 1689-1696.
- FRIESE, M. A. & FUGGER, L. 2005. Autoreactive CD8+ T cells in multiple sclerosis: a new target for therapy? *Brain*, 128, 1747-1763.
- FRITSCHY, J.-M. 2008. Is my antibody-staining specific? How to deal with pitfalls of immunohistochemistry. *European Journal of Neuroscience*, 28, 2365-2370.
- FUGGER, L., FRIESE, M. A. & BELL, J. I. 2009. From genes to function: the next challenge to understanding multiple sclerosis. *Nat Rev Immunol*, 9, 408-417.
- FULPIUS, T., SPERTINI, F., REININGER, L. & IZUI, S. 1993. Immunoglobulin heavy chain constant region determines the pathogenicity and the antigen-binding activity of rheumatoid factor. *Proceedings of the National Academy of Sciences*, 90, 2345-2349.

- GIESEKE, F., MANG, P., VIEBAHN, S., SONNTAG, I., KRUCHEN, A., ERBACHER, A., PFEIFFER, M., HANDGRETINGER, R. & MÜLLER, I. 2012. Siglec-7 tetramers characterize B-cell subpopulations and leukemic blasts. *European Journal of Immunology*, 42, 2176-2186.
- GIUNTI, D., BORSELLINO, G., BENELLI, R., MARCHESE, M., CAPELLO, E., VALLE, M. T., PEDEMONTI, E., NOONAN, D., ALBINI, A., BERNARDI, G., MANCARDI, G. L., BATTISTINI, L. & UCCELLI, A. 2003. Phenotypic and functional analysis of T cells homing into the CSF of subjects with inflammatory diseases of the CNS. *Journal of Leukocyte Biology*, 73, 584-590.
- GOVERMAN, J., WOODS, A., LARSON, L., WEINER, L. P., HOOD, L. & ZALLER, D. M. 1993. Transgenic mice that express a myelin basic protein-specific T cell receptor develop spontaneous autoimmunity. *Cell*, 72, 551-560.
- HAFLER, D. A., COMPSTON, A., SAWCER, S., LANDER, E. S., DALY, M. J., DE JAGER, P. L., DE BAKKER, P. I. W., GABRIEL, S. B., MIREL, D. B., IVINSON, A. J., PERICAK-VANCE, M. A., GREGORY, S. G., RIOUX, J. D., MCCAULEY, J. L., HAINES, J. L., BARCELLOS, L. F., CREE, B., OKSENBERG, J. R. & HAUSER, S. L. 2007. Risk alleles for multiple sclerosis identified by a genomewide study. *New England Journal of Medicine*, 357, 851-862.
- HARDY, R. R., CARMACK, C. E., LI, Y. U. E. S. & HAYAKAWA, K. 1994. Distinctive Developmental Origins and Specificities of Murine CD5+ B Cells. *Immunological Reviews*, 137, 91-118.
- HARRIS, D. P., GOODRICH, S., MOHRS, K., MOHRS, M. & LUND, F. E. 2005. Cutting Edge: The Development of IL-4-Producing B Cells (B Effector 2 Cells) Is Controlled by IL-4, IL-4 Receptor  $\alpha$ , and Th2 Cells. *The Journal of Immunology*, 175, 7103-7107.
- HARRIS, D. P., HAYNES, L., SAYLES, P. C., DUSO, D. K., EATON, S. M., LEPAK, N. M., JOHNSON, L. L., SWAIN, S. L. & LUND, F. E. 2000. Reciprocal regulation of polarized cytokine production by effector B and T cells. *Nat Immunol*, 1, 475-482.
- HAZENBOS, W. L. W., GESSNER, J. E., HOFHUIS, F. M. A., KUIPERS, H., MEYER, D., HEIJNEN, I. A. F. M., SCHMIDT, R. E., SANDOR, M., CAPEL, P. J. A., DAËRON, M., VAN DE WINKEL, J. G. J. & VERBEEK, J. S. 1996. Impaired IgG-Dependent Anaphylaxis and Arthus Reaction in Fc $\gamma$ RIII (CD16) Deficient Mice. *Immunity*, 5, 181-188.
- HEMMER, B., ARCHELOS, J. J. & HARTUNG, H.-P. 2002. New concepts in the immunopathogenesis of multiple sclerosis. *Nat Rev Neurosci*, 3, 291-301.
- HICKEY, W. F. 1991. Migration of Hematogenous Cells Through the Blood-Brain Barrier and the Initiation of CNS Inflammation. *Brain Pathology*, 1, 97-105.
- HIROSE, S., WAKIYA, M., KAWANO-NISHI, Y., YI, J., SANOKAWA, R., TAKI, S., SHIMAMURA, T., KISHIMOTO, T., TSURUI, H., NISHIMURA, H. & SHIRAI, T. 1993. Somatic diversification and affinity maturation of IgM and IgG anti-DNA antibodies in murine lupus. *European Journal of Immunology*, 23, 2813-2820.
- HOLMSETH, S., LEHRE, K. P. & DANBOLT, N. C. 2006. Specificity controls for immunocytochemistry. *Anatomy and Embryology*, 211, 257-266.
- HUSEBY, E. S., ÖHLÉN, C. & GOVERMAN, J. 1999. Cutting Edge: Myelin Basic Protein-Specific Cytotoxic T Cell Tolerance Is Maintained In Vivo by a Single Dominant Epitope in H-2k Mice. *The Journal of Immunology*, 163, 1115-1118.
- JACOBSON, B. A., SHARON, J., SHAN, H., SHLOMCHIK, M., WEIGERT, M. G. & MARSHAK-ROTHSTEIN, A. 1994. An isotype switched and somatically mutated rheumatoid factor clone isolated from a MRL-lpr/lpr mouse exhibits limited intraclonal affinity maturation. *The Journal of Immunology*, 152, 4489-99.
- JIANG, H., CURRAN, S., RUIZ-VAZQUEZ, E., LIANG, B., WINCHESTER, R. & CHESS, L. 2003. Regulatory CD8+ T cells fine-tune the myelin basic protein-reactive T cell receptor V $\beta$  repertoire during experimental autoimmune encephalomyelitis. *Proceedings of the National Academy of Sciences*, 100, 8378-8383.
- JOHNSTON, M., ZAKHAROV, A., KOH, L. & ARMSTRONG, D. 2005a. Subarachnoid injection of Microfil reveals connections between cerebrospinal fluid and nasal lymphatics in the non-human primate. *Neuropathology and Applied Neurobiology*, 31, 632-640.
- JOHNSTON, M., ZAKHAROV, A., KOH, L. & ARMSTRONG, D. 2005b. Subarachnoid injection of Microfil reveals connections between cerebrospinal fluid and nasal lymphatics in the non-human primate. *Neuropathol Appl Neurobiol*.
- JOHNSTON, M., ZAKHAROV, A., PAPAICONOMOU, C., SALMASI, G. & ARMSTRONG, D. 2004. Evidence of connections between cerebrospinal fluid and nasal lymphatic vessels in humans, non-human primates and other mammalian species. *Cerebrospinal Fluid Research*, 1, 2.

- KABAT, E. A., MOORE, D. H. & LANDOW, H. 1942. AN ELECTROPHORETIC STUDY OF THE PROTEIN COMPONENTS IN CEREBROSPINAL FLUID AND THEIR RELATIONSHIP TO THE SERUM PROTEINS 1. *The Journal of Clinical Investigation*, 21, 571-577.
- KANTOR, A. B., MERRILL, C. E., MACKENZIE, J. D., HERZENBERG, L. A. & HILLSON, J. L. 1995. Development of the Antibody Repertoire as Revealed by Single-Cell PCR of FACS-Sorted B-Cell Subsets. *Annals of the New York Academy of Sciences*, 764, 224-227.
- KIVISAKK, P., TUCKY, B., WEI, T., CAMPBELL, J. & RANSOHOFF, R. 2006. Human cerebrospinal fluid contains CD4+ memory T cells expressing gut- or skin-specific trafficking determinants: relevance for immunotherapy. *BMC Immunology*, 7, 14.
- KOH, L., ZAKHAROV, A. & JOHNSTON, M. 2005. Integration of the subarachnoid space and lymphatics: Is it time to embrace a new concept of cerebrospinal fluid absorption? *Cerebrospinal Fluid Research*, 2, 6.
- KRISHNAMOORTHY, G., HOLZ, A. & WEKERLE, H. 2007. Experimental models of spontaneous autoimmune disease in the central nervous system. *J Mol Med (Berl)*, 85, 1161-73.
- KRISHNAMOORTHY, G., LASSMANN, H., WEKERLE, H. & HOLZ, A. 2006. Spontaneous opticospinal encephalomyelitis in a double-transgenic mouse model of autoimmune T cell/B cell cooperation. *J Clin Invest*, 116, 2385-92.
- KRISHNAMOORTHY, G. & WEKERLE, H. 2009. EAE: an immunologist's magic eye. *Eur J Immunol*, 39, 2031-5.
- KURTZKE, J. F. 1993. Epidemiologic evidence for multiple sclerosis as an infection. *Clinical Microbiology Reviews*, 6, 382-427.
- LAFAILLE, J. J., NAGASHIMA, K., KATSUKI, M. & TONEGAWA, S. 1994. High incidence of spontaneous autoimmune encephalomyelitis in immunodeficient anti-myelin basic protein T cell receptor transgenic mice. *Cell*, 78, 399-408.
- LASSMANN, H., KITZ, K. & WISNIEWSKI, H. M. 1981. In vivo effect of sera from animals with chronic relapsing experimental allergic encephalomyelitis on central and peripheral myelin. *Acta Neuropathologica*, 55, 297-306.
- LASSMANN, H., RAINE, C. S., ANTEL, J. & PRINEAS, J. W. 1998. Immunopathology of multiple sclerosis: Report on an international meeting held at the Institute of Neurology of the University of Vienna. *Journal of Neuroimmunology*, 86, 213-217.
- LEONG, A. S.-Y. 2004. Pitfalls in Diagnostic Immunohistology. *Advances in Anatomic Pathology*, 11, 86-93.
- LEUNG, S., LIU, X., FANG, L., CHEN, X., GUO, T. & ZHANG, J. 2010. The cytokine milieu in the interplay of pathogenic Th1/Th17 cells and regulatory T cells in autoimmune disease. *Cell Mol Immunol*, 7, 182-189.
- LITZENBURGER, T., FASSLER, R., BAUER, J., LASSMANN, H., LININGTON, C., WEKERLE, H. & IGLESIAS, A. 1998. B lymphocytes producing demyelinating autoantibodies: development and function in gene-targeted transgenic mice. *J Exp Med*, 188, 169-80.
- LOSY, J., MEHTA, P. D. & WISNIEWSKI, H. M. 1990. Identification of IgG subclasses' oligoclonal bands in multiple sclerosis CSF. *Acta Neurologica Scandinavica*, 82, 4-8.
- LOW, P. A., SCHMELZER, J. D., YAO, J. K., DYCK, P. J., PARTHASARATHY, S. & BAUMANN, W. J. 1983. Structural specificity in demyelination induced by lysophospholipids. *Biochimica et Biophysica Acta (BBA) - Lipids and Lipid Metabolism*, 754, 298-304.
- LUND, F. E. 2008. Cytokine-producing B lymphocytes—key regulators of immunity. *Current Opinion in Immunology*, 20, 332-338.
- LÜNEMANN, J. D. & MÜNZ, C. 2009. EBV in MS: guilty by association? *Trends in Immunology*, 30, 243-248.
- LYONS, J.-A., SAN, M., HAPP, M. P. & CROSS, A. H. 1999. B cells are critical to induction of experimental allergic encephalomyelitis by protein but not by a short encephalitogenic peptide. *European Journal of Immunology*, 29, 3432-3439.
- MADSEN, L. S., ANDERSSON, E. C., JANSSON, L., KROGSGAARD, M., ANDERSEN, C. B., ENGBERG, J., STROMINGER, J. L., SVEJGAARD, A., HJORTH, J. P., HOLMDAHL, R., WUCHERPFENNIG, K. W. & FUGGER, L. 1999. A humanized model for multiple sclerosis using HLA-DR2 and a human T-cell receptor. *Nat Genet*, 23, 343-347.
- MAGLIOZZI, R., HOWELL, O., VORA, A., SERAFINI, B., NICHOLAS, R., PUOPOLO, M., REYNOLDS, R. & ALOISI, F. 2007. Meningeal B-cell follicles in secondary progressive multiple sclerosis associate with early onset of disease and severe cortical pathology. *Brain*, 130, 1089-1104.
- MATSUSHIMA, G. K. & MORELL, P. 2001. The Neurotoxicant, Cuprizone, as a Model to Study Demyelination and Remyelination in the Central Nervous System. *Brain Pathology*, 11, 107-116.

- MCCARTHY, D., RICHARDS, M. & MILLER, S. 2012. Mouse Models of Multiple Sclerosis: Experimental Autoimmune Encephalomyelitis and Theiler's Virus-Induced Demyelinating Disease. *In: PERL, A. (ed.) Autoimmunity*. Humana Press.
- MCCMAHON, E. J., BAILEY, S. L. & MILLER, S. D. 2006. CNS dendritic cells: Critical participants in CNS inflammation? *Neurochemistry International*, 49, 195-203.
- MCMENAMIN, P. G. 1999. Distribution and phenotype of dendritic cells and resident tissue macrophages in the dura mater, leptomeninges, and choroid plexus of the rat brain as demonstrated in wholemount preparations. *The Journal of Comparative Neurology*, 405, 553-562.
- MILLER, S. D., VANDERLUGT, C. L., BEGOLKA, W. S., PAO, W., YAUCH, R. L., NEVILLE, K. L., KATZ-LEVY, Y., CARRIZOSA, A. & KIM, B. S. 1997. Persistent infection with Theiler's virus leads to CNS autoimmunity via epitope spreading. *Nat Med*, 3, 1133-1136.
- MITSDOERFFER, M., LEE, Y., JÄGER, A., KIM, H.-J., KORN, T., KOLLS, J. K., CANTOR, H., BETTELLI, E. & KUCHROO, V. K. 2010. Proinflammatory T helper type 17 cells are effective B-cell helpers. *Proceedings of the National Academy of Sciences*, 107, 14292-14297.
- NIMMERJAHN, F., BRUHNS, P., HORIUCHI, K. & RAVETCH, J. V. 2005. FcγRIV: A Novel FcR with Distinct IgG Subclass Specificity. *Immunity*, 23, 41-51.
- O'CONNOR, K. C., APPEL, H., BREGOLI, L., CALL, M. E., CATZ, I., CHAN, J. A., MOORE, N. H., WARREN, K. G., WONG, S. J., HAFLER, D. A. & WUCHERPFENNIG, K. W. 2005. Antibodies from Inflamed Central Nervous System Tissue Recognize Myelin Oligodendrocyte Glycoprotein. *The Journal of Immunology*, 175, 1974-1982.
- OBERMEIER, B., MENTELE, R., MALOTKA, J., KELLERMANN, J., KUMPFEL, T., WEKERLE, H., LOTTSPEICH, F., HOHLFELD, R. & DORNMAIR, K. 2008. Matching of oligoclonal immunoglobulin transcriptomes and proteomes of cerebrospinal fluid in multiple sclerosis. *Nat Med*, 14, 688-93.
- OHNO, M., KOMIYAMA, A., MARTIN, P. M. & SUZUKI, K. 1993. MHC class II antigen expression and T-cell infiltration in the demyelinating CNS and PNS of the twitcher mouse. *Brain Research*, 625, 186-196.
- OLIVARES-VILLAGÓMEZ, D., WANG, Y. & LAFAILLE, J. J. 1998. Regulatory CD4+ T Cells Expressing Endogenous T Cell Receptor Chains Protect Myelin Basic Protein-specific Transgenic Mice from Spontaneous Autoimmune Encephalomyelitis. *The Journal of Experimental Medicine*, 188, 1883-1894.
- PATERSON, P. Y. 1960. TRANSFER OF ALLERGIC ENCEPHALOMYELITIS IN RATS BY MEANS OF LYMPH NODE CELLS. *The Journal of Experimental Medicine*, 111, 119-136.
- PERCHELLET, A., STROMNES, I., PANG, J. M. & GOVERMAN, J. 2004. CD8+ T cells maintain tolerance to myelin basic protein by 'epitope theft'. *Nat Immunol*, 5, 606-614.
- POLLINGER, B., KRISHNAMOORTHY, G., BERER, K., LASSMANN, H., BOSL, M. R., DUNN, R., DOMINGUES, H. S., HOLZ, A., KURSCHUS, F. C. & WEKERLE, H. 2009. Spontaneous relapsing-remitting EAE in the SJL/J mouse: MOG-reactive transgenic T cells recruit endogenous MOG-specific B cells. *J Exp Med*, 206, 1303-16.
- RANSOHOFF, R. M. & BROWN, M. A. 2012. Innate immunity in the central nervous system. *The Journal of Clinical Investigation*, 122, 1164-1171.
- RANSOHOFF, R. M. & CARDONA, A. E. 2010. The myeloid cells of the central nervous system parenchyma. *Nature*, 468, 253-262.
- RANSOHOFF, R. M. & ENGELHARDT, B. 2012. The anatomical and cellular basis of immune surveillance in the central nervous system. *Nat Rev Immunol*, 12, 623-635.
- RANSOHOFF, R. M., KIVISAKK, P. & KIDD, G. 2003. Three or more routes for leukocyte migration into the central nervous system. *Nat Rev Immunol*, 3, 569-581.
- RANSOHOFF, R. M. & PERRY, V. H. 2009. Microglial Physiology: Unique Stimuli, Specialized Responses. *Annual Review of Immunology*. Palo Alto: Annual Reviews.
- RIVERA-QUINONES, C., MCGAVERN, D., SCHMELZER, J. D., HUNTER, S. F., LOW, P. A. & RODRIGUEZ, M. 1998. Absence of neurological deficits following extensive demyelination in a class I-deficient murine model of multiple sclerosis. *Nat Med*, 4, 187-193.
- SALLUSTO, F., LENIG, D., FORSTER, R., LIPP, M. & LANZAVECCHIA, A. 1999. Two subsets of memory T lymphocytes with distinct homing potentials and effector functions. *Nature*, 401, 708-712.
- SCHEID, J. F., MOUQUET, H., FELDHAHN, N., WALKER, B. D., PEREYRA, F., CUTRELL, E., SEAMAN, M. S., MASCOLA, J. R., WYATT, R. T., WARDEMANN, H. & NUSSENZWEIG, M. C. 2009. A method for identification of HIV gp140 binding memory B cells in human blood. *Journal of Immunological Methods*, 343, 65-67.

- SCHLEY, D., CARARE-NNADI, R., PLEASE, C. P., PERRY, V. H. & WELLER, R. O. 2006. Mechanisms to explain the reverse perivascular transport of solutes out of the brain. *Journal of Theoretical Biology*, 238, 962-974.
- SERAFINI, B., ROSICARELLI, B., MAGLIOZZI, R., STIGLIANO, E. & ALOISI, F. 2004. Detection of Ectopic B-cell Follicles with Germinal Centers in the Meninges of Patients with Secondary Progressive Multiple Sclerosis. *Brain Pathology*, 14, 164-174.
- SHLOMCHIK, M. J., MARSHAK-ROTHSTEIN, A., WOLFOWICZ, C. B., ROTHSTEIN, T. L. & WEIGERT, M. G. 1987. The role of clonal selection and somatic mutation in autoimmunity. *Nature*, 328, 805-811.
- SMOLDERS, J., MENHEERE, P., KESSELS, A., DAMOISEAUX, J. & HUPPERTS, R. 2008. Association of vitamin D metabolite levels with relapse rate and disability in multiple sclerosis. *Multiple Sclerosis*, 14, 1220-1224.
- SOBEL, R. A. 2000. Genetic and epigenetic influence on EAE phenotypes induced with different encephalitogenic peptides. *Journal of Neuroimmunology*, 108, 45-52.
- SRIRAM, S. 2011. Role of glial cells in innate immunity and their role in CNS demyelination. *Journal of Neuroimmunology*, 239, 13-20.
- STORCH, M. K., STEFFERL, A., BREHM, U., WEISSERT, R., WALLSTRÖM, E., KERSCHENSTEINER, M., OLSSON, T., LININGTON, C. & LASSMANN, H. 1998. Autoimmunity to Myelin Oligodendrocyte Glycoprotein in Rats Mimics the Spectrum of Multiple Sclerosis Pathology. *Brain Pathology*, 8, 681-694.
- SUZUKI, K. & SUZUKI, K. 1995. The Twitcher Mouse: A Model for Krabbe Disease and for Experimental Therapies. *Brain Pathology*, 5, 249-258.
- SZENTISTVANYI, I., PATLAK, C. S., ELLIS, R. A. & CSERR, H. F. 1984. Drainage of interstitial fluid from different regions of rat brain. *American Journal of Physiology - Renal Physiology*, 246, F835-F844.
- TILLMAN, D. M., JOU, N. T., HILL, R. J. & MARION, T. N. 1992. Both IgM and IgG anti-DNA antibodies are the products of clonally selective B cell stimulation in (NZB x NZW)F1 mice. *The Journal of Experimental Medicine*, 176, 761-779.
- TREBST, C., LYKKE SØRENSEN, T., KIVISÄKK, P., CATHCART, M. K., HESSELGESSER, J., HORUK, R., SELLEBJERG, F., LASSMANN, H. & RANSOHOFF, R. M. 2001. CCR1+/CCR5+ Mononuclear Phagocytes Accumulate in the Central Nervous System of Patients with Multiple Sclerosis. *The American Journal of Pathology*, 159, 1701-1710.
- VARTDAL, F., VANDVIK, B. & NORRBY, E. 1980. Viral and bacterial antibody responses in multiple sclerosis. *Annals of Neurology*, 8, 248-255.
- VESCE, S., ROSSI, D., BRAMBILLA, L. & VOLTERRA, A. 2007. Glutamate Release from Astrocytes in Physiological Conditions and in Neurodegenerative Disorders Characterized by Neuroinflammation. In: GIACINTO BAGETTA, M. T. C. & STUART, A. L. (eds.) *International Review of Neurobiology*. Academic Press.
- VOLLERS, S. S. & STERN, L. J. 2008. Class II major histocompatibility complex tetramer staining: progress, problems, and prospects. *Immunology*, 123, 305-313.
- WALDNER, H., WHITTERS, M. J., SOBEL, R. A., COLLINS, M. & KUCHROO, V. K. 2000. Fulminant spontaneous autoimmunity of the central nervous system in mice transgenic for the myelin proteolipid protein-specific T cell receptor. *Proceedings of the National Academy of Sciences*, 97, 3412-3417.
- WALSH, M. J., TOURTELLOTTE, W. W. & SHAPSHAK, P. 1986. Immunoglobulin heavy chain associated protein in multiple sclerosis cerebrospinal fluid. *Molecular Immunology*, 23, 1117-1123.
- WEINSHENKER, B. G. 1998. The natural history of multiple sclerosis: Update 1998. *Seminars in Neurology*, 18, 301-307.
- WEKERLE, H. 2006. Breaking ignorance: the case of the brain. *Curr Top Microbiol Immunol*, 305, 25-50.
- WEKERLE, H., KOJIMA, K., LANNES-VIEIRA, J., LASSMANN, H. & LININGTON, C. 1994a. Animal models. *Annals of Neurology*, 36, S47-S53.
- WEKERLE, H., KOJIMA, K., LANNES-VIEIRA, J., LASSMANN, H. & LININGTON, C. 1994b. Animal models. *Ann Neurol*, 36 Suppl, S47-53.
- WEKERLE, H., LININGTON, C., LASSMANN, H. & MEYERMANN, R. 1986. Cellular immune reactivity within the CNS. *Trends in Neurosciences*, 9, 271-277.
- WEKERLE, H., SUN, D., OROPEZA-WEKERLE, R. L. & MEYERMANN, R. 1987. Immune reactivity in the nervous system: modulation of T-lymphocyte activation by glial cells. *J Exp Biol*, 132, 43-57.
- WELLER, R. 1998. Pathology of cerebrospinal fluid and interstitial fluid of the CNS: significance for Alzheimer disease, prion disorders and multiple sclerosis. *J Neuropathol Exp Neurol*, 57, 885 - 894.



- WELLER, R., DJUANANDA, E., YOW, H.-Y. & CARARE, R. 2009. Lymphatic drainage of the brain and the pathophysiology of neurological disease. *Acta Neuropathologica*, 117, 1-14.
- WU, Y.-C., KIPLING, D., LEONG, H. S., MARTIN, V., ADEMOKUN, A. A. & DUNN-WALTERS, D. K. 2010. High-throughput immunoglobulin repertoire analysis distinguishes between human IgM memory and switched memory B-cell populations. *Blood*, 116, 1070-1078.
- YOFFEY, J. M. & DRINKER, C. K. 1939. The cell content of peripheral lymph and its bearing on the problem of the circulation of the lymphocyte. *The Anatomical Record*, 73, 417-427.
- ZWAM, M., HUIZINGA, R., MELIEF, M.-J., WIERENGA-WOLF, A., MEURS, M., VOERMAN, J., BIBER, K. H., BODDEKE, H. G. M., HÖPKEN, U., MEISEL, C., MEISEL, A., BECHMANN, I., HINTZEN, R., 'T HART, B., AMOR, S., LAMAN, J. & BOVEN, L. 2009. Brain antigens in functionally distinct antigen-presenting cell populations in cervical lymph nodes in MS and EAE. *Journal of Molecular Medicine*, 87, 273-286.

## CHAPTER 9: CURRICULUM VITAE

## 9. Curriculum vitae

Zakeya Al Rasbi

BSc., MSc.

P.O. Box: 80305, Al-Ain, United Arab Emirates

**Cell phone:** +971(50) 33 43 913

**Office phone:** +971(3) 7137 515

**E-mail:** rasbi@uaeu.ac.ae

### Personal details

**Gender:** Female

**Status:** Single

**Date of Birth:** October 6, 1983

### Profile

I possess well-developed leadership qualities, as well as interpersonal and communication skills with the excellent ability to work either independently or in a team in a multi-cultural environment. I am seeking to expand and develop my analytical skills in a leading organization.

### Scholarships and awards

- **2009-2013:** Fellowship grant from the Emirates Foundation for PhD project
- **2009:** best poster prize in the third Al-Ain international Immunology Meeting
- **2007-2009:** Scholarship from the President's Office of United Arab Emirates for MSc Project
- **2001-2007:** Scholarship from the United Arab Emirates' Ministry of Higher Education and Scientific Studies for BSc. Degree

### Academic qualifications

<b>2013-present</b>	Master/diploma of Medical Parasitology London School of Hygiene and Tropical Medicine Keppel Street London, United Kingdom <b>Graduation Date:</b>
<b>2009-2013</b>	Doctorate of Human Biology Major: Neuroimmunology

Max Planck Institute of Neurobiology  
Department of Neuroimmunology  
Martinsried 82152  
Munich, Germany

**Graduation Date:**

**2007-2009**

Master of Medical Science  
Major: Immunology and Microbiology  
United Arab Emirates University  
Al-Ain, United Arab Emirates  
**Graduation Date:** March 2010

**2004-2007**

Bachelor of Biomedical Science  
Monash University  
Melbourne, Australia  
**Graduation Date:** December 2006

**2003**

Monash University Foundation Year (MUFY)  
Taylors College  
Melbourne, Australia

**2002**

English Course  
Taylors College  
Melbourne, Australia

**2001**

High School Certificate  
Al-Ain Secondary School  
Science Stream  
Al-Ain, United Arab Emirates  
**Over all Grades: 92%**

## Professional experience

- August 2013-present**
- Organization:** United Arab Emirates University  
**Department:** Department of Medical Microbiology and Immunology  
**Position:** Teaching Assistant of Parasitology  
**Address:** Department of Medical Microbiology and Immunology  
 Faculty of Medicine and Health Sciences  
 United Arab Emirates University  
 P.O. Box 17666  
 Al Ain, United Arab Emirates
- Job Duties:** Training program to gain qualifications in clinical and diagnostic parasitology; lecturing medical students; performing research in immunoparasitology.
- October 2009-2013**
- Organization:** Max Planck Institute of Neurobiology  
**Department:** Department of Neuroimmunology  
**Position:** PhD student  
**Address:** Am Klopferspitz 18  
 82152 Martinsried  
 Munich, German
- Job Duties:** The work focused on the role of B cells in spontaneous EAE (MS-like disease) in RR mice. Endogenously recruited myelin oligodendrocyte glycoprotein (MOG)-binding B cells have been observed in relapsing remitting (RR) experimental autoimmune encephalomyelitis (EAE) mice where all T cells are transgenic and specific for MOG<sub>92-106</sub> peptide, which has raised the interest in the contribution of B cells to EAE in RR mice.
- June 2006-2010**
- Organization:** United Arab Emirates University  
**Department:** Department of Medical Microbiology and Immunology  
**Position:** Master's Student  
**Address:** Department of Medical Microbiology and Immunology  
 Faculty of Medicine and Health Sciences  
 United Arab Emirates University

- P.O. Box 17666  
Al Ain, United Arab Emirates
- Job Duties:** Studied multiple sclerosis (MS) using the immunized EAE animal model. My studies focused on resistance to EAE galectin knockout mice and elucidating the contribution of galectins in molecular basis of EAE pathology.
- April-June 2006**
- Organization:** United Arab Emirates University  
**Department:** Department of Biochemistry  
**Position:** Trainee (Volunteer)  
**Address:** Department of Biochemistry  
Faculty of Medicine and Health Sciences  
United Arab Emirates University  
P.O. Box 17666  
Al Ain, United Arab Emirates
- Job Duties:** Studied Parkinson's disease using several techniques such as ELISA; expressed human recombinant  $\alpha$ -synuclein protein in cells to find a peptide that could block its accumulation and thus affect the dopamine pathway, which is believed to influence the clinical presentation of Parkinson's disease.
- 18/11/2005 - 20/02/2006**
- Organization:** United Arab Emirates University  
**Department:** Department of Medical Microbiology and Immunology  
**Position:** Trainee (Volunteer)  
**Address:** Department of Medical Microbiology and Immunology  
Faculty of Medicine and Health Sciences  
United Arab Emirates University  
P.O. Box 17666  
Al Ain, United Arab Emirates
- Job Duties:** Examined different types of viral infections in birds' ticks. Using advanced molecular techniques such as real-time PCR and conventional PCR
- 08/03/2006 - 20/05/2006**
- Organization:** Immunology and Stem Cell Laboratories  
**Department:** Neuroimmunology

	<b>Position:</b>	Trainee (Volunteer)
	<b>Address:</b>	Monash Immunology and Stem Cell Laboratories (MISCL) STRIP1, Level 3 Monash University Clayton 3800
	<b>Job Duties</b>	Performed histological work on MS animal models (EAE), to examine demyelination of the axons compare with its normal counterpart; quantified the amount of immune cell infiltration into the central nervous system compared to normal tissue
<b>July 2006</b>	<b>Organization:</b>	Monash Institute of Medical Research (MIMR)
	<b>Department:</b>	Center of inflammatory diseases
	<b>Position:</b>	Trainee (Volunteer)
	<b>Address:</b>	27-31 Wright Street, Clayton, 3168 Victoria, Australia
	<b>Job Duties:</b>	Learned the small interfering RNA (siRNA) technique and reviewed several scientific papers.

### Research interest

I wish to investigate the cellular and molecular networks underlying self-destructive (autoimmune) diseases, and which are believed to be mainly influenced by bacteria, fungus, and parasites in the gastrointestinal tract of human/animal body. I hope to ultimately develop methods that will impede disease progression and improve diagnosis in the early stages of disease. Additionally, I am interested in the mechanism underlying disease progression to elucidate targets for potential intervention.

### Professional skills

- Protein Synthesis: trained at **United Arab Emirates University** and **Max Planck Institute of Neurobiology**.
- RT-PCR and PCR: trained at **Monash University**, **United Arab Emirates University**, and **Max Planck Institute of Neurobiology**.
- Animal handling and injection: trained at **United Arab Emirates University** and **Max Planck Institute of Neurobiology**.

- GST-fusion protein expression, extraction and purification, protein detection, SDS-PAGE and Western blotting: trained at **United Arab Emirates University** and **Max Planck Institute of Neurobiology**.
- Cell Culture: trained at **United Arab Emirates University** and **Max Planck Institute of Neurobiology**.
- Enzyme linked immunosorbent assay (ELISA): trained at **Monash University, United Arab Emirates University**, and **Max Planck Institute of Neurobiology**.
- Enzyme linked immunospot (ELISPOT) assay: trained at **Max Planck Institute of Neurobiology**.
- Antibody purification and hybridoma creation: trained at the **Max Planck Institute of Neurobiology**.
- Flow cytometry: trained at **Max Planck Institute of Neurobiology**.
- Immunohistochemistry: trained at **Max Planck Institute of Neurobiology**.

### **Duties and responsibilities**

- Handled orders and managed payments of purchased equipment and reagents following University procedures.
- Designed experiments in accordance with the hypothesis under investigation.
- Analyzed results, including statistical analyses.
- Carried out troubleshooting of experiments.
- Wrote scientific articles and commentaries for prestigious scientific journals.
- Built and established effective collaborations with other laboratories.
- Taught and lectured students

### **Relevant skills**

- Excellent communication skills, ambitious and motivated to achieve and exceed set goals.
- Willing to train and learn new skills so as to advance oneself and organization.
- **Language Skills:**                   **Arabic** (Excellent writing, speaking, and reading)  
  **English** (Excellent writing, speaking, and reading)
- **Computer skills:** Microsoft Office, SPSS/STATA, Endnote Software.
- **TOEFL (iBT)** - Test of English as a Foreign Language (Internet-based Testing)
- Intermediate First aid (Australian Red Cross)
- UAE Driving License



**Activities and conferences****November 2010****SFB 571 Meeting**

Presented a 15 minutes talk based on my Ph.D. project and the techniques I developed to learn more about the role of MOG-binding B cells in spontaneous RR-EAE.

**January 2009****The 6<sup>th</sup> International Scientific Conference for Medical Students in GCC Countries**

Presented a 15 minutes talk based on my Master's project entitled, Galectin-3 is required in the initial and effector phases of T cell-mediated neuropathology.

**November 2008****The 2<sup>nd</sup> International Genetic Conference in Al Ain**

The conference was held in Al Ain and I obtained 20 credit hours for attending 4 days of lectures and activities.

**April 2008****The First Educational Distinction Conference**

I hosted this event, which allowed me to step out of my comfort zone and learn how to present my findings to the scientific community.

**April 2008****9<sup>th</sup> Annual Research Conference**

The research group I worked with presented two lectures based on our work on autoinflammatory disease in the EAE animal model of multiple sclerosis, which is one of the most common inflammatory diseases of the central nervous system worldwide.

**April 2008****3<sup>rd</sup> Al-Ain International Immunology Meeting**

The Immunology conference was held in Al Ain and I obtained 14 credit hours for attending 3 days of lectures and activities; I was awarded a prize for active participation.

July 2007

**Diabetes. Knowledge. Action. (Takatof membership)**

A public awareness campaign to educate people about diabetes and its potential risk to one's health. The campaign aimed to reduce the burden on UAE national health system and help people adopt a healthier life style and ultimately avoid Type 2 diabetes.

**Posters and publications**

1. Berer K, Mues M, Koutrolos M, **Rasbi ZA**, Boziki M, Johner C, Wekerle H, Krishnamoorthy G. Commensal microbiota and myelin autoantigen cooperate to trigger autoimmune demyelination. *Nature*. 2011 Oct 26; 479(7374): 538-41.
2. **Z.AI-Rasebi**, A. Shahin, A, AL-Awadhi, N, saif, M, Al-Marzouqi, E.Mensah-Brown and M.L. Lukic, Galectin-3 is required for the induction of experimental allergic encephalomyelitis. Department of Microbiology and Immunology, Department of Anatomy Faculty of Medicine and Health Sciences, UAE University, Al-Ain, P.O.Box 17666, united Arab Emirates. (Poster)
3. Jiang HR, **AI Rasebi Z**, Mensah-Brown E, Shahin A, Xu D, Goodyear CS, Fukada SY, Liu FT, Liew FY, Lukic ML. Galectin-3 deficiency reduces the severity of experimental autoimmune encephalomyelitis. *J Immunol*. 2009 Jan 15; 182(2): 1167-73.
4. Mensah-Brown EPK, **AI Rasebi Z**, Shahin A, Al Shamsi M, Arsenijevic N, Hsu DK, Liu F-T, Lukic ML. (2008) Targeted disruption of the galectin-3 gene results in decreased susceptibility to multiple low dose streptozotocin- induced diabetes in mice. *Clinical immunology*. Volume 130, Issue 1, January 2009, Pages 83-88

## References

### **Prof. Basal Ramadi**

Microbiology and Immunology Department Chairman  
Department of Medical Microbiology and Immunology  
Faculty of Medicine and Health Sciences  
United Arab Emirates University  
P.O. Box 17666  
Al Ain, United Arab Emirates  
Phone: +971 3 7137 529  
Fax: +971 3 7671966  
E-Mail: ramadi.b@uaeu.ac.ae

### **Prof. MD. Hartmut Wekerle**

Hertie Senior Professor  
Director emeritus of the Max Planck Institute of Neurobiology  
Max-Lebsche-Platz 31  
81377 Munich  
Germany  
Phone: +49 89 7095 8381  
Fax: +49 89 7095 8380  
E-Mail: hwekerle@neuro.mpg.de

### **Professor Claude Bernard**

Monash Immunology and Stem Cell Laboratories (MISCL)  
Monash University  
Clayton 3800  
Phone: +61 3 9905 0623  
Fax: +61 3 9905 0680  
E-Mail: claud.bernard@med.monash.edu.au